



# PACS Observer's Manual

HERSCHEL-HSC-DOC-0832, Version 2.2  
07-April-2011

---

## PACS Observer's Manual

Published version 1.0, 01 February 2007

Published version 1.1, 14 March 2007

Published version 1.2, 04 June 2007

Published version 1.3, 04 July 2007

Published version 1.4, 08 October 2007

Published version 1.5, 17 October 2007

Published version 2.0, 18 May 2010

Published version 2.1, 01 June 2010

Published version 2.2, 07 April 2011

Published

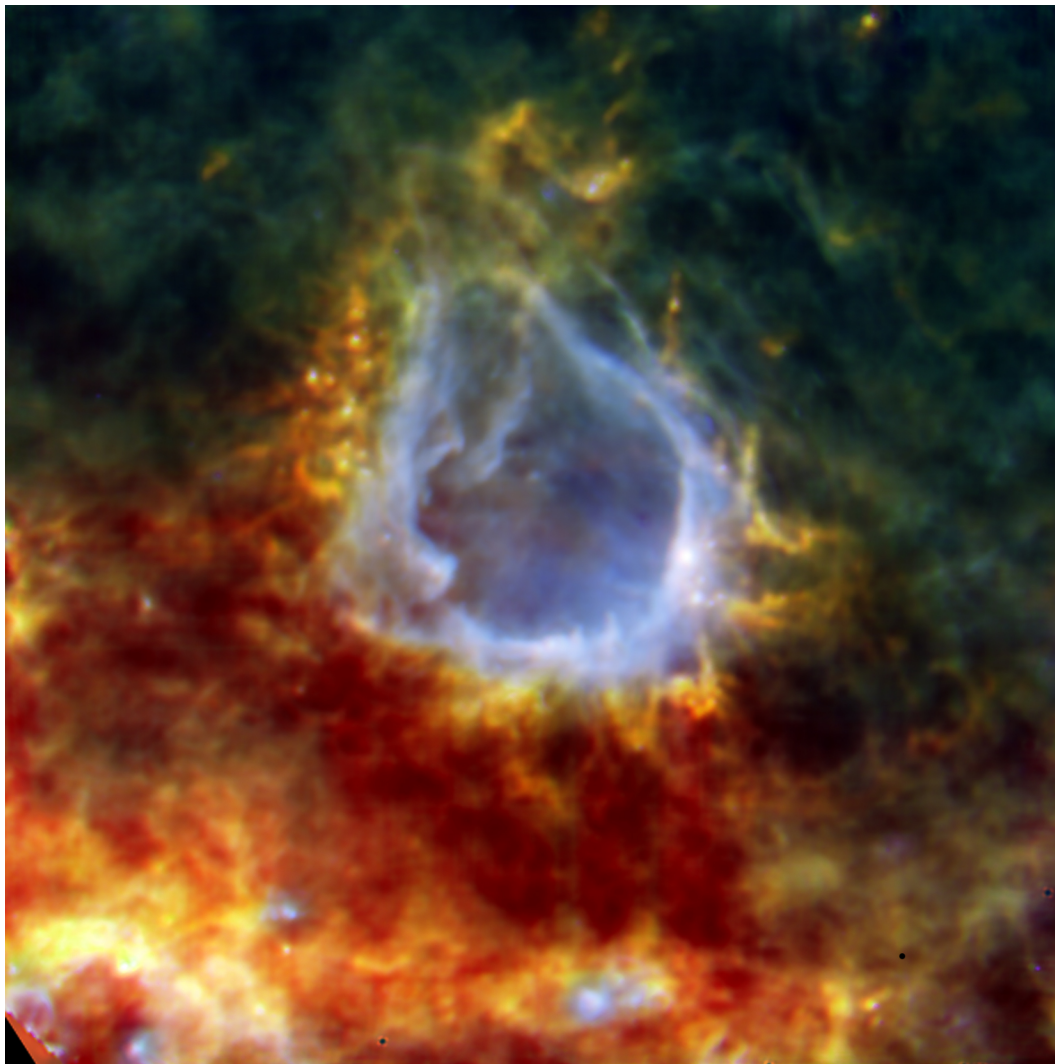


**Figure 1. RCW 120 HII emission nebula : PACS100+160  $\mu\text{m}$  + SPIRE250 $\mu\text{m}$  colour composite image Zavagno, A., et al., "Star formation triggered by the Galactic HII region RCW 120", A&A, 2010**

---

---

---

---

# Table of Contents

|  |    |
|--|----|
| 1. Introduction .....  | 1  |
| 1.1. Purpose of document .....   | 1  |
| 1.2. Background .....  | 1  |
| 1.3. Acknowledgements .....  | 2  |
| 1.4. Acronyms .....  | 2  |
| 2. The PACS instrument .....   | 3  |
| 2.1. Overview: instrument concept .....  | 3  |
| 2.2. Common Optics .....   | 5  |
| 2.2.1. Entrance Optics .....   | 5  |
| 2.2.2. Calibration sources .....   | 5  |
| 2.2.3. Chopper .....   | 6  |
| 2.3. Photometer .....  | 6  |
| 2.3.1. Filters .....   | 6  |
| 2.3.2. Bolometer arrays .....  | 7  |
| 2.3.3. Cooler .....  | 7  |
| 2.4. Spectrometer .....  | 8  |
| 2.4.1. Instrument design .....   | 8  |
| 2.4.2. Image slicer .....  | 8  |
| 2.4.3. Grating .....   | 10 |
| 2.4.4. Order sorting Filters .....   | 11 |
| 2.4.5. Photoconductor arrays .....   | 11 |
| 3. PACS photometer scientific capabilities .....                                   | 14 |
| 3.1. Point spread function .....   | 14 |
| 3.2. Photometer filters .....  | 17 |
| 3.3. Photometer flux calibration .....   | 18 |
| 3.4. Photometer bad pixels .....   | 19 |
| 3.5. Photometer sensitivity .....  | 20 |
| 3.6. Astrometric accuracy .....  | 21 |
| 4. PACS spectrometer scientific capabilities .....                                 | 22 |
| 4.1. Diffraction Losses .....  | 22 |
| 4.2. Grating efficiency .....  | 22 |
| 4.3. Spectrometer filters .....  | 23 |
| 4.4. Spectrometer relative spectral response function .....                        | 24 |
| 4.5. Spectrometer field-of-view and spatial resolution .....                       | 26 |
| 4.6. Spectrometer Point Spread Function (PSF) .....                                | 27 |
| 4.6.1. Measured vs. model PSF .....  | 27 |
| 4.6.2. Detector sampling of the PSF .....  | 28 |
| 4.6.3. Measured beam efficiencies .....  | 28 |
| 4.7. Spectrometer spectral resolution and instrumental profile .....               | 29 |
| 4.7.1. Spectrometer spectral resolution .....                                      | 29 |
| 4.7.2. Wavelength calibration .....  | 33 |
| 4.7.3. Instrumental profile .....  | 33 |
| 4.8. Spectral leakage regions .....  | 35 |
| 4.9. Spectrometer flux calibration .....   | 38 |
| 4.9.1. Recovering full beam line fluxes and flux densities for point sources ..... | 38 |
| 4.9.2. Absolute flux calibration, using the calibration block .....                | 38 |
| 4.10. Spectrometer sensitivity .....   | 41 |
| 4.11. Spectrometer saturation limits .....   | 44 |
| 5. Observing with the PACS photometer .....  | 49 |
| 5.1. Chop-nod point-source photometry mode .....                                   | 49 |
| 5.1.1. Chopper avoidance angle in point-source mode .....                          | 51 |
| 5.2. Scan mapping mode .....   | 52 |
| 5.2.1. Scan maps in instrument reference frame .....                               | 54 |
| 5.2.2. Scan maps in sky coordinates .....  | 55 |
| 5.2.3. Scan maps sensitivity .....   | 58 |
| 5.3. Gain setting for bright sources .....   | 59 |
| 5.4. Mini-scan map mode .....  | 60 |

|   |    |
|---|----|
| 6. Observing with PACS spectrometer .....   | 62 |
| 6.1. Line Spectroscopy AOT .....  | 63 |
| 6.1.1. Flux estimates and dynamic range .....   | 64 |
| 6.1.2. Spectral leakage regions .....   | 64 |
| 6.1.3. Pointed mode .....   | 64 |
| 6.1.4. Pointed with dither mode .....   | 65 |
| 6.1.5. Mapping mode .....   | 65 |
| 6.1.6. Standard chopping-nodding mode .....   | 67 |
| 6.1.7. Bright lines chopping-nodding mode .....   | 73 |
| 6.1.8. Unchopped grating scan mode .....  | 74 |
| 6.1.9. Wavelength switching mode .....  | 76 |
| 6.2. Range Spectroscopy AOT .....   | 80 |
| 6.2.1. Flux estimates and dynamic range .....   | 81 |
| 6.2.2. Spectral leakage regions .....   | 81 |
| 6.2.3. Pointed mode .....   | 82 |
| 6.2.4. Pointed with dither mode .....   | 82 |
| 6.2.5. Mapping mode .....   | 82 |
| 6.2.6. Range scan modes .....   | 82 |
| 6.2.7. SED mode .....   | 86 |
| 7. Pipeline processing and data products .....  | 91 |
| 7.1. PACS photometer standard data processing .....                                       | 91 |
| 7.1.1. Scan map pipeline processing issues .....  | 91 |
| 7.1.2. Level 2 pipeline products for scan maps generated with HCSS in the HSA archive ... | 92 |
| 7.2. Spectroscopy processing levels and data products .....                               | 93 |
| 8. Change record .....  | 95 |
| References .....  | 96 |

---

# Chapter 1. Introduction

## 1.1. Purpose of document

The PACS Observer's manual is intended to support astronomers in the definition of their observations with the PACS instrument. The purpose of this document is to provide relevant information about the PACS instrument on-board Herschel Space Observatory to plan PACS observations in HSpot. The information is mainly targeted to be a general overview of the instrument and its performance, in order to help the astronomer to plan, prepare and execute scientific observations with PACS.

The structure of this observer's manual is as follows: we first describe the instrument (Chapter 2) and its scientific capabilities of the photometer and spectrometer (Chapter 3 & 4), the use of astronomical observation templates (AOTs) to enter PACS observations in HSpot( Chapter 5 & 6) and the manual ends with a description of the pipeline (Chapter 7).



### Note

The [Herschel Observers' Manual](#) provides further information about Herschel pertinent to using the observatory from the perspective of an observer.

## 1.2. Background

The Herschel Space Observatory is an ESA cornerstone mission, for high spatial resolution observations in the FIR and sub-millimeter regime, launched on the 14th of May 2009 aboard an Ariane 5 rocket together with Planck. It was placed on a Lissajous 700 000 km diameter orbit 1.5 million kilometers away from Earth at the second Lagrange point of the Earth-Sun system.

The mission is named after Sir William Herschel, who discovered the infrared radiation in 1800.

It is the first space observatory to cover the full far-infrared and submillimetre waveband. It performs photometry and spectroscopy in the 55-670  $\mu\text{m}$  range, with its 3.5m diameter radiatively cooled telescope, with three science instruments housed inside a superfluid helium cryostat.

Herschel is designed to observe the "cool universe". The main scientific objectives of the mission are:

- to study the formation of galaxies in the early universe and their subsequent evolution;
- to investigate the formation of stars and their interaction with the interstellar medium;
- to observe the chemical composition of the atmospheres and surfaces of comets, asteroids, planets and satellites;
- to examine the molecular chemistry of the universe.

Herschel is operated as an observatory facility for three years of routine observations. Roughly two thirds of the observing time are "open time", and will be offered through a standard competitive proposal procedure.

The Photodetector Array Camera & Spectrometer (PACS) is one of the three science instruments of the Herschel observatory. PACS provides the Herschel Space Telescope with the capabilities for spectroscopy and imaging/photometry in the 55-210  $\mu\text{m}$  range.

PACS has been designed and built by a consortium of institutes and university departments from across Europe under the leadership of the Principal Investigator Albrecht Poglitsch at Max-Planck-Institute for Extraterrestrial Physics, Garching, Germany. Consortium members are from

Austria: UVIE; from Belgium: IMEC, KUL, CSL; from France: CEA, OAMP; from Germany: MPE, MPIA; from Italy: IFSI, OAP/OAT, OAA/CAISMI, LENS, SISSA; from Spain: IAC.

The PACS web site is : <http://pacs.mpe.mpg.de>

## 1.3. Acknowledgements

The PACS instrument is the result of many years of work by a large group of dedicated people in several institutes and companies across Europe. It is their efforts that have made it possible to create such a powerful instrument for use in the Herschel Space Observatory. We would first like to acknowledge their work.

This manual is edited by Bruno Altieri and Roland Vavrek (ESAC) on behalf of the PACS ICC consortium. This Observer's Manual also uses the knowledge contained in numerous PACS technical documents and various discussions.

## 1.4. Acronyms

- AOR : Astronomical Observation Request
- AOT : Astronomical Observation Template
- CRE : Cryogenic Readout Electronics
- DDCS : Double Differential Correlated Sampling (mode)
- DMC : Detector and Mechanics Controller
- DTCP : Daily TeleCommunications Period
- ESA : European Space Agency
- FM : Flight Model
- FOV : Field-Of-View
- FPU: Focal Plane Unit
- FWHM : Full Width Half Maximum
- HSpot: Herschel planning observations tool
- ICC: Instrument Control Centre
- ICS: Internal Calibration Source
- ILT: Integrated (Instrument) Level Tests
- NEP: Noise Equivalent Power
- OD: Observation Day
- PACS : Photodetector Array Camera & Spectrometer
- QLA : Quick Look Analysis
- QM: Qualification Model
- RSRF: Relative Spectral Response Function
- SED: Spectral Energy Distribution
- SPU: Signal Processing Unit

---

# Chapter 2. The PACS instrument

## 2.1. Overview: instrument concept

The PACS instrument comprises two sub-instruments which offer **two basic and mutually exclusive modes** in the wavelength band 55-210  $\mu\text{m}$  :

- Imaging dual-band photometry (60-85  $\mu\text{m}$  or 85-125  $\mu\text{m}$  and 125-210  $\mu\text{m}$ ) over a field of view of 1.75'x3.5', with full sampling of the telescope point spread function (diffraction/wavefront error limited)
- Integral-field spectroscopy between 51 and 220  $\mu\text{m}$  with a resolution of  $\sim 75\text{-}300\text{km/s}$  and instantaneous coverage of  $\sim 1500\text{ km/s}$ , over a field of view of 47"x47".

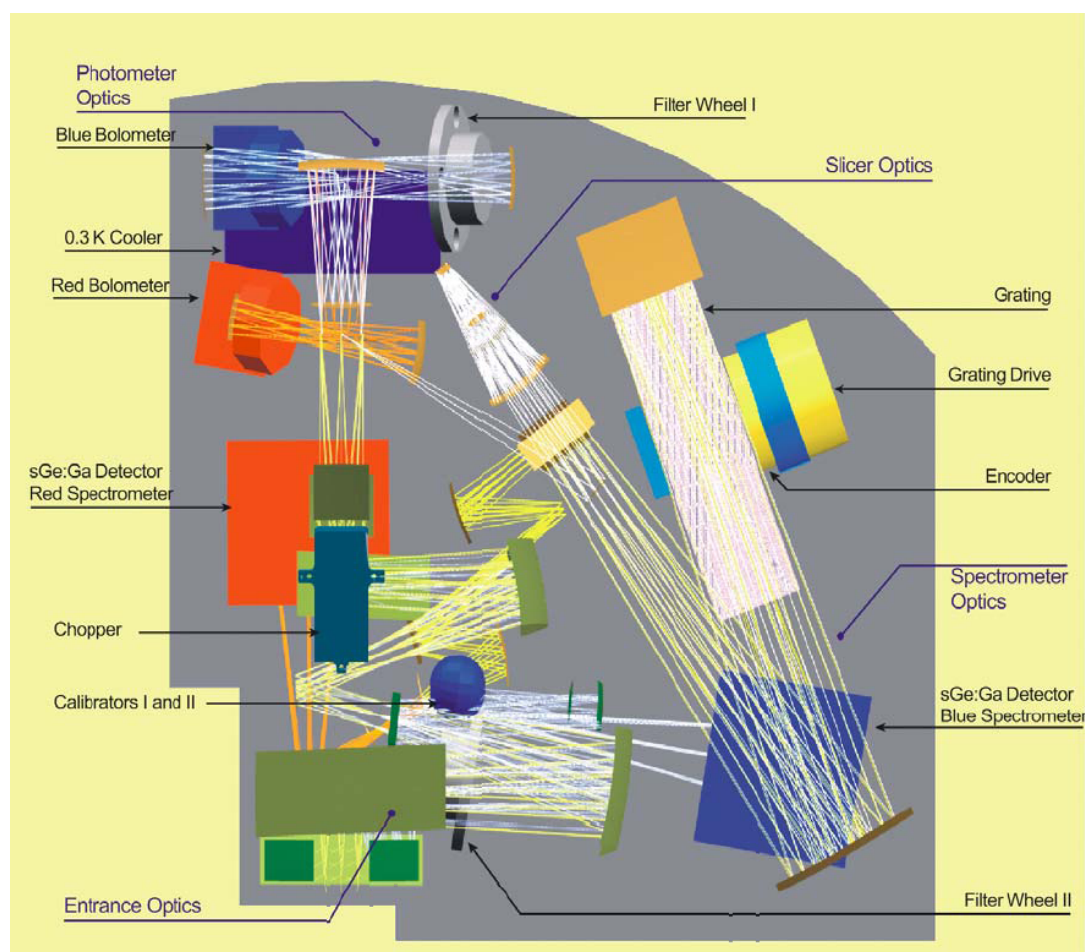


**Figure 2.1. Optical layout.** After the common entrance optics with calibration sources and the chopper, the field is split into the spectrometer train and the photometer trains. In the latter a dichroic beam splitter feeds separate re-imaging optics for the two bolometer arrays. In the spectrometer train, the image slicer converts the square field into an effective long slit for the Littrow-mounted grating spectrograph. The dispersed light is distributed to the two photoconductor arrays by a dichroic beam splitter which acts as an order sorter for the grating.

Figure 2.1 shows how the functional groups are distributed in the spatial instrument envelope.



Figure 2.2 shows an optical circuit block diagram of the major functional parts of PACS. At the top, the entrance and calibration optics is common to all optical paths through the instrument. On the right, the spectrometer serves both, the short-wavelength (“blue”), and long-wavelength (“red”) photoconductor arrays. A fixed dichroic beam splitter separates blue from red spectrometer light at the very end of the optical path. On the left, the bolometer fixed dichroic beam splitter comes before the blue and red imaging branches since they require different magnification. Directly in front of their baffle enclosures the blue detectors have filter wheel mechanisms which contain the band pass filters for short wavelength photometry, and the order selection band passes for 2nd and 3rd order operation of the grating spectrometer, respectively.

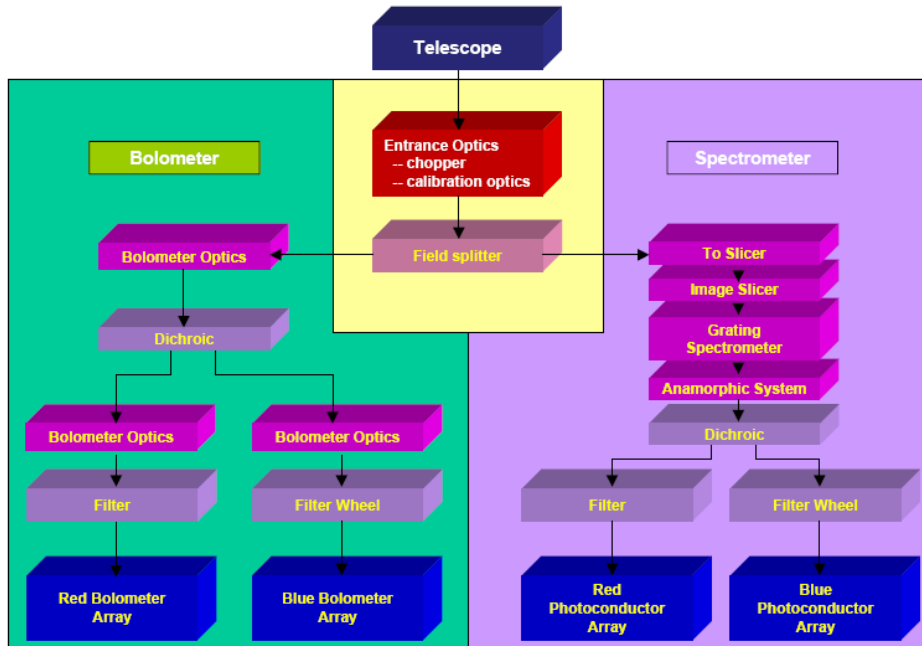
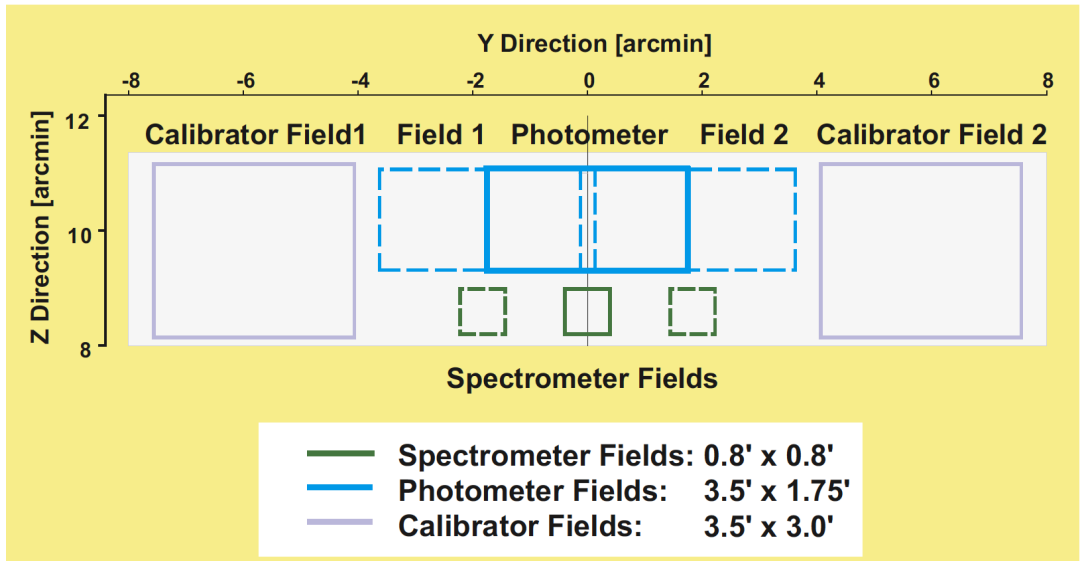


Figure 2.2. Functional block diagram of PACS overall optics

The focal plane sharing of the instrument channels is shown in Figure 2.3. The photometric bands, which can be observed simultaneously, cover the same field-of-view. The field-of-view of the spectrometer is offset from the photometer field (see Figure 2.3). However, this has no effect on the observing efficiency.

The focal plane unit provides photometric and spectroscopic capabilities through five functional units :

- common input optics with the chopper, calibration sources and a focal plane splitter;
- a photometer optical train with a dichroic beam splitter and separate re-imaging optics for the two short-wavelength bands (60-85  $\mu\text{m}$ / 85-125  $\mu\text{m}$ ) selectable via a filter wheel and the long-wavelength band (125-210  $\mu\text{m}$ ), respectively;
- two bolometer arrays with cryogenic buffers/multiplexers and a common 0.3 K sorption cooler;
- a spectrometer optical train with an image slicer unit for integral field spectroscopy, an anamorphic collimator, a movable diffraction grating in Littrow mount, anamorphic re-imaging optics, and a dichroic beam splitter for separation of diffraction orders. The blue channel contains an additional filter wheel for selecting its short or long wavelength part;
- two photoconductor arrays with attached cryogenic readout electronics (CRE).



PACS focal plane usage. Long-wavelength and short wavelength photometry bands cover practically identical fields-of-view. The spectrometer FOV is offset in the  $-Z$  direction (closer to the optical axis of the telescope). Chopping is done along the  $Y$  axis (left-right in this view) and also allows observation of the internal calibrators on both sides of the used area in the telescope focal plane. The maximum chopper throw for sky observations is  $\sim 3.5$  arcmin for photometry and 6 arcmin for spectroscopy. In photometry, object and reference fields are almost touching at 3.5 arcmin throw.

Figure 2.3. PACS field-of-view footprint in the telescope focal plane.

## 2.2. Common Optics

### 2.2.1. Entrance Optics

The entrance optics fulfill the following tasks: they create an image of the telescope secondary mirror (the entrance pupil of the telescope) on the focal plane chopper; this allows spatial chopping with as little as possible modulation in the background received by the instrument.

It also provides for an intermediate pupil position where the Lyot stop and the first blocking filter, common to all instrument channels, can be positioned. It allows the chopper, through two field mirrors adjacent to the used field of view in the telescope focal surface, to switch between a (chopped) field-of-view on the sky and two calibration sources (see also Figure 2.3).

The chopped image is then re-imaged onto an intermediate focus where a fixed field mirror splits off the light into the spectroscopy channel. The remaining part of the field of view passes into the photometry channels. A "footprint" of the focal-plane splitter is shown in Figure 2.3.

### 2.2.2. Calibration sources

The calibration sources are placed at the entrance of the instrument to have the same light path for the sky observation and internal calibration. This is essential for removing detector baseline drifts as well as possible, a serious task with a warm telescope and the associated high thermal background. To eliminate non-linearity or memory problems with the detector/readout system, the calibration sources are low emissivity gray-body sources providing FIR radiation loads at two slightly different signals around the level of the telescope background. This is achieved by diluting the radiation from a (small) black source with a temperature near the telescope temperature inside a cold diffusor sphere with a (larger) exit aperture. The temperature of the radiator ( $\sim 80\text{K}$ ) is stable to within a few mK.

### 2.2.3. Chopper

Differential measurements are required to extract faint signals from celestial sources from the dominant thermal background radiation of the warm (~80K) Herschel mirror. For this purpose a small tilting mirror, the chopper, flips alternately on the astronomical source and on a nearby sky position, with a variable throw up to 6 arcmin on the sky for the spectrometer and 3.5 arcmin for the photometer. This allows full separation of an object field and a reference field.

The chopper is also used to alternatively look at the two internal calibration sources (ICS) which are located at the left and right side of the instrument FOV (see Figure 2.3) for frequent calibration measurements.

The chopper is capable of following staircase waveforms with a resolution of 1", and delivers a duty-cycle of ~90% at chop frequency of 5 Hz. The chopper axis is stabilized in its central position by flexular pivots and rotated by a linear motor. The chopper design allows a low heat load in the PACS FPU.

## 2.3. Photometer

After the intermediate focus provided by the entrance optics, the light is split into the long-wavelength and short-wavelength channels by a dichroic beam-splitter with a transition wavelength of 125  $\mu\text{m}$  and is re-imaged with different magnification onto the respective Si bolometer arrays.

The blue channel offering two filters, 60-85  $\mu\text{m}$  and 85-125  $\mu\text{m}$ , has a 32x64 pixels arrays, while the red channel with a 125-210  $\mu\text{m}$  filter has a 16x32 pixels array. Both channels cover a field-of-view of ~1.75'x3.5', with full beam sampling in each band. The two short-wavelength bands are selected by two filters via a filter wheel. The field-of-view is nearly filled by the square pixels, however the arrays are made of sub-arrays which have a gap of ~1 pixel in-between.

The incident infrared radiation is registered by each bolometer pixel by causing a tiny temperature difference.

### 2.3.1. Filters

The PACS filters, in combination with the detectors, define the photometric bandpass of the instrument. There are in total 3 bands in the PACS photometer: 60-85  $\mu\text{m}$ , 85-125  $\mu\text{m}$  and 125-210  $\mu\text{m}$ . The PACS filter scheme is shown in Figure 2.4 and the filter transmission of the photometer filters in Figure 3.4.

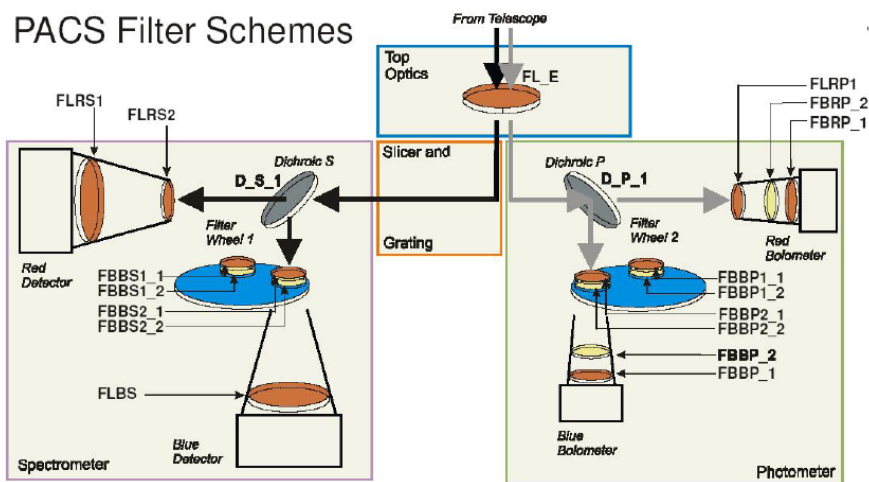
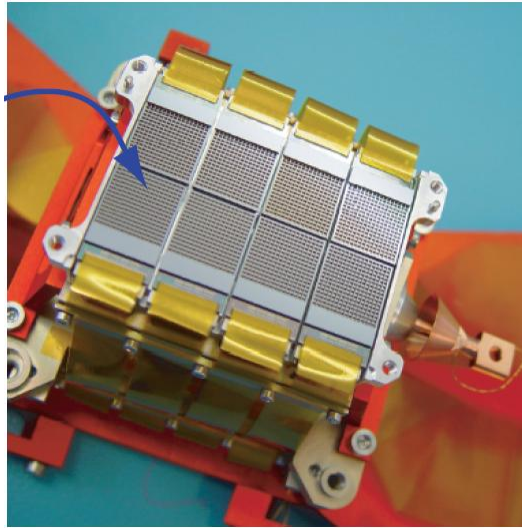


Figure 2.4. Overview of the filter arrangements in PACS. The selection of the blue photometer filter is done via commanding of the filter wheel 2.

## 2.3.2. Bolometer arrays

Figure 2.5 shows a cut-out of the 64x32 pixel bolometer array assembly. 4x2 monolithic matrices of 16x16 pixels are tiled together to form the short-wave focal plane array.



**Figure 2.5. Bolometer matrices assembly: 4x2 matrices from the focal plane of the short-wave bolometer assembly. The 0.3 K multiplexers are bonded to the back of the sub-arrays. Ribbon cables lead to the 3K buffer electronics.**

In a similar way, 2 matrices of 16x16 pixels, are tiled together for the long-wavelength focal plane array.

The matrices are mounted on a 0.3K carrier which is thermally isolated from the surrounding 2K structure. The buffer/multiplexer electronics are split in two levels; a first stage is part of the indium-bump bonded back plane of the focal plane arrays, operating at 0.3K. Ribbon cables connect the output of the 0.3K readout to a buffer stage running at 2K.

For science observations the multiplexing readout samples each pixel at a rate of 40 Hz. Because of the large number of pixels, data compression by the SPU is required. The raw data are therefore binned to an effective 10 Hz sampling rate. After that, the same lossless compression algorithm is applied as with the spectrometer data.

## 2.3.3. Cooler

The photometer operates at sub-Kelvin temperatures, which are achieved using a  $^3\text{He}$  cooler. This type of refrigerator uses porous material which absorbs or releases gas depending on the mode: cooling or heating. The use of the  $^3\text{He}$  isotope instead of the common  $^4\text{He}$  is dictated by two reasons: it is not super fluid at cryogenic temperatures below 2.2 K and it is a superior cryogen. This sorption cooler is run from a cold stage provided by the Herschel cryostat. The refrigerator contains 6 litres of  $^3\text{He}$  and can in principle be recycled infinitely, with an efficiency of more than 95% with a lifetime limited only by the cold stage from which it is run. Gas-gap heat switches, which are coupled to the Herschel 3K system with thermal straps, control the mode of operations. The evaporation of  $^3\text{He}$  provides a very stable thermal environment under constant heat load. The design of the cooler is well suited for work in space as there are no moving parts and the heat load is small.

This sorption cooler is nearly identical to the unit developed for SPIRE. It provides a stable temperature environment at 300 mK for more than 48 hours under normal observing and operational circumstances. The recycling is performed during DTCP periods, when the PACS photometer is selected for the following observing day and has a hold time of ~60h, allowing of up to 2.5 consecutive ODs of operations.

## 2.4. Spectrometer

The power emitted or absorbed by a single spectral line in the far-infrared is normally several orders of magnitudes lower than the power in the dust continuum over a typical photometric band. Sensitivity is thus the most important parameter for optimisation; with background-limited detector performance the best sensitivity is obtained if the spectrometer satisfies the following conditions: the detection bandwidth should not be greater than the resolution bandwidth, which in turn should be matched to the line width of the source, and, the line flux from the source must be detected with the highest possible efficiency in terms of system transmission, spatial and spectral multiplexing. Subtraction of the high telescope background has to be achieved by appropriate spatial and/or spectral modulation techniques.

### 2.4.1. Instrument design

The integral-field spectrometer covers the wavelength range from 51 $\mu\text{m}$  to 220 $\mu\text{m}$ , in two channels that operate simultaneously in the blue (51-105 $\mu\text{m}$ ) and red (102-220 $\mu\text{m}$ ) band. It provides a resolving power between 1000 and 4000 (i.e. a spectral resolution of  $\sim 75\text{-}300\text{km/s}$ ) depending on wavelength, for a fixed grating position the instantaneous coverage is  $\sim 1500\text{km/s}$ . It allows simultaneous imaging of a 47"x47" field of view, resolved into 5x5 pixels. An image slicer employing reflective optics is used to re-arrange the 2 dimensional field-of-view along a 1x25 pixels entrance slit for the grating, as schematically shown in Figure 2.6.

This integral-field concept with spectral and spatial multiplexing allows for the most efficient detection of weak individual spectral lines with sufficient baseline coverage and high tolerance to pointing errors without compromising spatial resolution, as well as for spectral mapping of extended sources regardless of their intrinsic velocity structure.

The grating is Littrow-mounted, i.e. the entrance and exit optical paths coincide. It is operated in first, second or third order, respectively, to cover the full wavelength range. The first order covers the range 102-210 $\mu\text{m}$ , the second order 71-105 $\mu\text{m}$ , and the third order 51-73 $\mu\text{m}$ . Anamorphic collimating optics expands the beam to an elliptical cross section to illuminate the grating over a length required to reach the desired spectral resolution. The grating is actuated by a cryogenic motor with arcsec precision which allows spectral scanning/stepping for improved spectral flat-fielding and for coverage of extended wavelength ranges. The settling time for typical motions used in the PACS-AOTs is sufficiently short to allow for grating scans at various sampling densities.

The light from the first diffraction order is then separated from the light of the two other orders by a dichroic beamsplitter and passed into two optical trains feeding the respective detector arrays (stressed/unstressed) for the wavelength ranges 102-220 $\mu\text{m}$  and 51-105 $\mu\text{m}$ . Anamorphic re-imaging optics is employed to independently match the spatial and spectral resolution of the system to the square pixels of the detector arrays. The filter wheel in the short-wavelength path selects the second or third grating order.

It is possible to operate both spectrometer detector arrays simultaneously. For wide scans, full spectra can so be obtained in both selected grating orders. In a spectral line mode in the grating order-of-interest, the other array yields narrow-band continuum data, or in suitably line-rich sources, serendipitous lines.

### 2.4.2. Image slicer

The image slicer's main function is to transform the 5x5 pixel image at its focal plane into a linear 1x25 pixel entrance slit for the grating spectrometer. The slicer assembly consists of 3 set of mirrors:

- The *slicer stack*: 5 identical spherical field mirrors, individually tilted, which forms separate pupil images for each "slice" on the set of 5 capture mirrors.
- The *capture mirrors* re-combine the separate beams into the desired linear image on the set of 5 spherical mirrors at the exit of the slicer assembly.

- The *field mirrors* at the exit re-combine the pupils separated in the slicer into a common virtual pupil. The collimators of the spectrometer will later form an (anamorphic) image of this virtual pupil onto the grating. At the same time, the field mirror apertures serve as the entrance slit of the grating spectrometer.

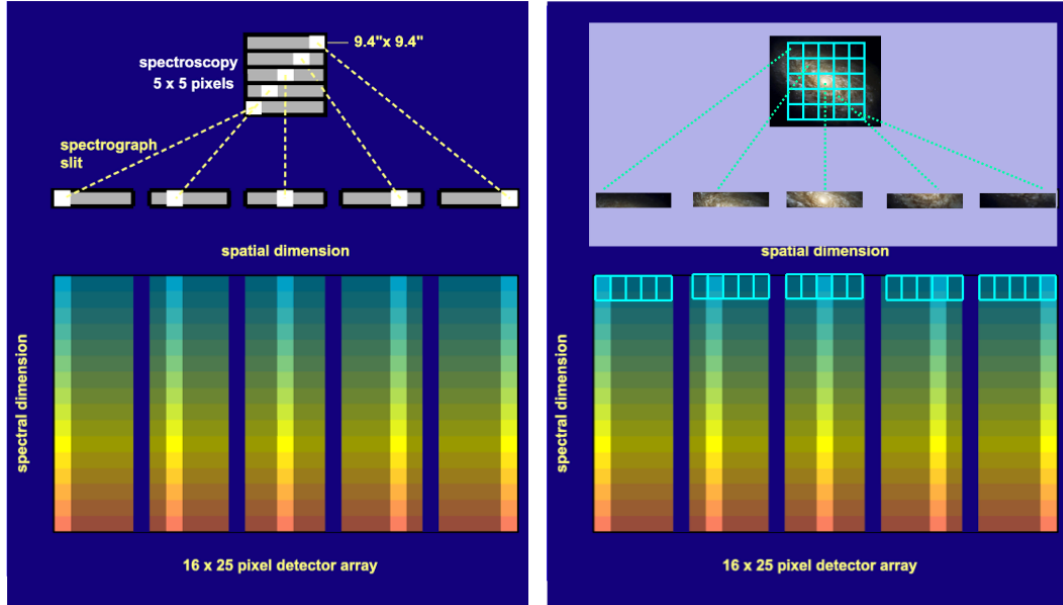
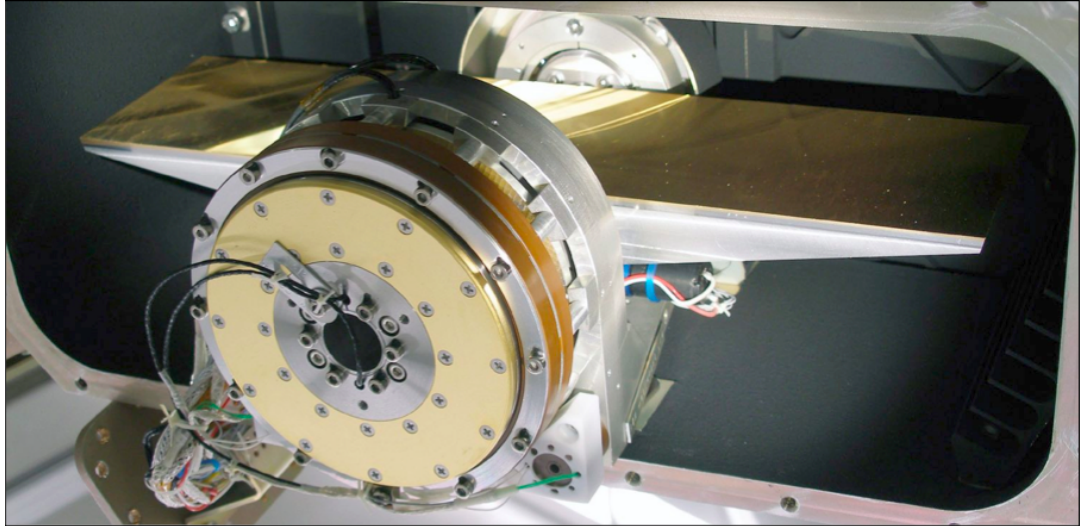


Figure 2.6. Integral-field spectrometer concept : projection of the focal plane onto the detector arrays in spectroscopy mode. The image slicer re-arranges the 2D field along the entrance slit of the grating spectrograph such that, for all spatial elements in the field, spectra are observed simultaneously. Note, the blank space left between the slices to reduce crosstalk between left- and rightmost pixels of adjacent slices (see also Figure 2.9 ). On the right-hand side the spatial slicing scheme is illustrated by the image of an extended structure.

### 2.4.3. Grating

The grating assembly consists of a Littrow-mounted grating, a mounting bracket that interfaces with the FPU structure, the actuator with redundant coils that provides positioning of the grating, the redundant position sensors, a launch lock mechanism with redundant coils for the launch lock actuator, the redundant temperature sensors and the duplicated cryo-harness (see Figure 2.7).



**Figure 2.7. Flight model grating unit. A torquer motor is used to actuate the grating angle which is measured with sub-arcsecond precision by an inductosyn angular resolver.**

The grating blank has a length of 320mm with a groove period of  $8.5 \pm 0.05$  grooves/mm, with a total of approximately 2720 grooves. The reflection grating is operated in the first (102-210  $\mu\text{m}$ ), the second (72-102  $\mu\text{m}$ ) and the third diffraction order (51-72  $\mu\text{m}$ ). Grating deflections from 25 degrees to 70 degrees are possible to cover the full wavelength range of each order. A graphical correlation of the grating angle of incidence versus order and wavelength is given in Figure 2.8.

Grating angle – wavelength relation in Littrow configuration

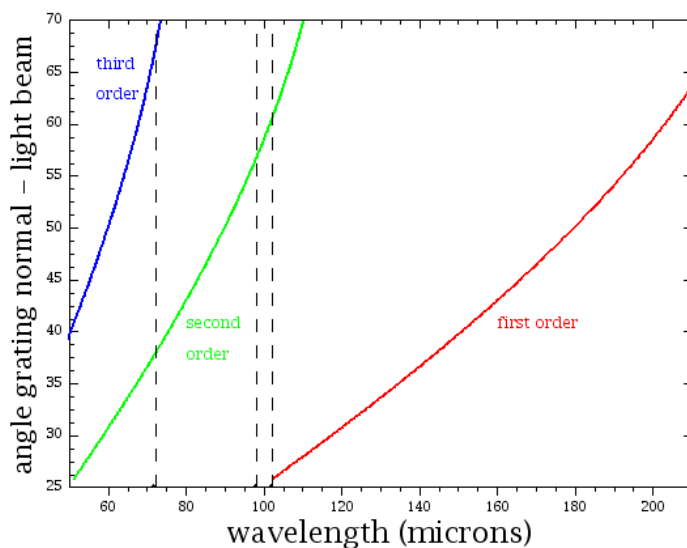


**Figure 2.8. Relation between grating angle and wavelength**

## 2.4.4. Order sorting Filters

The PACS order sorting filters enable the spectral purity of the selected band by suppressing contributions by other orders the detector is sensitive to. There are in total 3 bands in the PACS spectrometer: 55-72  $\mu\text{m}$ , 72-102  $\mu\text{m}$  and 102-210  $\mu\text{m}$ . The filter transmission is shown in Figure 4.3. The filter train of both the photometer and spectrometer channels is illustrated in Figure 2.4.

## 2.4.5. Photoconductor arrays

The spectrometer employs two Ge:Ga photoconductors arrays (low and high stressed) with 16x25 pixels on which the 16 spectral elements of the 25 spatial pixels are imaged.

The Ge:Ga photoconductor arrays have a modular design: they are made of 25 linear modules of 16 pixels each are stacked together to form a 2-dimensional array. Ge:Ga photoconductors are sensitive in the wavelength range 40-110/120  $\mu\text{m}$  without any stress. A stress is therefore applied to improve the long wavelength sensitivity. The stressing mechanism ensures homogeneous stress on each pixel along the entire pile of 16 spectral elements. The low-stressed blue detectors has a mechanical stress on the pixels which is reduced to about 10% of the level needed for the long-wavelength response of the red detectors.

Light cones in front of the actual detector block provide an area-filling light collection in the focal plane and feed the light into the individual integrating cavities around each individual, mechanically stressed detector crystal. The light cones also act as a very efficient means of straylight suppression because their solid angle acceptance is matched to the re-imaging optics such that out-of-beam light is rejected.

Responsivity measurements of both stressed and unstressed modules show sufficiently homogeneous spectral and photometric response within each module and between modules. Absolute responsivity calibration for optimum bias under in-orbit conditions is under way and will most likely give numbers of  $\sim 10$  A/W for the unstressed detectors and  $\sim 40$  A/W for the stressed detectors. The detectors are operated at (stressed) or slightly above (unstressed) the “Level 0” cryostat temperature ( $\sim 1.65$  K). Each linear module of 16 detectors is read out by a cryogenic amplifier/multiplexer circuit (CRE) in CMOS technology. The readout electronics is integrated into the detector modules, but operates at “Level 1” temperature (3...5 K). Measurements of the NEP of both arrays after integration into the instrument flight model at characteristic wavelengths and with representative flux levels have confirmed the performance measured at module level. Only a small fraction of pixels suffers from excess noise. Median NEP values are  $8.9 \times 10^{-18} \text{WHz}^{-1/2}$  for the stressed and  $2.1 \times 10^{-17} \text{WHz}^{-1/2}$  for the unstressed detectors, respectively. The achievable in-orbit performance was expected to depend critically on the effects of cosmic rays on the detector response. Proton irradiation tests performed at the synchrotron source of the Universite Catholique de Louvain (Louvain la Neuve, Belgium) complemented by a  $\gamma$ -ray radiation test programme at MPIA indicated that NEPs close to those measured without irradiation should actually be achievable in flight. In-flight measurements performed during the commissioning phase of Hershel confirmed these findings.



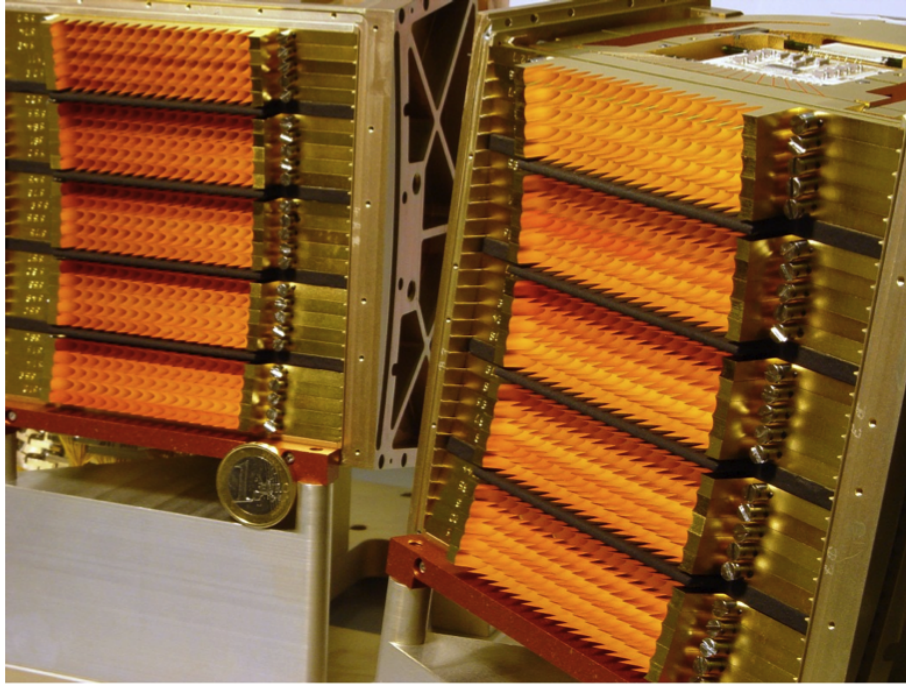


**Figure 2.9. Array close-ups: The 25 stressed and low-stress modules (corresponding to 25 spatial pixels) in the red- and blue arrays are integrated into their housing. Stress is applied to the whole stack of 16 Ge crystals, providing the instantaneous spectral coverage for each of the 25 spatial fields on the sky. Light cones provide for area-filling collection onto the individual detectors.**

Each module is attached to an 18 channel cold readout electronics (CRE) amplifier/multiplexer circuit in CMOS technology. The photocurrent from the detector crystals is integrated on a capacitor. The capacitance is switchable between 4 values from 0.14 to 1.15pF to provide sufficient dynamic range for the expected flux range. The integration process is reset after preset interval. During the integration the voltage signal is regularly read in a non-destructive way with a frequency of 1/256s leading to an integration ramp with 256 / (reset interval) samples.

The extensive PV program aimed at optimising the AOT parameters led to ramps of 32 samples, i.e. 1/8 second, for all all spectrometer AOTs. The scientific signal corresponds to the slope of these integrating ramps, and, for bandwidth reasons, these are fitted on-board. Hence, a spectrometer observation of n seconds always results in 18 x 25 x 8n samples for each camera, i.e. red and blue: 18 spectral pixels for each of the 25 spaxels, each providing 8 measures per second.

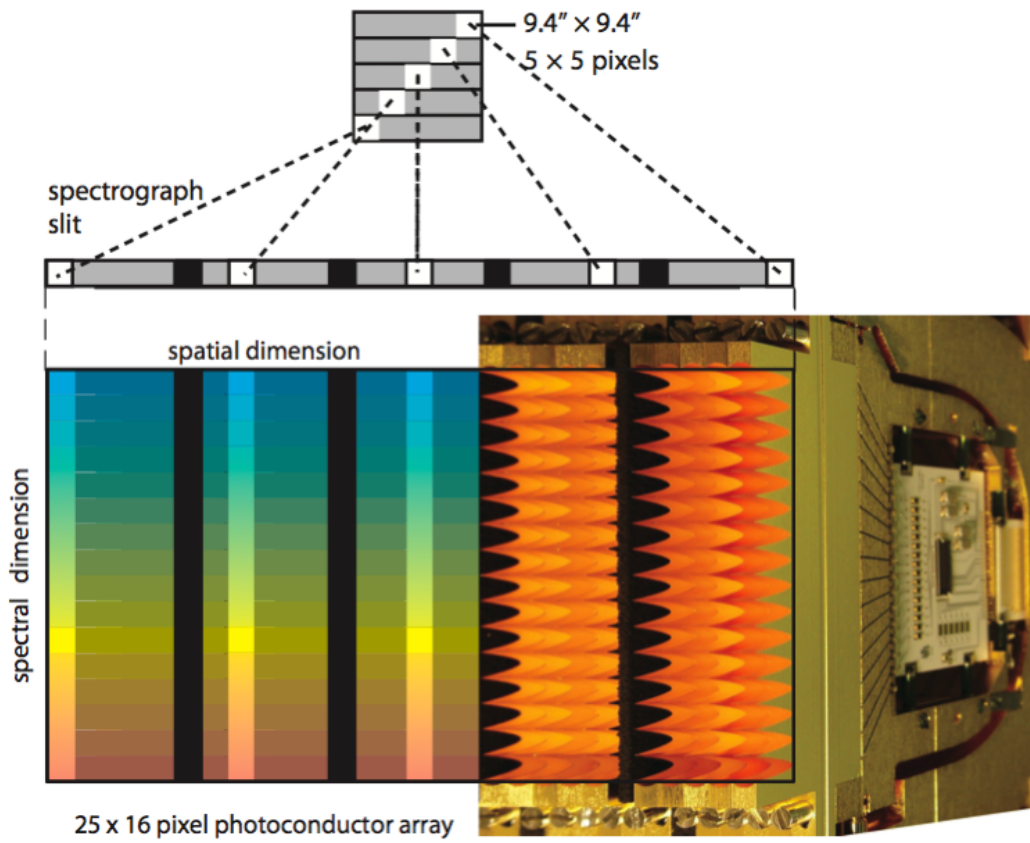


Figure 2.10. The optical image slicer re-arranges the 2-dimensional field along the entrance slit of the grating spectrograph such that for each spatial element in the field of view, a spectrum can be simultaneously observed with a 2D detector array. On the right, part of the red photoconductor array with its area-filling light-cones and CREs are shown scaled to the schematic picture of the 25 by 16 array.

---

# Chapter 3. PACS photometer scientific capabilities

## 3.1. Point spread function

The photometer optics delivers diffraction-limited image quality (Strehl ratio >95%). Therefore PACS preserves the image quality provided by the Herschel telescope and is diffraction-limited on its whole energy range. The photometer PSF (see Figure 3.1) is dominated by the telescope and characterised by:

- A narrow core which is round in the blue bands but slightly elongated in spacecraft Z direction in red.
- A tri-lobe pattern seen at the several % level in all bands, most clearly in the blue with its strongest signal, and ascribed to imperfect mirror shape due to the secondary mirror tripod.
- Knotty structure at sub-percent level, clearly seen in blue and indicated in green.

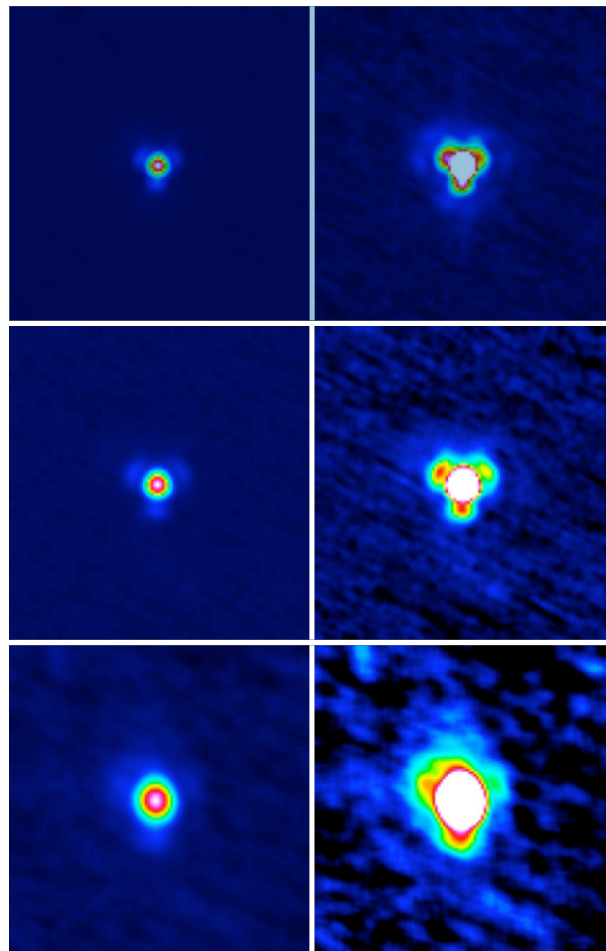


**Figure 3.1.** The photometer PSF in blue, green and red (top to bottom) derived from scans performed at 10 arcsec/s. Left-hand panels display the image with a linear scale up to the peak, while right-hand panels show up to 10% of the peak.

For fast scans in normal and parallel mode, this PSF structure is smeared by detector time constants

and data averaging. Quantitative information on the PSF is given in Table 1.

These PSFs and derived quantities reflect the intrinsic optical quality of Herschel+PACS. In a scan-map reduction they will be very slightly smeared, in particular at short wavelengths, because of the data averaging on-board (from 40Hz to 10Hz sampling), but also due to detector time constants telescope pointing jitter and drifts. For more detailed information on the PACS photometer PSF we refer to the PACS technical note [PICC-ME-TN-033](#) (version 0.3, Nov. 10, 2009)

The photometer focal plane geometry, initially established on ground by scanning a back-illuminated hole mask across the bolometer arrays, has been adapted to the actual telescope by optical modeling. The in-flight verification required a small change in scale and a slight rotation to fit to the results of a 32x32 raster on the star  $\alpha$ Her. In particular these measurements also show that the possibilities to further improve the calibration of detailed distortions are limited by short-term pointing drifts of the satellite. Residual measured inter-band offsets between blue/green (0.3 arcsec) and green/red (1.2 arcsec) have been characterised and are implemented in the astrometric processing chain. Current best point spread functions (PSF) have been determined on asteroid Vesta. The observed 3-lobe structure of the PSF (Figure 3.1) can be explained qualitatively by the secondary mirror support structure and has been verified in detail by ray tracing calculations taking the telescope design and known wave-front errors into account. The spatial resolution, expressed as encircled energy as a function of angular separation from PSF centre, is in reasonable agreement with expectations from telescope and instrument design.

**Table 3.1. Results of fitting 2-dimensional gaussians to the PSF. Note these are fits to the full PSF including the lobes/wings. Position angles (east of North) are listed only for beams with clearly elongated core. The scan angle was 63 degrees for these observations.**

| Band  | Speed (arcsec/s)   | FWHM (arcsec) | PA (deg) |
|-------|--------------------|---------------|----------|
| Blue  | 10                 | 5.26 x 5.61   |          |
|       | 20                 | 5.46 x 5.76   |          |
|       | 60                 | 5.75 x 9.0    | 62.0     |
|       | 60 (parallel mode) | 5.86 x 12.16  | 63.0     |
| Green | 10                 | 6.57 x 6.81   |          |
|       | 20                 | 6.69 x 6.89   |          |
|       | 60                 | 6.89 x 9.74   | 62.3     |
|       | 60 (parallel mode) | 6.98 x 12.7   | 63.0     |
| Red   | 10                 | 10.46 x 12.06 | 7.6      |
|       | 20                 | 10.65 x 12.13 | 9.3      |
|       | 60                 | 11.31 x 13.32 | 40.9     |
|       | 60 (parallel mode) | 11.64 x 15.65 | 53.4     |

Further details on the PACS PSF can be found in the technical note [PICC-ME-TN-033 Version 1.01](#). The aperture correction factors for the are listed in the table in section Table 3.2.

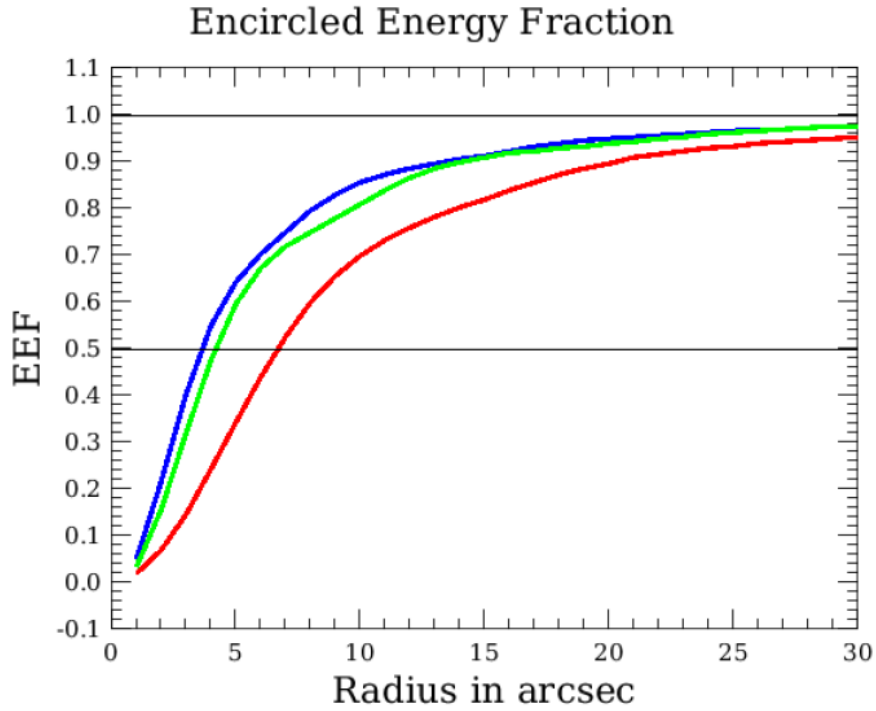


Figure 3.2. Encircled energy fraction as a function of circular aperture radius for the three bands. Derived from slow scan OD160 Vesta data. The EEF fraction shown is normalized to the signal in aperture radius 60 arcsec, with background subtraction done in an annulus between radius 61 and 70 arcsec.

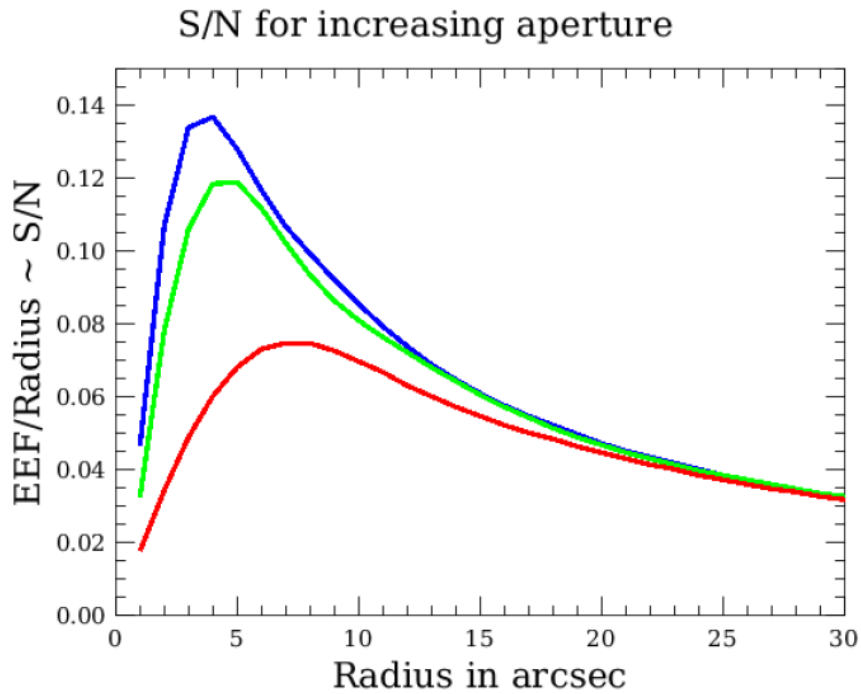


Figure 3.3. The signal-to-noise curve under the assumption that noise scales linearly with aperture radius. Note that this assumption is not met for scanmaps with  $1/f$  noise.

**Table 3.2.** Encircled energy fraction as a function of circular aperture radius for the three bands. Derived from slow scan OD160 Vesta data in the three photometer bands. The EEf fraction shown is normalized to the signal in aperture radius 60 arcsec, with background subtraction done in an annulus between radius 61 and 70 arcsec.

| Radius (arcsec) | EEF blue | EEF green | EEF red |
|-----------------|----------|-----------|---------|
| 1               | 0.047    | 0.032     | 0.018   |
| 2               | 0.214    | 0.156     | 0.069   |
| 3               | 0.402    | 0.318     | 0.146   |
| 4               | 0.548    | 0.474     | 0.241   |
| 5               | 0.642    | 0.595     | 0.341   |
| 6               | 0.701    | 0.672     | 0.438   |
| 7               | 0.750    | 0.718     | 0.524   |
| 8               | 0.794    | 0.749     | 0.597   |
| 9               | 0.830    | 0.778     | 0.656   |
| 10              | 0.856    | 0.809     | 0.700   |
| 12              | 0.886    | 0.866     | 0.759   |
| 14              | 0.904    | 0.900     | 0.801   |
| 16              | 0.922    | 0.917     | 0.838   |
| 18              | 0.938    | 0.928     | 0.871   |
| 20              | 0.949    | 0.938     | 0.897   |
| 25              | 0.966    | 0.963     | 0.934   |
| 30              | 0.976    | 0.977     | 0.953   |
| 40              | 0.988    | 0.989     | 0.982   |
| 50              | 0.995    | 0.997     | 0.995   |
| 60              | 1.0      | 1.0       | 1.0     |

## 3.2. Photometer filters

The transmission of the filter chain in each of the instrument channels has been calculated from measurements of the individual filters. All filters have been measured at room temperature; some filters or samples taken from the same filter sheet as used for the flight filter have also been measured in a contact gas cryostat near Helium temperature. Generally, filters show a small gain in transmission at cryogenic temperatures, but since not all of the actual filters could be measured we assume their ambient temperature performance as a good and somewhat conservative estimate. The filter transmission curves for the three photometer bands are plotted in Figure 3.4. The photometer transmission curves are available in HCSS as *PCalPhotometer\_FilterTransmission\_FM\_v1.fits* and the bolometer response in the *PCalPhotometer\_Absorption\_FM\_v2.fits*.

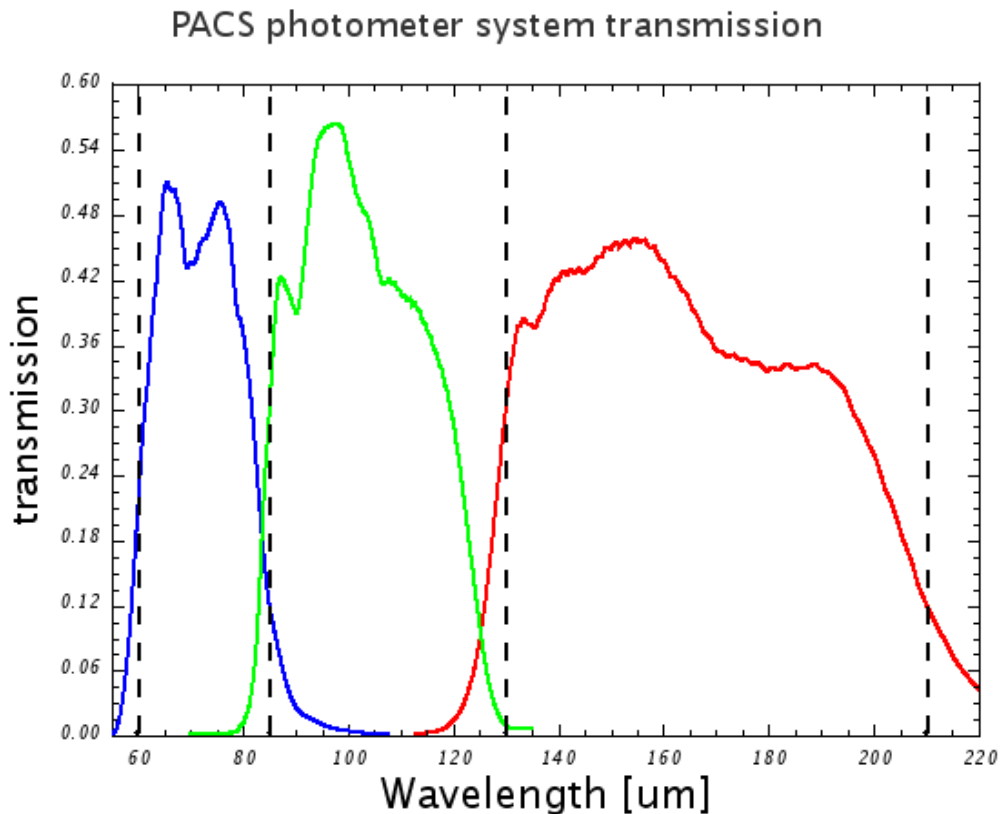


**Figure 3.4.** Filter transmissions of the PACS filter chains. The graph represents the overall transmission of the combined filters with the dichroic and the detector relative response in each of the three bands of the photometer. The dashed vertical lines mark the original intended (design values) of the band edges.

The reference wavelengths chosen for the 3 photometer filters are **70, 100 and 160 μm**. These rounded values are close to the wavelengths that minimize the colour correction terms with the flight model filters.

No indications of any near- or mid-infrared filter leakage could be identified. Required colour-corrections for the photometric PACS reference wavelengths (70, 100, 160 μm) which have been determined from the photometer filter transmission curves and bolometer responses (See Figure 3.4) are quite small. Suitable corrections factors for a wide sample of SED shapes can be found in Poglitsch et al. (2010).

### 3.3. Photometer flux calibration

The absolute flux calibration of the photometer is based on models of standard stars in the 0.6-15 Jy flux range in the three filters:  $\alpha$ Boo (Arcturus),  $\alpha$ Tau,  $\alpha$ CMa (Sirius),  $\alpha$ Ceti &  $\gamma$ Dra (see Dehaes et al. 2010) and on thermophysical models for a set of more than 10 asteroids (Müller & Lagerros 1998, 2002), building up on similar approaches for ISOPHOT (Schulz et al. 2002) and Akari-FIS (Shirahata et al. 2009). Together they cover a flux range from below 100 mJy up to 300 Jy. Both types of sources agree very well in all 3 PACS bands, and the established absolute flux calibration is consistent within 5%. Neptune and Uranus with flux levels of several hundred Jansky are already close to the saturation limits, but have been used for flux validation purposes. At those flux levels, a reduction in response of up to 10% has been observed. For comparison, the latest FIR flux model of Neptune is considered to be accurate to better than 5% (Raphael Moreno, priv. comm. & Fletcher et al. 2010).

For the 5 primary PACS standard stars, the measured absolute flux accuracy is within 5% of pre-

dicted values (Aussel et al. 2010) in the blue and green filters, and within 10% of the predicted values in the red filter. For the full set of primary and secondary standards, the measured absolute flux accuracy is within 10% in the blue and green, and better than 20% in the red filter.

Absolute flux calibration uncertainties should improve over the mission, with better statistics of available celestial calibration observations.

The calibration itself comprises: (i) flat-fielding, (ii) responsivity correction -- conversion of engineering units, volts, to Jy/pixel, and (iii) gain drift correction to account to small drifts in gain with time.

The flux calibration of the PACS photometer assumes:

- that the detectors are linear in the full dynamic flux range observable by PACS.
- a spectral convention of  $\nu * F_{\nu} = \text{constant}$  & reference filter wavelengths at 70, 100 and 160 $\mu\text{m}$ .
- a set of celestial flux calibrators that are mostly stars and asteroids for which model spectra are available that allow either color-correction of the measured spectral densities in order to compare them with the predicted monochromatic model fluxes or computation of the expected measured spectral densities.

## 3.4. Photometer bad pixels

The flight model bolometer blue array displays about 2% of dead pixels (or very low responsivity pixels), including one row of 16 pixels, as can be seen on Figure 3.5 and Figure 3.6 in the upper right matrix.

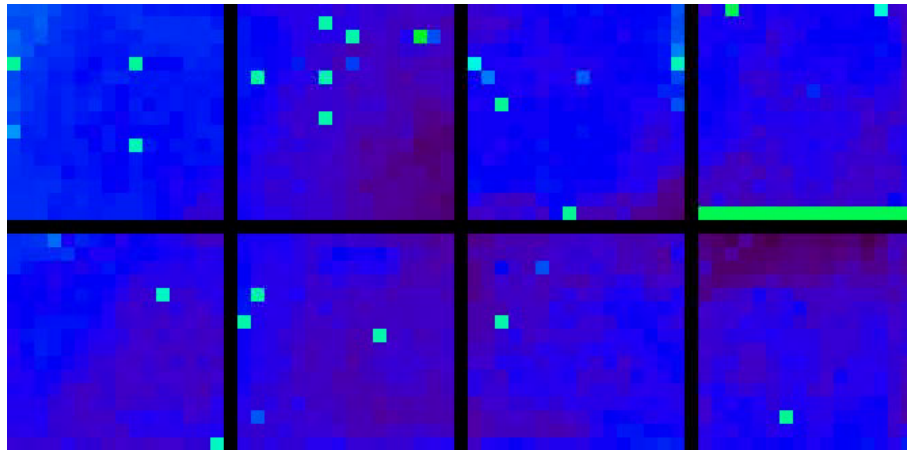


Figure 3.5. FM blue array with low illumination



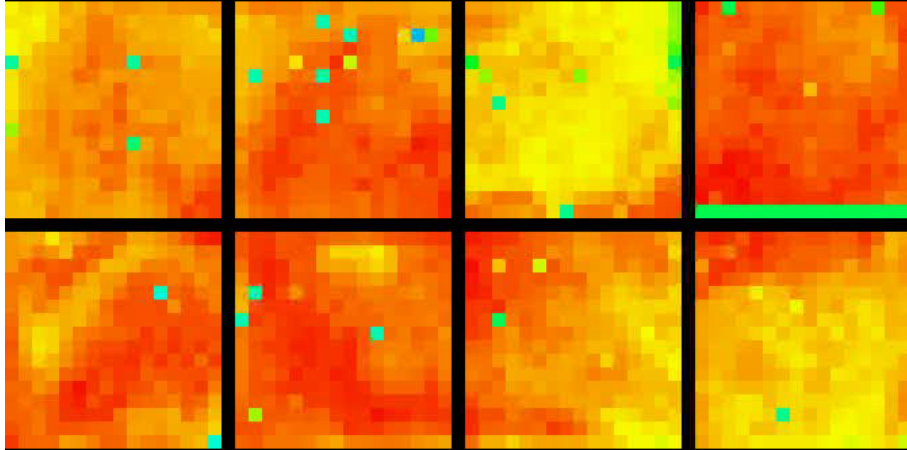


Figure 3.6. FM blue array with high illumination

### 3.5. Photometer sensitivity

The photometer sensitivity is driven by the foreground thermal noise emission, mostly from the telescope and the electrical noise of the readout electronics.

The point-source sensitivities have been updated in HSpot 5.0 to the in-flight measured sensitivities on deep fields maps. However, the achieved sensitivity is a strong function of data processing and scan strategy.

The given sensitivities in Table 3.3 refer to scan maps processed with a high-pass filtering, with a very short width (typically a half-width of 16 in the blue/green bands and 25 in the red band) to mitigate the effect of 1/f noise and gain/detector responsivity drifts in time, at the expense of removing any extended emission beyond the scale of this filter length. Maps processed with MADmap, which preserve extended emission at any scale, cannot reach this sensitivity yet.

Based on in-flight performance, we recommend that observers:

- Use the medium (20"/sec) scan speed to get optimum point-source sensitivity. The fastest (60"/sec) scan speed should be used if a wide area is to be mapped.
- Use concatenated cross-scans for observations that cannot benefit from high-pass filter reductions (e.g. fields with spatially complex, extended and diffuse emission). The cross-scans are also useful to obtain higher photometric accuracy for faint sources.

Table 3.3. PACS photometer sensitivity

| central wavelength                        | 70 $\mu$ m | 100 $\mu$ m | 160 $\mu$ m |
|---|------------|-------------|-------------|
| scan mapping 1 $\sigma$ -1second (mJy)    | 30.6       | 36.0        | 68.5        |
| mini-scan mapping 5 $\sigma$ -1hour (mJy) | 4.7        | 5.5         | 10.5        |

To a first order the sensitivity in all mode scales with the inverse of the square root of the on-source observation time. This scaling is used for the sensitivities and S/N ratios reported by HSpot.

The on-array chopping technique is only used in point-source photometry mode : the sensitivity reached is worse than in min-scan mapping mode as the  $1/f$  noise cannot be filtered out by chopping at 0.8Hz as efficiently as in the spatial modulation of the scan mapping. See chapter 4 for more information on the observing modes.

## 3.6. Astrometric accuracy

The absolute pointing accuracy for Herschel is measured to be 2 arc-seconds at the 1-sigma level on pointed observations. However, some larger deviations, as large as 5 arc-seconds (solid shift), have been reported for some scan map observations. Deviations of the actual telescope pointing from the scan legs (great circles in the sky) that is reported in the pointing product cause a smearing of the PACS PSF in the reconstructed scanmap, in particular in the blue/green bands. The jittering along scan legs is estimated to be usually around 1 arcsec level, therefore the effect is rather small even in the blue band.

The scan speed profile sometimes exhibits significant bumps above the average speed, see example in Figure 3 on two different scan legs. These events are relatively rare. The cause of these jumps has been traced down to warm star tracker (STR) CCD pixels. When a guide star of 5-6 magnitude approaches such a pixel, the STR gets confused, producing a wrong attitude estimate. During the speed bump the attitude is unreliable and could be up to several tens of arcsec off.

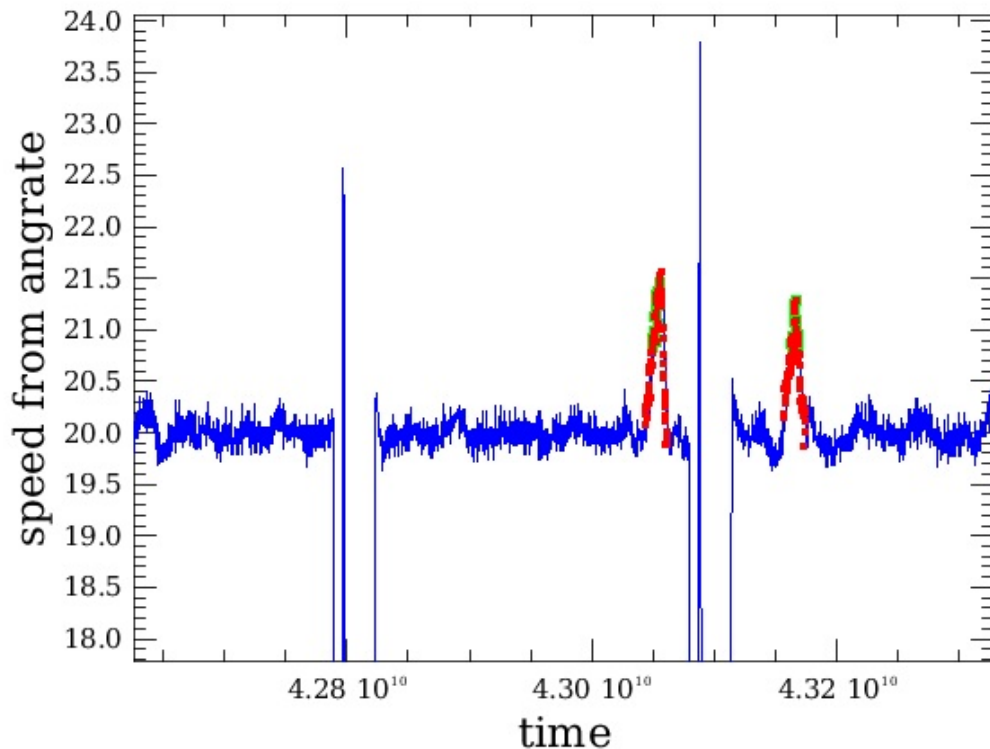


Figure 3.7. Example of two 'speed bumps' in a scan map at 20 arcsec/s scan speed

The time interval during the speed bumps shall currently not be used in the map projection. HSC is investigating methods to propagate the gyroscope angular rate to reconstruct the right attitude during these bump.

The STR CCD temperature was lowered since OD320 to mitigate the effects of these warm pixels, no obvious speed bump has been observed since.

---

# Chapter 4. PACS spectrometer scientific capabilities

## 4.1. Diffraction Losses

The image slicer is the most critical element of the PACS optics, in the figures below the effect of diffraction/vignetting by the entrance field stop and Lyot stop have been included. For the Lyot stop a worst-case loss of 10% is used. For the losses in the spectrometer the fraction of power arriving at the detector is shown in Figure 4.1.

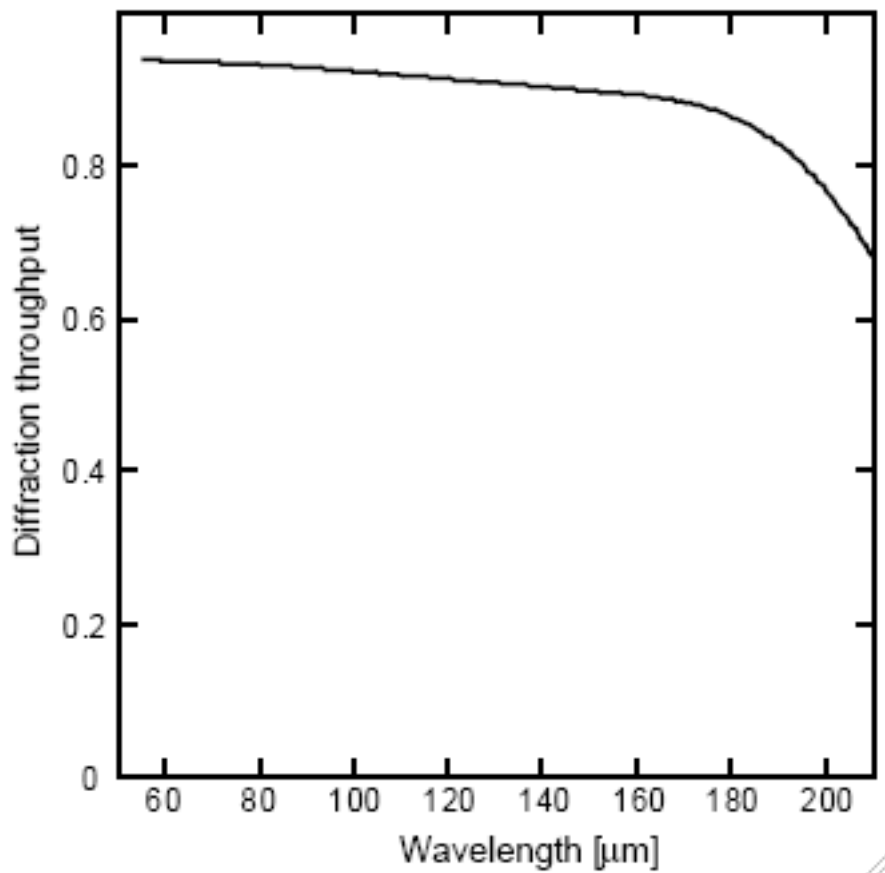


Figure 4.1. Diffraction throughput of the spectrometer optics; the diffraction losses mainly occur in the image slicer.

## 4.2. Grating efficiency

The calculated grating efficiency, i.e. the fraction of the incident power that is diffracted in the used grating order, as a function of wavelength, is shown in Figure 4.2.

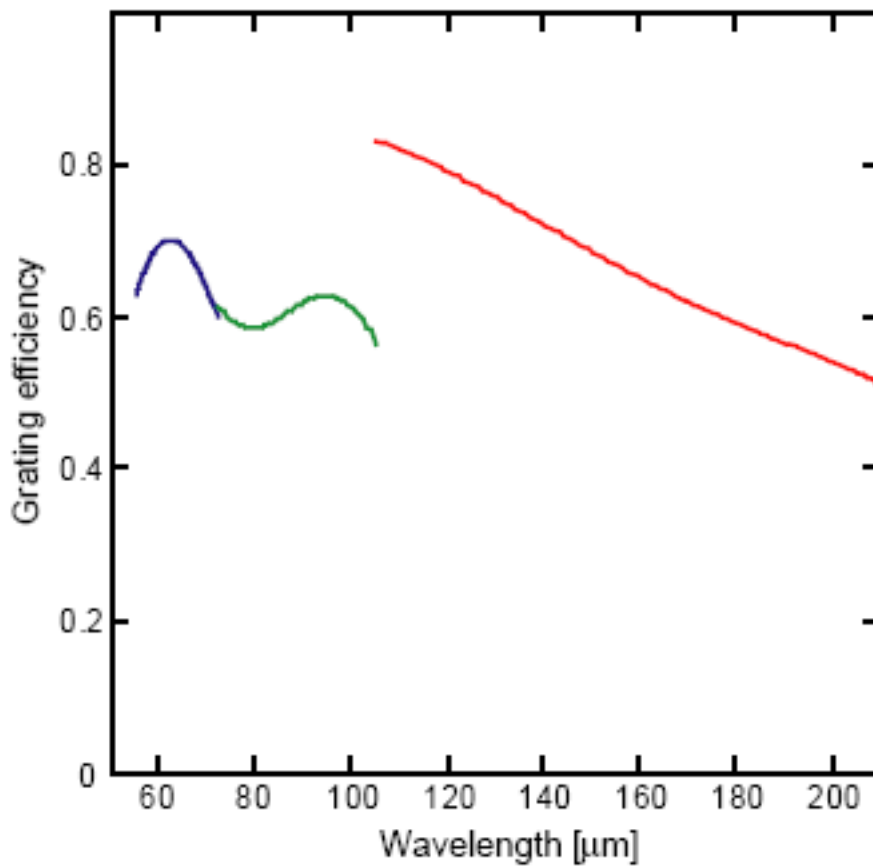


Figure 4.2. Calculated PACS grating efficiency.

### 4.3. Spectrometer filters

The transmission of the filter chain in each of the instrument channels has been calculated from measurements of the individual filters (see Photometer filters section). The filter transmission curves for the three grating orders are plotted in Figure 4.3.

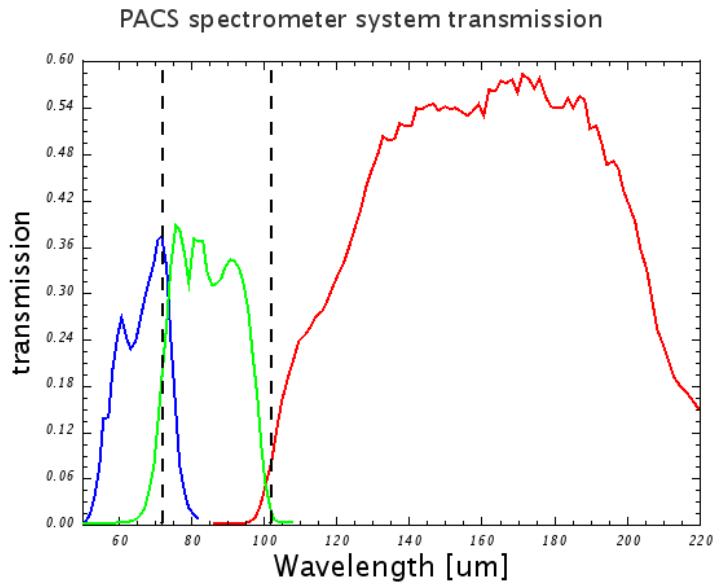


Figure 4.3. Transmissions of the spectrometer filter chains. The graph represents the overall transmission of the combined filters in each of the three grating orders of the spectrometer. The vertical lines mark the edges between spectral bands.

## 4.4. Spectrometer relative spectral response function

The relative spectral response function (RSRF) gives the combined system efficiency including filter transmission and detector sensitivity. The on-ground measured RSRF, during PACS flight-module black-body measurements is displayed in Figure 4.4. Besides the overall trend of the RSRF, one of the most important issue is to calibrate with a high accuracy the ripples on short wavelength scales. It is particularly important for faint line detection and identification. The RSRF is very stable over the mission lifetime, however, an updated version will be made available to PACS observers if it is appropriate.

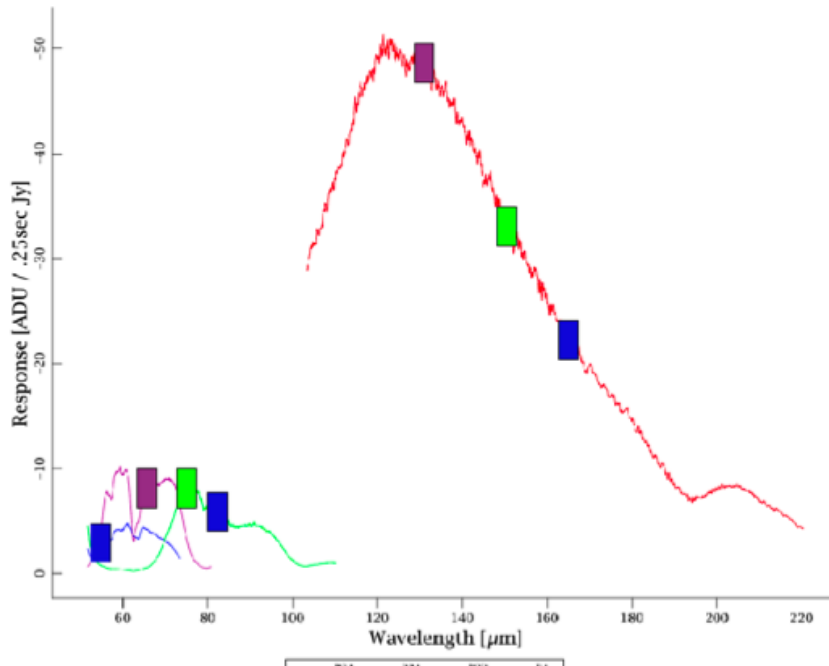


Figure 4.4. PACS spectrometer relative spectral response function measured on-ground, colored signs show the key wavelengths measured in the calibration block of every single observation.

The wavelength dependence of the absolute response of each spectrometer pixel is characterised by an individual relative spectral response function. Since this calibration file has been derived from the extended laboratory black-body measurements, its application to point sources requires additional diffraction corrections. The required correction curve is provided in Figure 4.5; however, partly extended sources may consequently show deviating spectral shapes according to their size and morphology (see more in Section 4.9).

In the data reduction environment (HIPE), this curve is available as a calibration product. For a point-source, the flux derived from the central spaxel of the 5x5 intergral-field array has to be multiplied by the correction factor at the corresponding wavelength. This flux represents the total line flux of the source, however, for (slightly) extended sources the total flux must be extracted from the 25 spaxels even if S/N is lower for the neighbouring spaxels comparing to the central one.

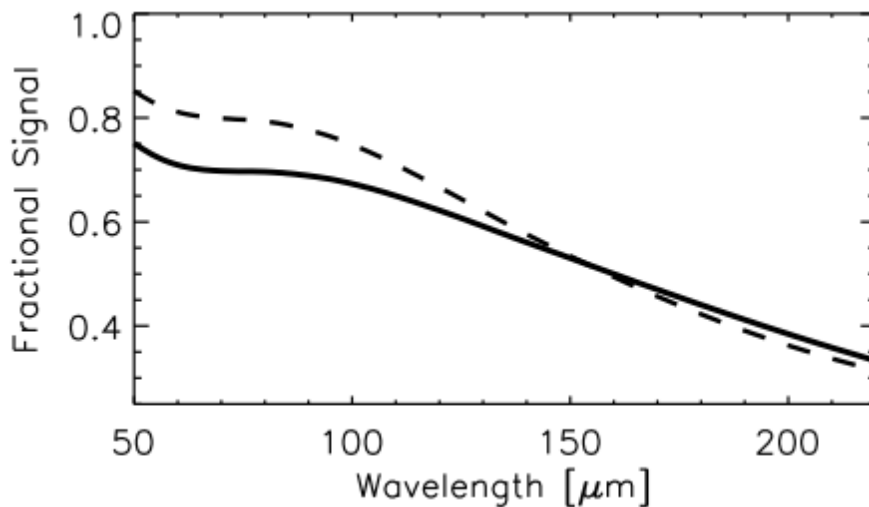


Figure 4.5. Point source correction: The fraction of signal seen by the central PACS spectrometer spaxel.

Dashed line: theoretical calculation from idealised PSF; solid line: 3rd order polynomial fit to results from rasters on Neptune.

## 4.5. Spectrometer field-of-view and spatial resolution

The spectrometer, and in particular its image slicer, is used over a large wavelength range. The photometer pixel size of 9.4x9.4 arcseconds is a compromise between resolution at short wavelengths and observing efficiency (mapped area) at long wavelengths. The principle of integral field spectroscopy is illustrated in Figure 2.6. Full spatial sampling requires a fine raster with the satellite, for spectral line maps with full spatial resolution. For the sensitivity calculation this is neglected as the line flux will always be collected with the filled detector array.

It was confirmed during the Performance Verification Phase that no flux is lost in the integral-field unit, i.e. point source flux can be fully recovered from a single pointing if the source photocenter is on the central spaxel. Although the observed noise level is varying over the 5x5 field-of-view, the flux can be recovered by integrating over the neighbouring spaxels.

The spatial calibration of the PACS spectrometer section consists of the detailed characterization of the relative locations on the sky of the 5x5 spatial pixels (“spaxels”) in the blue and red sections and for all operational chopper positions ( $\pm 3'$ ,  $\pm 1.5'$ ,  $\pm 0.5'$ ,  $0'$ ). Detailed extended rasters on point sources (HIP21479 and Neptune) have been carried out during the Performance Verification Phase at a few wavelengths and the resulting spaxel geometries are stored as calibration files within the data processing environment (HIPE). Figure 4.6 shows, as an example, the result for chopper position zero in relative spacecraft units with respect to the virtual aperture of the PACS spectrometer, which is defined as the central pixel of the blue field of view. Asymmetrical optical distortions between chopper on and off positions cause unavoidable slight misalignment (smaller than 2") for individual spaxels between spacecraft nod A and B within the double differential data acquisition scheme.

As shown on Figure 4.7 the apparent field-rotation becomes larger with increasing chopper throw.

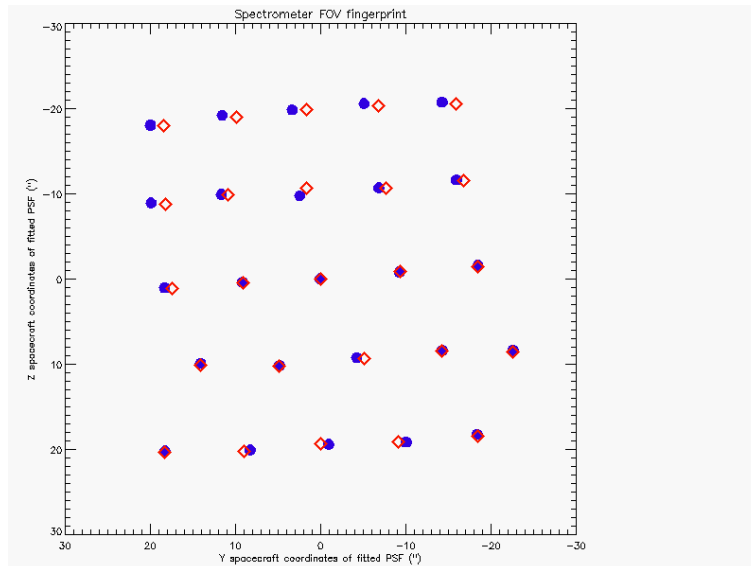


Figure 4.6. Spectrometer field of view for blue (circles) and red (squares) spaxels in spacecraft Y and Z coordinates for chopper position zero.

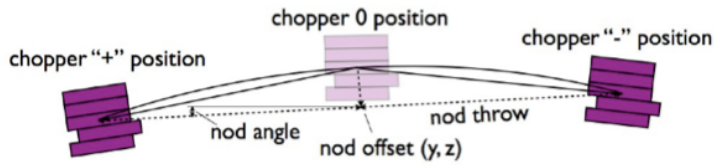


Figure 4.7. Apparent field rotation for the two chopper positions in a symmetric chopper pattern.

## 4.6. Spectrometer Point Spread Function (PSF)

### 4.6.1. Measured vs. model PSF

A further result of extended rasters on Neptune has been the verification of the point spread function of the spectrometer. Remarkable agreement with predictions from telescope and instrument modeling has been found. A measurement for a typical spatial pixel of the PACS spectrometer can be compared in Figure 4.8 and Figure 4.9 to a convolution of a calculated PSF (from actual telescope model including known wave-front errors) with a square pixel of 9.4"x9.4".

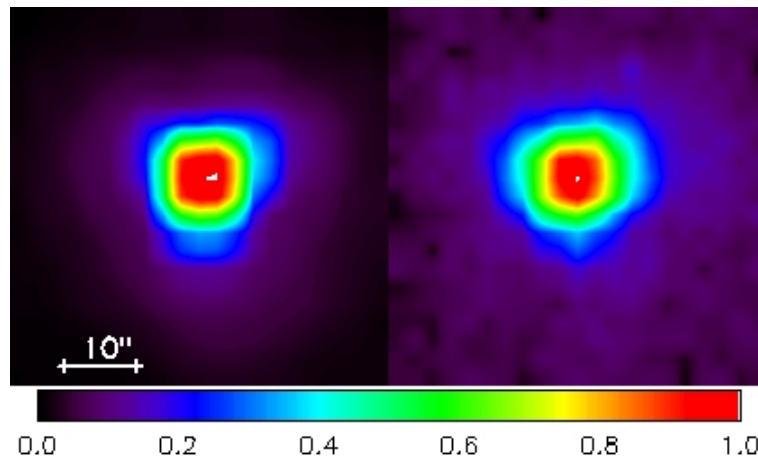


Figure 4.8. Calculated spectrometer PSF at 62  $\mu\text{m}$  (left) and measurement on Neptune (right) done at the same wavelength. Both are normalised to the peak and scaled by square-root, to enhance the faint wing pattern. The calculation includes the predicted telescope wave-front error, which dominates the overall aberrations.

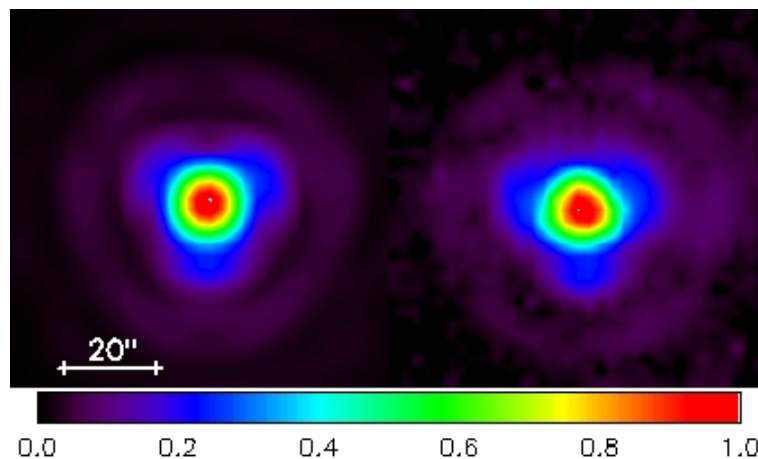




Figure 4.9. Same as Figure 4.8 at 124  $\mu\text{m}$ .

## 4.6.2. Detector sampling of the PSF

The PACS spectrometer spaxels sample a part of the PSF delivered by the Herschel telescope. The telescope PSF becomes larger with wavelength, and shows substantial departure from a Gaussian profile due to the telescope wavefront errors, mainly caused by the three-point mount of the telescope dish. At different wavelengths, different fractions of the PSF structure are seen by the different spaxels. This is illustrated in Figure 4.10. Given the pointing accuracy of the spacecraft, this means that the fraction of the PSF falling onto the central spaxel can vary substantially. This is presently the main limitation of the flux calibration. The full wavelength-dependent characterisation of the PSF is ongoing at the PACS Instrument Control Centre (P-ICC).

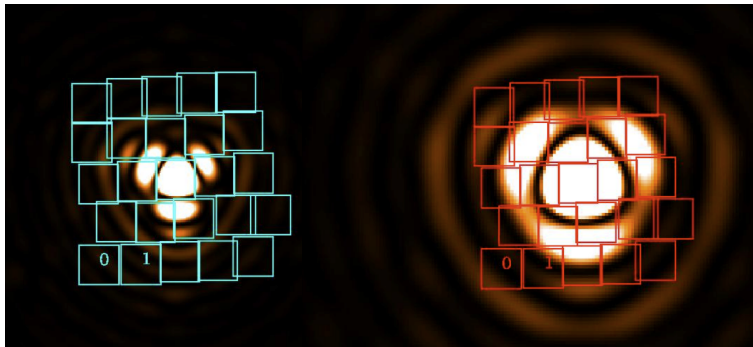


Figure 4.10. PACS spectrometer detector sampling of the telescope PSF at 75  $\mu\text{m}$  (left) and 150  $\mu\text{m}$  (right). Color scaling of the PSF is chosen to enhance the lobes and wings of the psf.

## 4.6.3. Measured beam efficiencies

A full characterisation of the spectrometer beam efficiencies is ongoing. The beam efficiencies have been measured via raster maps on Neptune at a few selected wavelengths. The Neptune visibility window in spring 2011 is being used to complete these measurements at different wavelengths in every spectral band. Together with the detailed telescope PSF models this will allow us to provide reliable model beam efficiencies well sampled across the PACS spectral coverage. In Figure 4.11 the measured beam efficiencies are shown at 62, 75, 125 and 150  $\mu\text{m}$ . The pixel size dominates the width of the beam efficiency up to 150  $\mu\text{m}$ .

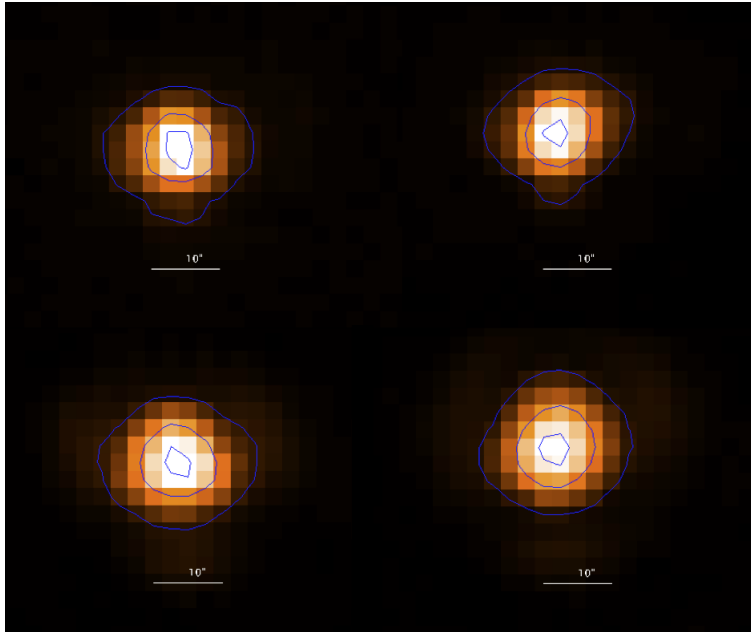


Figure 4.11. PACS spectrometer beam efficiency as measured from raster maps on Neptune. From top left, to bottom right: 62  $\mu\text{m}$ , 75  $\mu\text{m}$ , 125  $\mu\text{m}$ , 150  $\mu\text{m}$ . The contours indicate 10%, 50% and 90% of the peak response.

## 4.7. Spectrometer spectral resolution and instrumental profile

### 4.7.1. Spectrometer spectral resolution

The spectrometer effective resolution for the three orders is plotted in Figure 4.12 and Figure 4.13. The effective resolution is the quadratic sum of the grating resolution and the spectral pixel resolution. The achieved resolution is in the range  $c\delta\lambda/\lambda \sim 55\text{-}320$  km/s (or  $\lambda/\delta\lambda \sim 940\text{-}5500$ ). The instantaneous 16 pixel spectral coverage varies from 600 to 2900 km/s, corresponding to 0.15-1.0  $\mu\text{m}$  wavelength coverage.



#### Note

The main thrust of the PACS spectrometer resides in its high spectral resolution. The spectrometer is aimed at the study of emission/absorption lines rather than continuum sources, although a SED mode in the Range Scan spectroscopy AOT is available too.

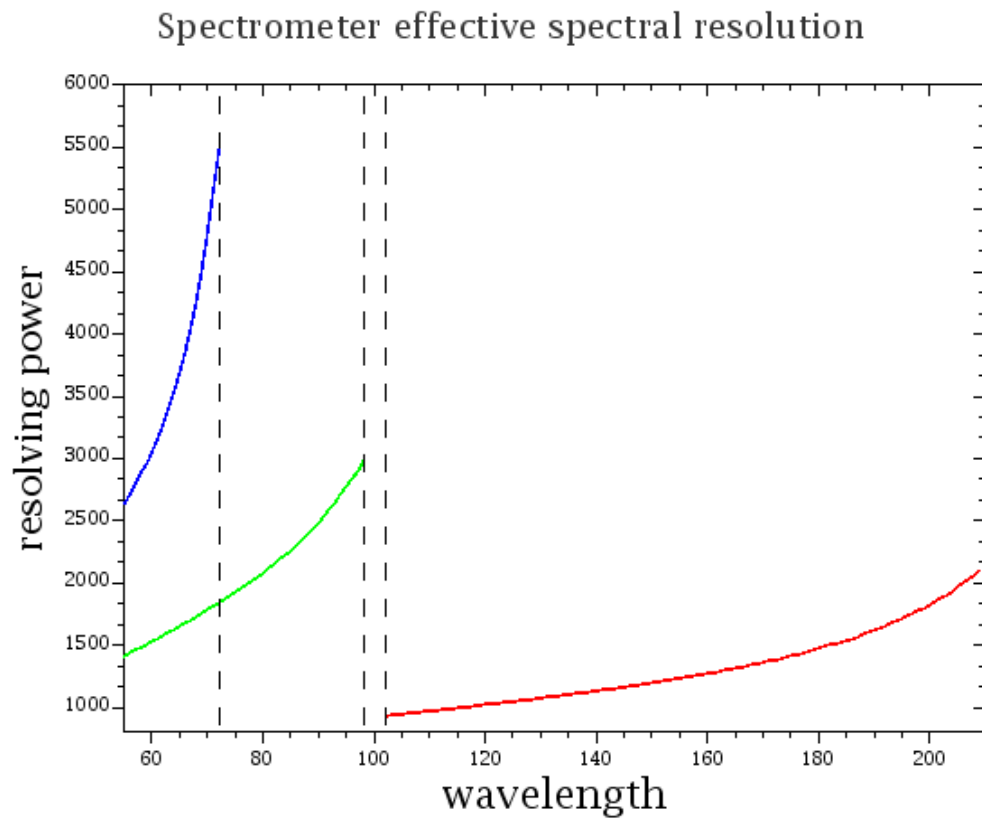
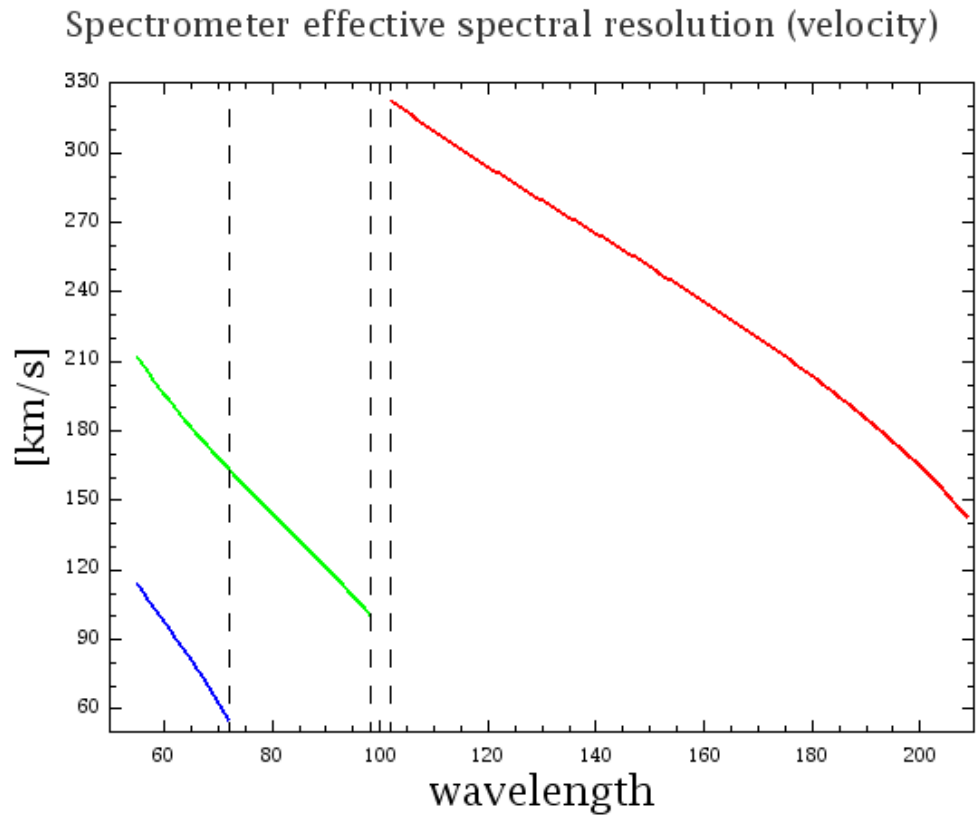


Figure 4.12. Spectrometer resolving power, design values



**Figure 4.13. Spectrometer effective spectral resolution (velocity), design values**

Table 4.1 summarizes the grating characterisation in terms of velocity resolution, spectral coverage and typical grating step sizes for a given order/wavelength.

Table 4.1. PACS grating/pixel spectral characterisation

| grating order | wavelength        | FWHM of an unresolved line |                   | instantaneous spectral coverage (16 pixels) |                   | pixel per FWHM |
|---------------|-------------------|----------------------------|-------------------|---|-------------------|----------------|
|               | [ $\mu\text{m}$ ] | [km/s]                     | [ $\mu\text{m}$ ] | [km/s]                                      | [ $\mu\text{m}$ ] |                |
| 3             | 55                | 114                        | 0.021             | 1420  | 0.26              | 1.20           |
| 3             | 60                | 98                         | 0.020             | 1400  | 0.28              | 1.06           |
| 3             | 72                | 55                         | 0.013             | 580   | 0.14              | 1.38           |
| 2             | 75                | 156                        | 0.039             | 1720  | 0.43              | 1.37           |
| 2             | 90                | 121                        | 0.036             | 1220  | 0.236             | 1.53           |
| 1             | 105               | 318                        | 0.111             | 3030  | 1.06              | 1.56           |
| 1             | 158               | 239                        | 0.126             | 1650  | 0.87              | 2.16           |
| 1             | 175               | 212                        | 0.124             | 1340  | 0.78              | 2.37           |
| 1             | 210               | 140                        | 0.098             | 715   | 0.50              | 3.58           |

The spectral resolution of the instrument, measured in the laboratory with a methanol far-infrared laser setup, follows closely the predicted values of the figures above. Spectral lines in celestial standards (planetary nebulae, HII regions, planets, etc.) are typically doppler broadened to 10-40 km/s, which has to be taken into account for any inflight analysis of the spectral resolution. The double differential chop-nod observing strategy leads to slight wavelength shifts of spectral profile centres due to the finite pointing performances. Averaging nod A and nod B data can therefore lead to additional profile broadening causing typical observed FWHM values that are up to ~10% larger.

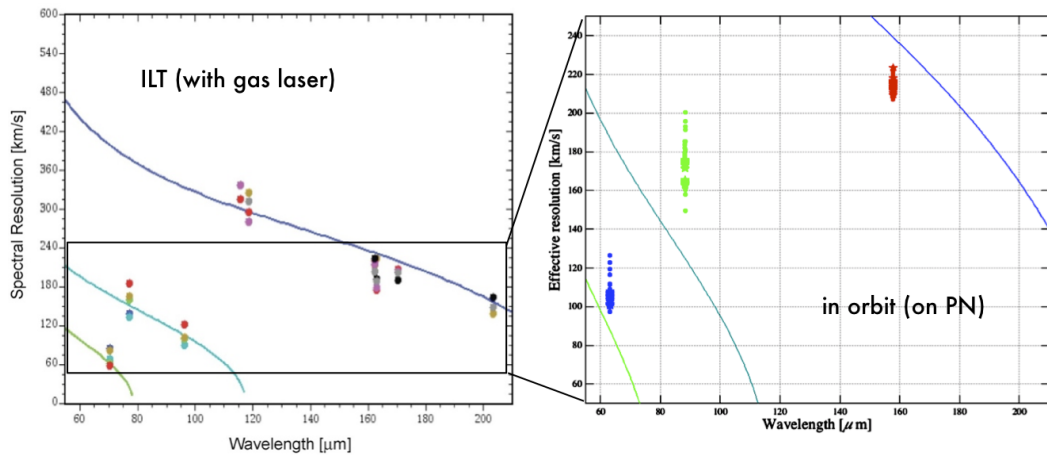


Figure 4.14. Comparison of pre-flight spectral resolution (left) with in-orbit performance (right). Continuous curves represent the design values respective, signs overplotted shows the measured laser line widths in the laboratory during the PACS flight-module tests, and on the right data are derived from planetary nebulae measurements and corrected for internal velocity broadening.

## 4.7.2. Wavelength calibration

The wavelength calibration of the PACS spectrometer relates the grating angle to the central wavelength "seen" by each pixel. Due to the finite width of the spectrometer slit, a characterisation of the wavelength scale as a function of (point) source position within the slit is required as well. The calibration derived from the laboratory water vapour absorption cell is still valid in-flight. For ideal extended sources the required accuracy of better than 20% of a spectral resolution is met throughout all bands. While at band borders, due to leakage effects and lower S/N, the RMS calibration accuracy is closer to 20%, values even better than 10% are obtained in band centres. However, for point sources the wavelength calibration may be dominated by pointing accuracy. Three  $4 \times 4$  raster observations ( $3''$  step size in instrument coordinates) of the point-like planetary nebula IC2501 on the atomic fine structure lines [N III] ( $57 \mu\text{m}$ ), [O III] ( $88 \mu\text{m}$ ) and [C II] ( $158 \mu\text{m}$ ) have been compared with predictions from instrument design. Figure 4.15 shows good agreement between measured spectral line centre positions and the predicted offsets from the relative source position in the slit. Observed wavelength offsets for individual point source observations are therefore expected to fall within the dashed colour lines, given the nominal pointing uncertainty of the spacecraft (consult the Observatory Manual).

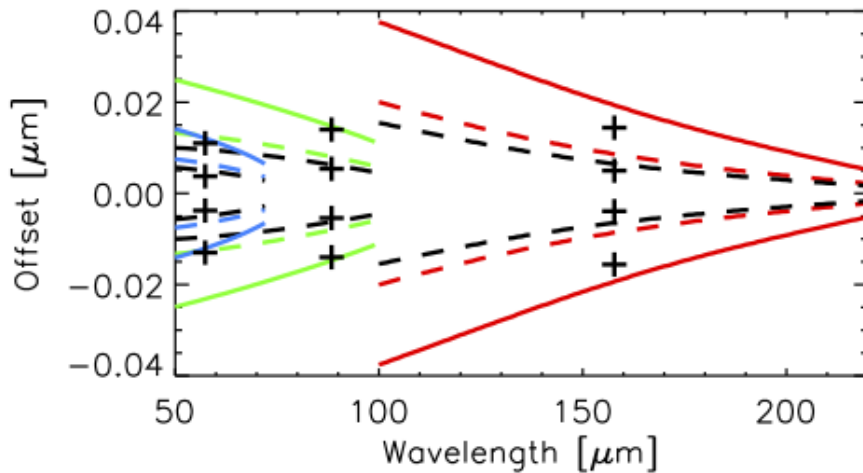


Figure 4.15. Calculated wavelength offsets for point source positions: at the slit border (solid colour lines), for typical pointing errors up to  $2''$  (dashed colour lines) and measured line centre offsets for  $\pm 1.5''$  (dashed black line and crosses) and slit border (black crosses) for three spectral lines on the point like planetary nebula IC2501.

## 4.7.3. Instrumental profile

When observing point sources, for a single spectral line we expect to see a Gaussian instrumental profile (IP) in all spaxels in which the point sources contributes to the flux (strictly-speaking, the profile will be not 100% Gaussian, but it is very close - see below). As the five-by-five PACS spaxel arrangement on the sky is fed into the image slicer, it is re-arranged into a 1-by-25 entrance slit for the grating. When the light from this slit falls on the grating and the point source is centred in the middle of the spaxel, the grating will output a Gaussian profile. However, if the point source is offset in the slit direction, a skewness is introduced in the line profile (as happens with standard slit spectroscopy). This shifts the central wavelength and changes the line width, and it also reduces the line fluxes as some of the flux now falls on neighbouring spaxels. This dependence is depicted in Figure 4.16. Line profiles with well characterised photocentre position on the slit of the central spaxel are shown in Figure 4.17: the skewness of line profiles, the shift of the peak wavelength, as well as loss of line flux as a function of photocentre offset can be well seen.

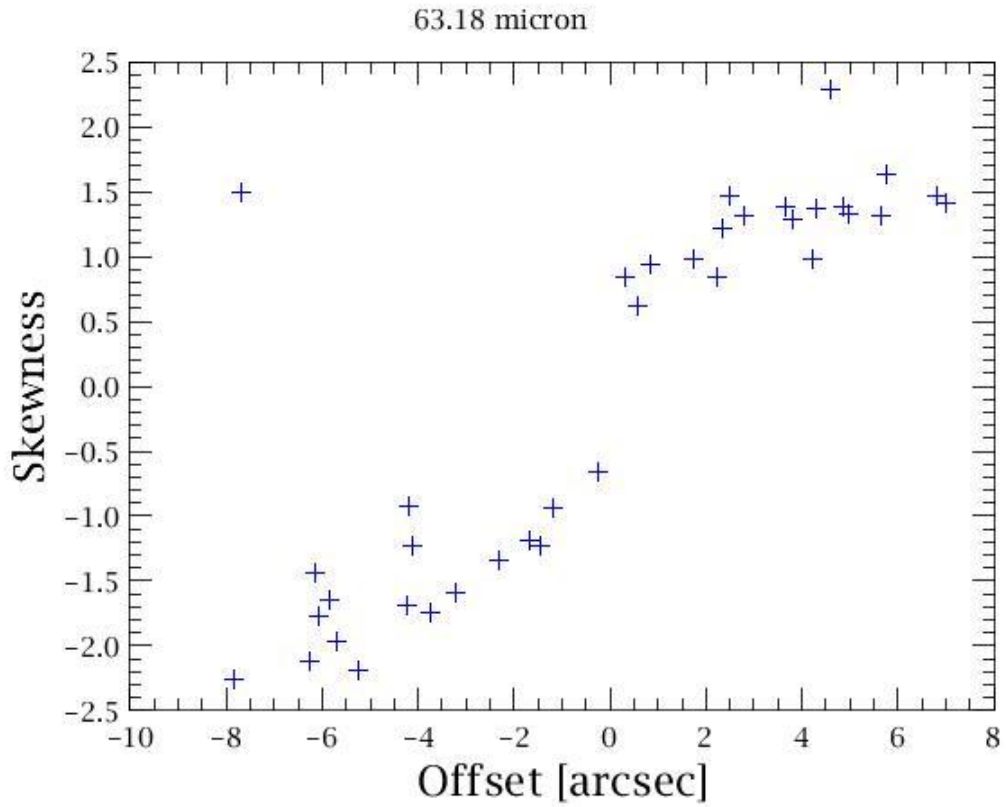


Figure 4.16. Line profile skewness varies with offset from the slit centre. Consider module 12 (spaxel 2,2). If the point source is nicely centred, the offset and skew are zero. As the point source moves off-centre in one direction, for example towards module 7, the skew increases as the offset increases. If the point source moves in the other direction, towards module 17, the skew becomes more negative as the offset increases.

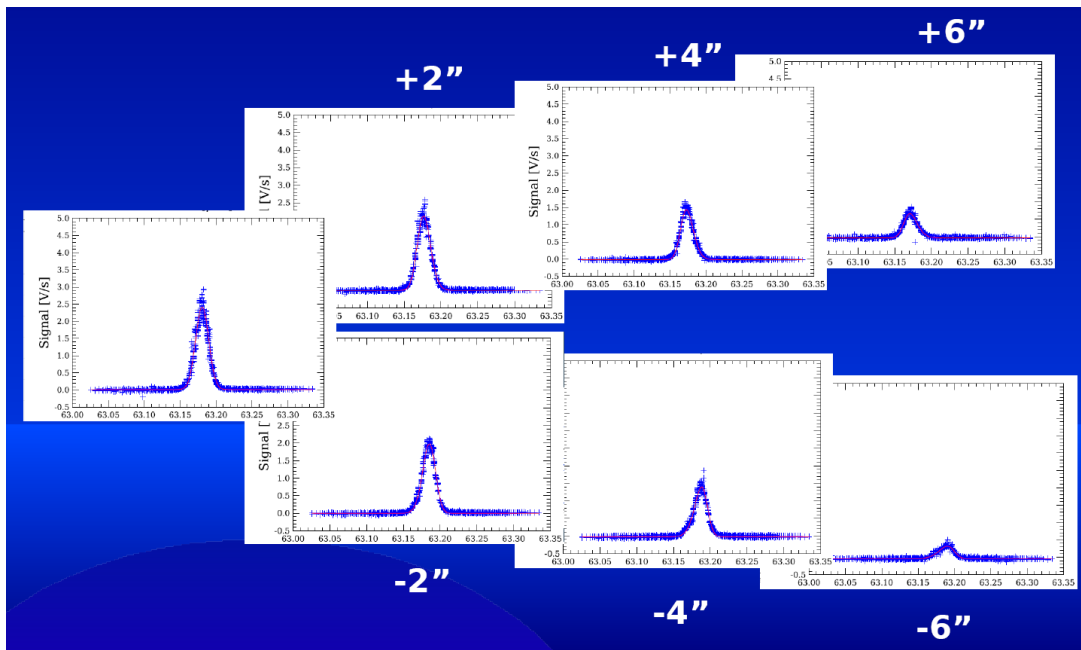


Figure 4.17. Line profile skewness varies with offset from the slit centre. Consider module 12 (spaxel 2,2), profiles are plotted for a point source. Skewness and the wavelength offset of the line peak increases as

the point source moves off-centre perpendicular the slit direction. Red lines are fitted skewed Gaussians.

The instrumental profile is defined as the instrument response when scanning over a line which is intrinsically much narrower i.e. unresolved, than the profile itself. The IP characterization on ground has been done by fitting parametric models to the measured intensity profile of laser lines. In the first order approximation, Gaussian profiles are fitted. These fitting parameters obtained at laser wavelengths have been used as input for phase matching of a numerically calculated profile derived from the sinc square function. The peak of the profile closely follows a Gaussian model, at about 10% level of the peak signal, ripples start to shape the extended line wings at the longest PACS wavelengths (around 200 microns). The full profile model matches the line wings on a few percent accuracy, although wings show an increasing level of asymmetry in the blue half of the 1st diffraction order (from 102 to about ~160 microns) which is not modeled at present. Data obtained on line wings follow very closely the same trend during grating up- and down scans. This confirms that wing shapes are predominantly related to grating dispersion instead of memory effects of the strongly illuminated detectors.

In the process of optimal spectrum extraction, line flux is usually determined from Gaussian- or skewed-Gaussian fitted profiles. The power conserved in line wings has to be corrected by applying a profile correction factor for point-sources. Fitting of the line wings after the first minima would very difficult for faint-lines especially at wavelength shorter than ~150 microns, therefore the profile correction factor is advised to use.

Profiles of various narrow lines, typically observed in the PACS wavelength range are shown in Figure 4.18. The Gaussian fitted model provides reliable flux estimation over the entire wavelength range. Figures were made by standard data reduction pipeline, plotted spectra are created on a wavelength grid corresponding to the Nyquist sampling of the spectral resolution at the line peak wavelength respectively.

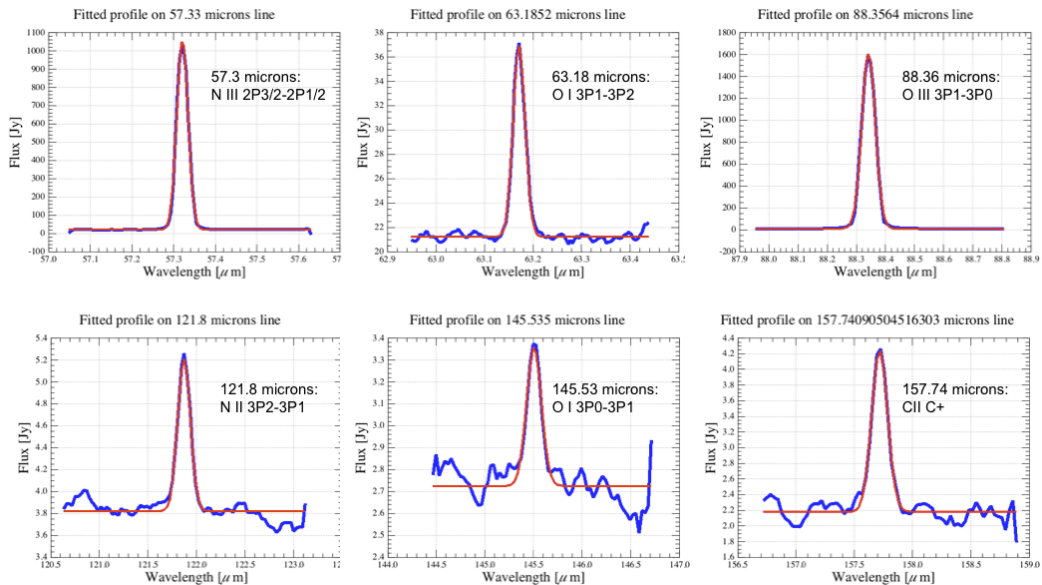


Figure 4.18. Frequently observed lines in the PACS bands, in this example from observations on planetary nebula NGC6543. The rebinned spectra taken from the central spaxel are produced by the standard pipeline, the fitted model is a Gaussian plus zero order polynomial representing the continuum. Data were taken in faint-line mode (high grating sampling density) applying single line repetition and single nodding cycle, therefore S/N strongly varies with lines in this example.

## 4.8. Spectral leakage regions

The precision of the relative spectral response is affected by spectral leakage (order overlap due to



finite steepness of order sorting filter cut-off edges) from grating order  $n+1$  into grating order  $n$ . At wavelengths of  $70\text{--}73\mu\text{m}$ ,  $98\text{--}105\mu\text{m}$  and  $190\text{--}220\mu\text{m}$  the next higher grating order wave- lengths of  $52.5\text{--}54.5\mu\text{m}$ ,  $65\text{--}70\mu\text{m}$  and  $95\text{--}110\mu\text{m}$  do overlap respectively (leakage regions on measured spectra are shown in Figure 4.19, Figure 4.20 and Figure 4.21). Continuum shapes and flux densities in these border ranges are therefore less reliable than in band centres. Band B2A is not affected by spectral leakage.

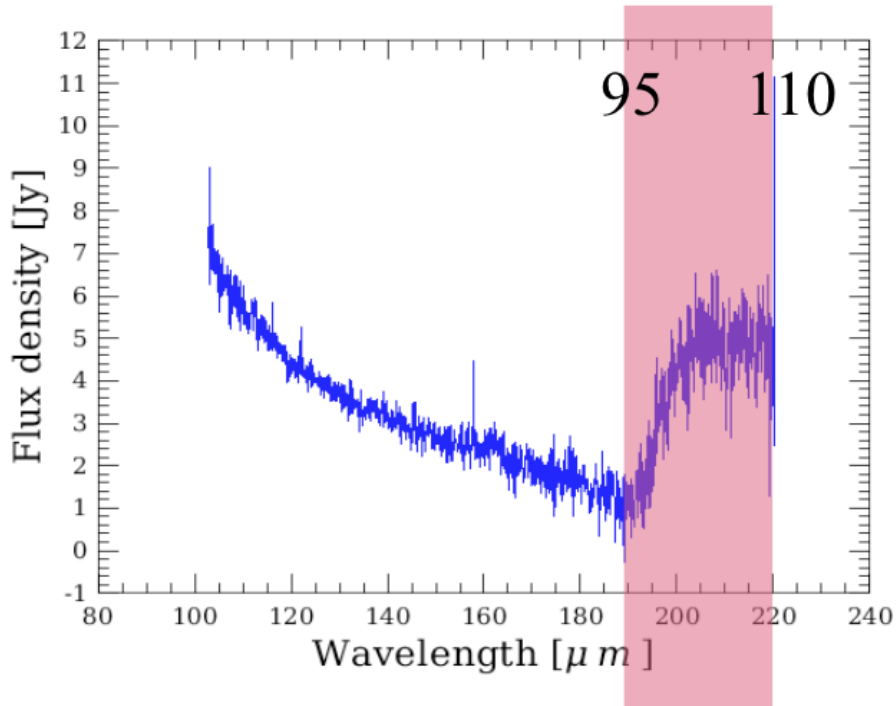


Figure 4.19. Spectral leakage in band R1: the spectrum between  $190\text{--}220\mu\text{m}$  has an unreliable (line) flux calibration, and shows superimposed spectral features from order 2 ( $95\text{--}110\mu\text{m}$ ).

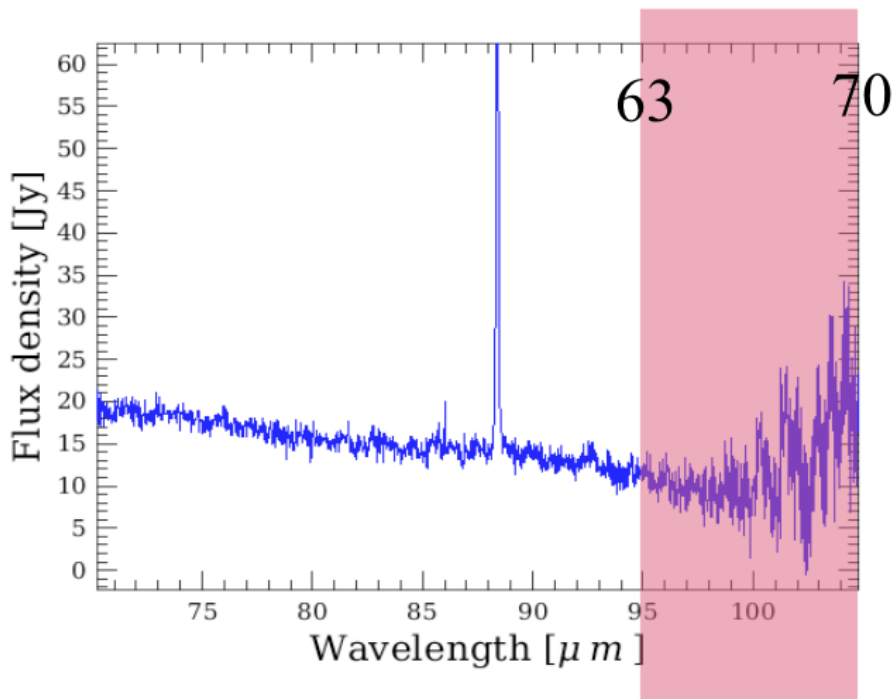


Figure 4.20. Spectral Spectral leakage in band B2B: beyond  $98\mu\text{m}$  the response is very low, and spectral

features from order 3 (63-70  $\mu\text{m}$ ) are superimposed on the spectrum.

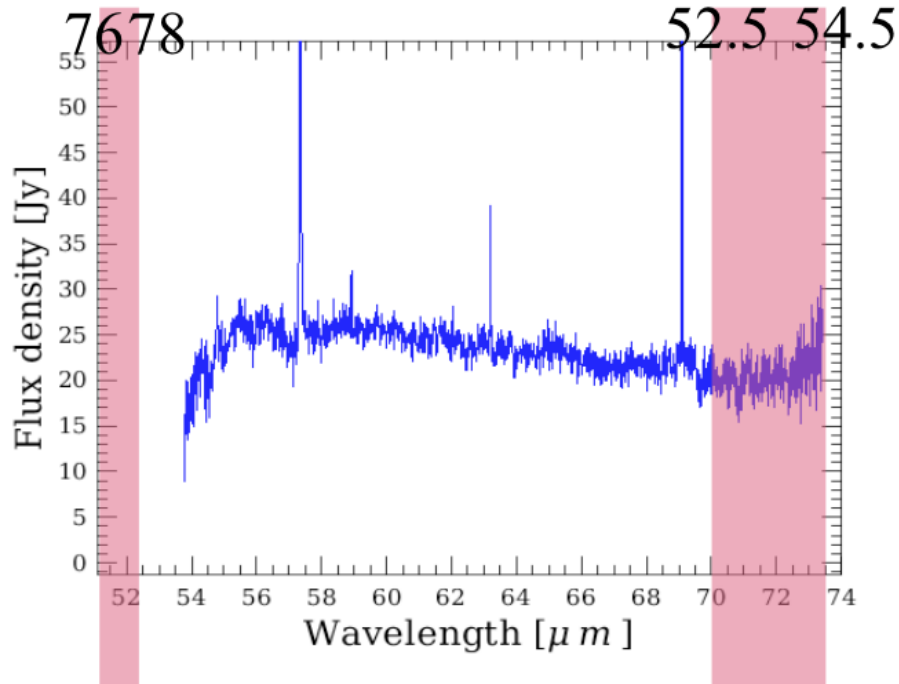


Figure 4.21. Spectral leakage in band B3A: beyond 70  $\mu\text{m}$ , the order 4 (52,5-54.5  $\mu\text{m}$ ) spectrum is added to the 70-73  $\mu\text{m}$  order 3 spectrum. The 51-52  $\mu\text{m}$  order 3 spectrum also shows the 76-78  $\mu\text{m}$  order 2 spectrum. At 69  $\mu\text{m}$ , the leakage is of the order of 2%. This can still be important in the few cases where the OIII line at 51.8  $\mu\text{m}$  is extremely bright, as in the example displayed.

## 4.9. Spectrometer flux calibration

### 4.9.1. Recovering full beam line fluxes and flux densities for point sources

The fraction of the Herschel+PACS PSF seen in one spaxel varies with wavelength. In order to recover full beam line fluxes or flux densities for point sources, a wavelength dependent correction factor needs to be applied to the line fluxes or flux densities as measured in the central spaxel only (see Section 4.4). The wavelength dependent fraction between the point source flux seen in the central spaxel and the full beam flux has been modelled and scaled to actual measurements of the PACS spectrometer PSF maps measured on Neptune. The correction curve is depicted in Figure 4.5. This correction curve assumes a point source perfectly centred on the central spaxel. In the current version of the pipeline this curve is not applied, but can be found in the calibration table `cal-Tree.spectrometer.pointSourceLoss`.

Alternatively, the full flux or flux density of a source can be recovered by co-adding the spectra obtained from several spaxels ("aperture photometry"). In this case, of course, no correction factor needs to be applied. However, if accurate line shapes are to be preserved, at the level of the instrumental resolution or below, it is not recommended to co-add the spectra obtained in different spaxels. As with all slit spectrographs, a different position of the source photocenter in the dispersion direction of the slit induces wavelength shifts and line profile skews (Section 4.7.3). Co-adding line profiles in different spaxels will therefore result in broadened and skewed line shapes. Work on proper optimal extraction and fitting of spectral lines is under way in the PACS ICC.

### 4.9.2. Absolute flux calibration, using the calibration block

The PACS pipeline uses a flux conversion based on the calibration block performed at the start of every AOR. During the calibration block, the differential signal between the two internal calibration sources is measured at a key wavelength within the spectral order that is being used in the AOR. That signal is known in absolute terms, as it is regularly calibrated on celestial standards, for which we dispose of state of the art models. Figure 4.22 to Figure 4.25 illustrate the comparison between observations calibrated with that strategy and models, for all calibration measurements obtained after the focal plane geometry of the instrument was established. The flux calibration accuracy of the PACS spectra is currently of 30%. Various further improvements are being investigated at the PACS ICC. Nevertheless, a fraction of the inaccuracy is suspected to be related to the pointing of the satellite: it can be shown that the dispersion observed in these figures is significantly reduced when one considers the co-addition of the flux in all spatial pixels instead of just the central one.

Broad spectral features (a few resolution elements) and continuum shape difference of ~10% in the blue bands and ~20% in the red band can be introduced by transient effects and features in the relative spectral response function. Corrections for these effects are under study. In the mean time, such features should not be interpreted blindly. A first check is to compare with the shape of the relative spectral response function at the wavelength where the feature is observed.

The same 10% (blue bands) and 20% (red bands) accuracy applies when comparing line fluxes within one spectral band. When comparing line fluxes across different bands, the 30% absolute uncertainty applies on the individual line fluxes.

The accuracies quoted above include the effect of detector response drifts, transients and signal losses due to the pointing accuracy limits.

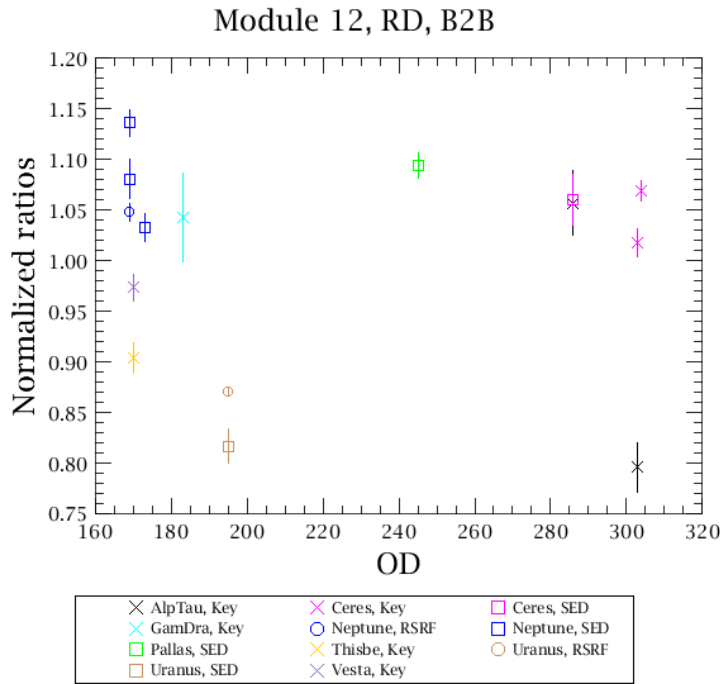


Figure 4.22. Average observed PACS spectrum of sky flux calibrators, corrected with the response derived from the calibration block, divided by model predictions - band B2A.

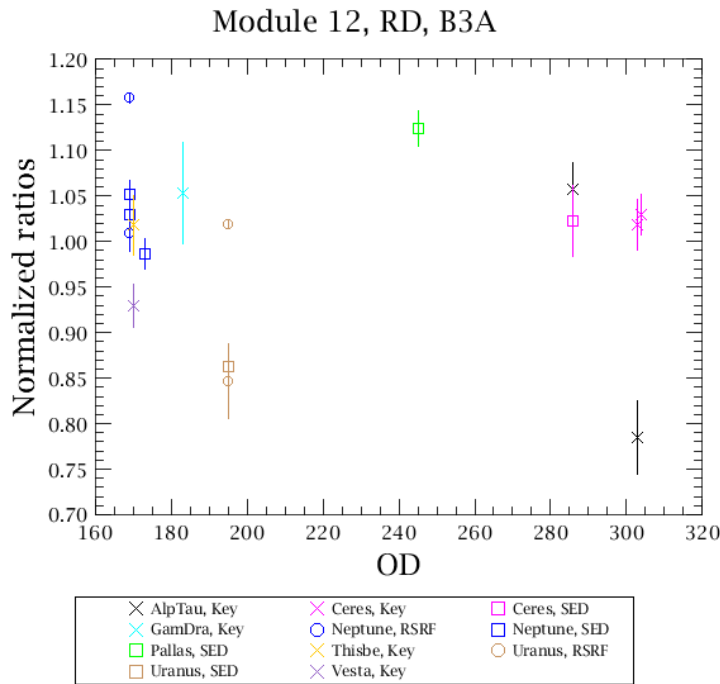


Figure 4.23. Average observed PACS spectrum of sky flux calibrators, corrected with the response derived from the calibration block, divided by model predictions - band B3A.

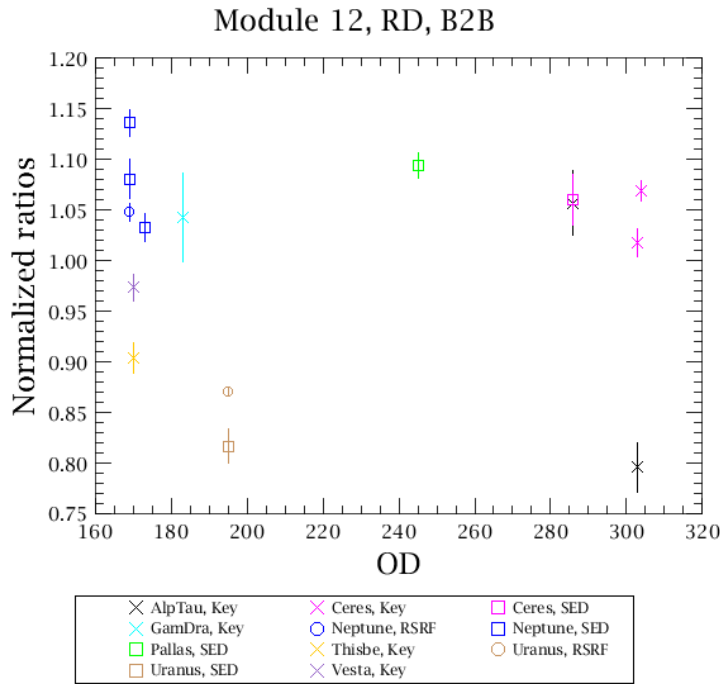


Figure 4.24. Average observed PACS spectrum of sky flux calibrators, corrected with the response derived from the calibration block, divided by model predictions - band B2B.

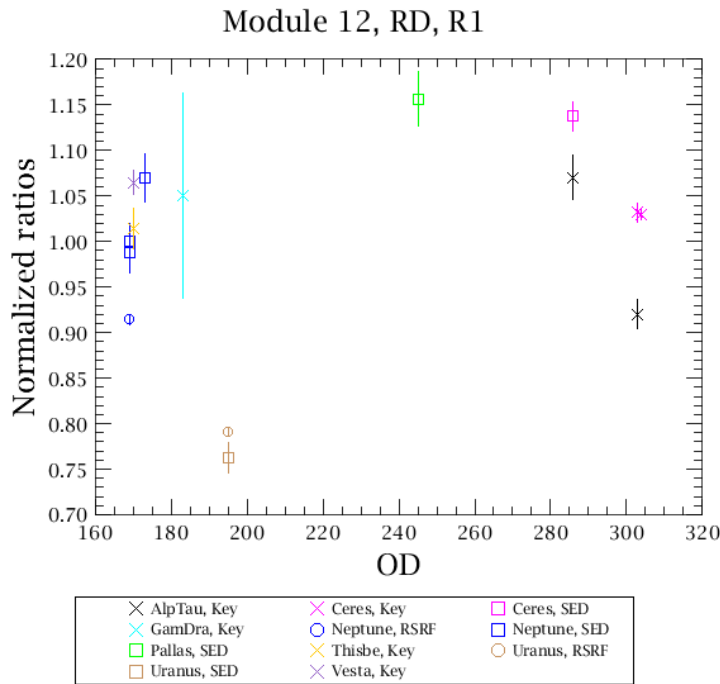


Figure 4.25. Average observed PACS spectrum of sky flux calibrators, corrected with the response derived from the calibration block, divided by model predictions - band R1.

## 4.10. Spectrometer sensitivity

Photoconductors of the type used in PACS have been demonstrated to have (dark) noise-equivalent powers (NEP) of less than  $9 \times 10^{-18} \text{WHz}^{-1/2}$  (for the high stressed array). Such a noise level would ensure background-noise limited performance of the spectrometer. Tests of the high-stress detectors done at module level in a test cryostat and with laboratory electronics indicate a significant noise contribution from the readout electronics.

These measurements can be consistently described by a constant contribution in current noise density from the CREs and a noise component proportional to the photon background noise, where this proportionality can be expressed in terms of an (apparent) quantum efficiency, with a peak value of 26%. The NEP of the Ge:Ga photoconductor system is then calculated over the full wavelength range of PACS based on the CRE noise and peak quantum efficiency determination at detector module level for the high-stress detectors. The quantum efficiency as a function of wavelength for each detector can be derived from the measured relative spectral response function. Similarly, the absolute responsivity as a function of wavelength is derived from the relative spectral response function and an absolute reference point measured in the laboratory.

The in-orbit performance depends critically on the effects of cosmic rays, in particular, high-energy protons. Analysis of in-orbit data as well as proton irradiation tests on ground indicate a permanently changing detector responsivity: cosmic ray hits lead to instantaneous increase in responsivity, followed by a curing process due to the thermal IR background radiation.

The HSpot prediction of spectrometer sensitivity in the high-sampling mode, used in the AOTs line spectroscopy mode and range spectroscopy (with the option "high-sampling") are shown in figures Figure 4.26 and Figure 4.27 for the continuum and line detection respectively.

The HSpot prediction of spectrometer sensitivity in the SED mode, used in AOT range spectroscopy, with the option "Nyquist sampling" are shown in figures Figure 4.28 and Figure 4.29 for continuum and line detection respectively.

The in-orbit performance verification results indicate that with optimized detector bias settings and modulation schemes (chopping + spectral scanning), NEPs measured in laboratory can actually be achieved. The line- and continuum sensitivities as a function of observing time have been verified in-orbit and are consistent with pre-launch predictions. Figure 4.30 shows the comparison of pre-launch sensitivity predictions with in-orbit line scan observations.



### Note

Sensitivity plots can be easily produced in HSpot: go to the Range Spectroscopy AOT, define a full wavelength range in Nyquist- or high sampling density and adjust the repetition factors. By clicking on 'Observation estimation' and then 'Range sensitivity plots' a pop-up window will show both line- and continuum sensitivities as a function of wavelength for the integration time defined in the AOR.

The best **5σ/1 hour sensitivity** in the first order corresponds to about **100 mJy** for the continuum ,  **$2 \times 10^{-18} \text{Wm}^{-2}$**  for the line sensitivity and a factor 2.5 worse roughly in the 2nd and 3rd order.



### Note

Sensitivities in the 2nd generation unchopped grating scan mode have not yet been verified on photometric standards. The 1st generation AOT mode - wavelength switching - had a performance very close to the chopped mode, however, did not reach the same level of sensitivity. The unchopped mode is expected to be superior with respect to wavelength switching, sensitivity numbers will be provided to the PACS observers community.

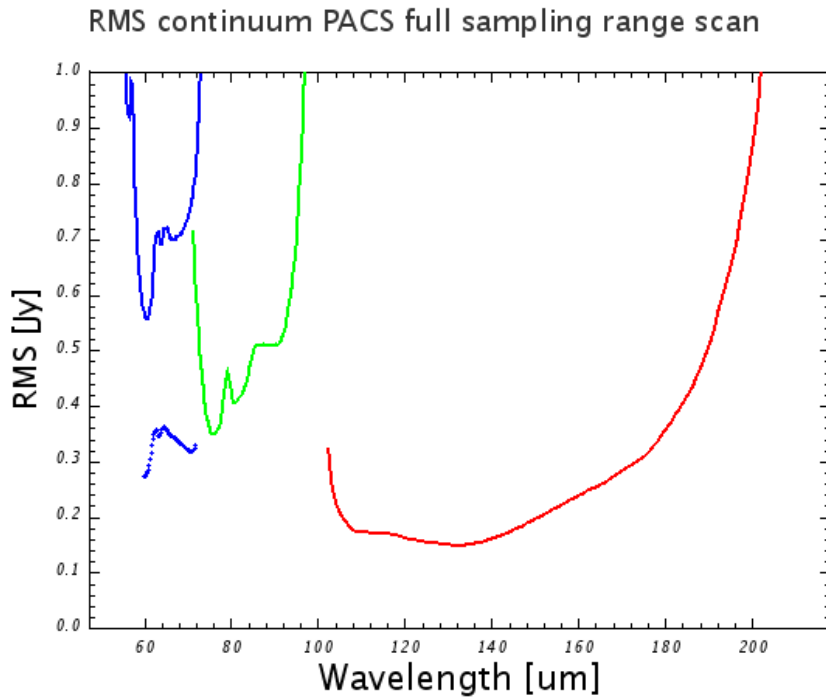


Figure 4.26. Spectrometer point-source continuum sensitivity in high-sampling density mode, for both line/range repetition and nodding repetition factors equal to one, in the line spectroscopy or range spectroscopy AOTs. Solid blue line: third grating order filter A (B3A), dotted blue line : second order with filter A (B2A), green: second order with filter B (B2B), red: first order (R1).

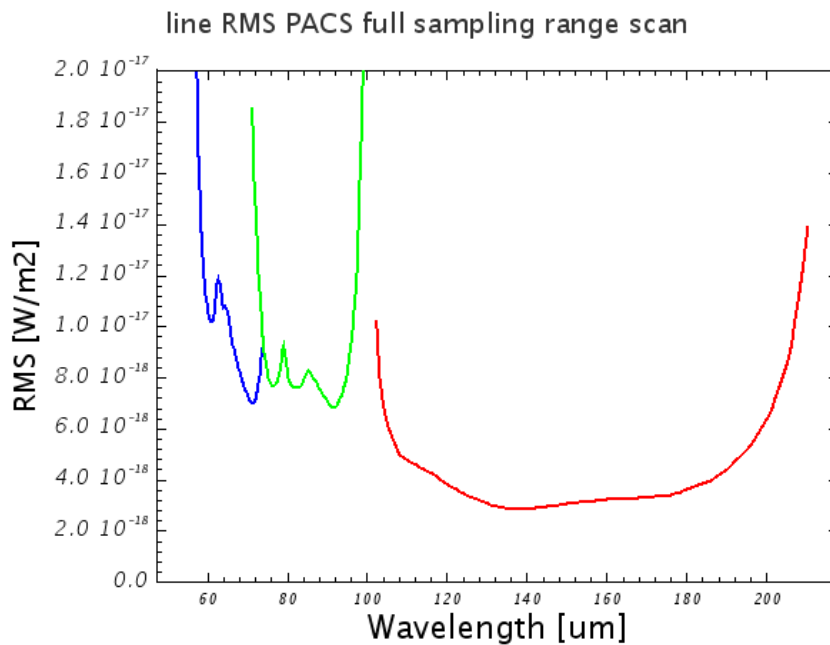


Figure 4.27. Spectrometer point-source line sensitivity in high-sampling density mode, for both line/range repetition and nodding repetition factors equal to one, in the line spectroscopy or range spectroscopy AOTs. Blue: third grating order filter A (B3A), green: second order filter B (B2B), red: first order (R1).

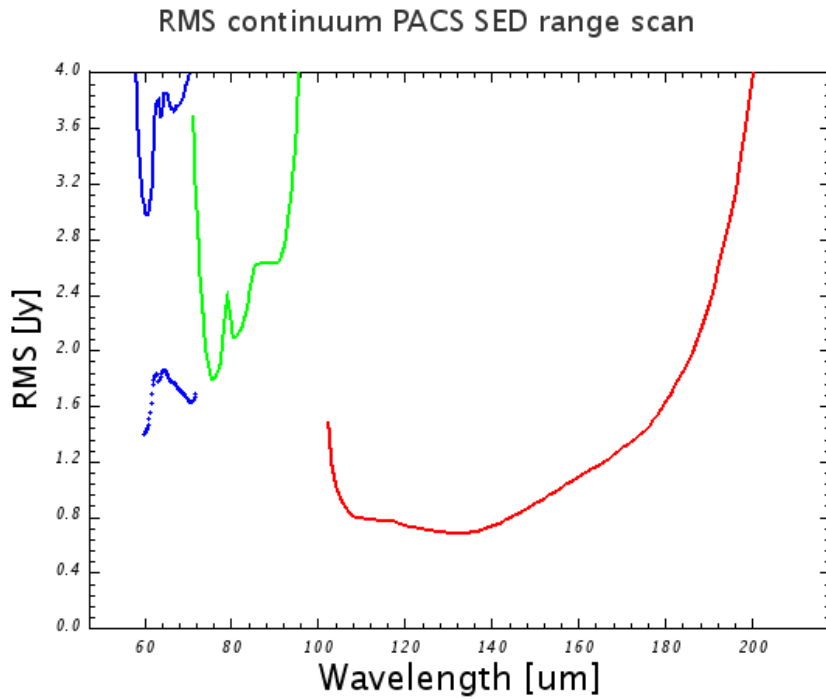


Figure 4.28. Spectrometer point-source continuum sensitivity in SED mode (range spectroscopy AOT), for both range repetition and nodding repetition factors equal to one. Solid blue line: third grating order filter A (B3A), dotted blue line : second order with filter A (B2A), green: second order with filter B (B2B), red: first order (R1).

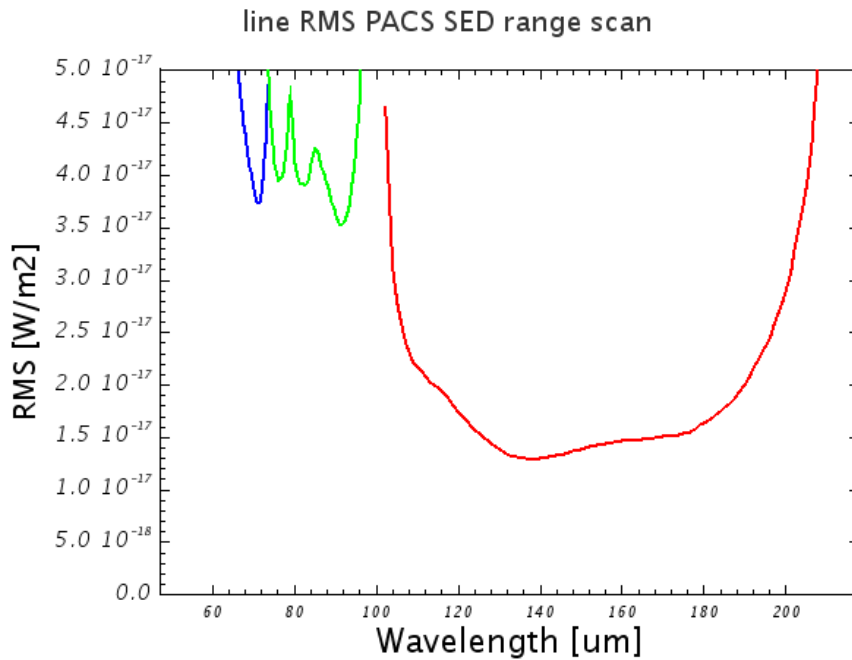


Figure 4.29. Spectrometer point-source line sensitivity in SED mode (range spectroscopy AOT), for both range repetition and nodding repetition factors equal to one. Blue: third grating order filter A (B3A), green: second order filter B (B2B), red: first order (R1).



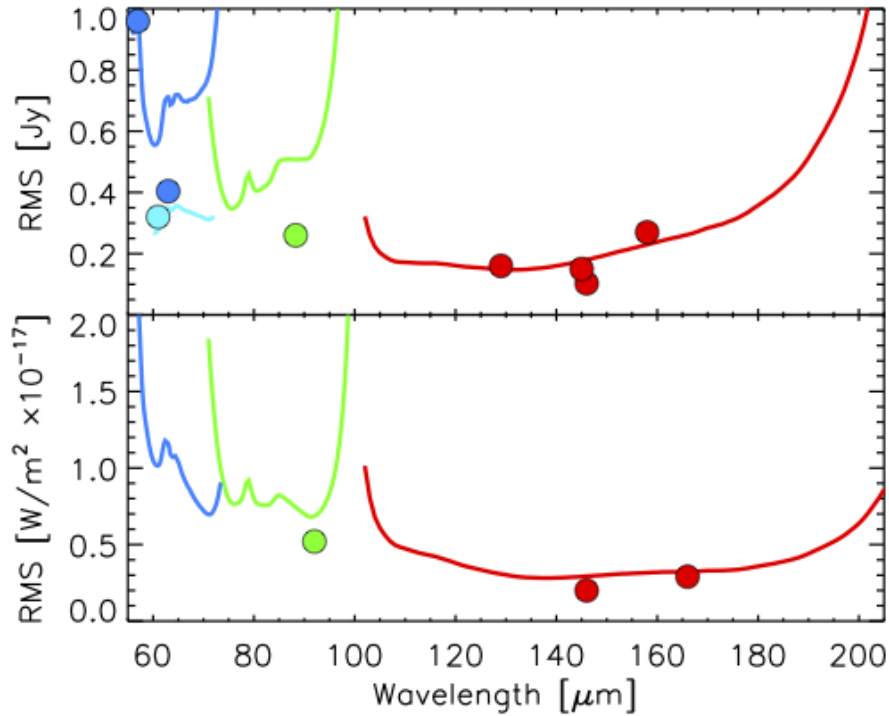


Figure 4.30. One sigma continuum sensitivity (upper plot) and line sensitivity (lower plot) for a number of faint line detections in comparison to the HSpot predictions for a single Nod and single up-down scan by the grating, with a total execution time of 400. . . 440 s, depending on wavelength. The different colours represent the different spectral PACS bands and grating orders. Nyquist binning (two bins per FWHM) has been used to derive the measured line detection sensitivity in each bin, while the HSPOT prediction refers to total line flux. Thus, the actual sensitivity values shown here are very conservative.

## 4.11. Spectrometer saturation limits

The PACS spectrometer gives access to a large dynamic range in flux densities by selecting 4 different integrating capacitances. The uplink logic automatically selects the integrating capacitance based on estimated continuum and line fluxes. Figure 4.31 shows the saturation limit in Jansky for the default integration capacitance. This is the limit for continuum and peak line flux together. Figure 4.32 shows the default capacitance saturation limits for unresolved lines on a zero continuum. Both figures should allow to judge if the observation can be executed with the default integration capacitance. If continuum and expected line fluxes are higher than the saturation limits for the default capacitance, it is mandatory to enter the expected continuum and line flux for every range at the time the observation is designed and filled in HSpot. Figures Figure 4.33 to Figure 4.36 show the flux limits at which a larger integrating capacitance is selected. If an observation contains lines that fall in different flux regimes, the largest capacitance will be chosen for the entire observation. If lines in the same observation fall in different flux regimes, it is recommended to split the observation into separate observations per flux regime. Figure Figure 4.37 and Figure 4.38 show the saturation limits using the largest integrating capacitance. If the expected line flux and continuum flux are higher than these limits then detectors may run into saturation and flux calibration becomes unreliable.

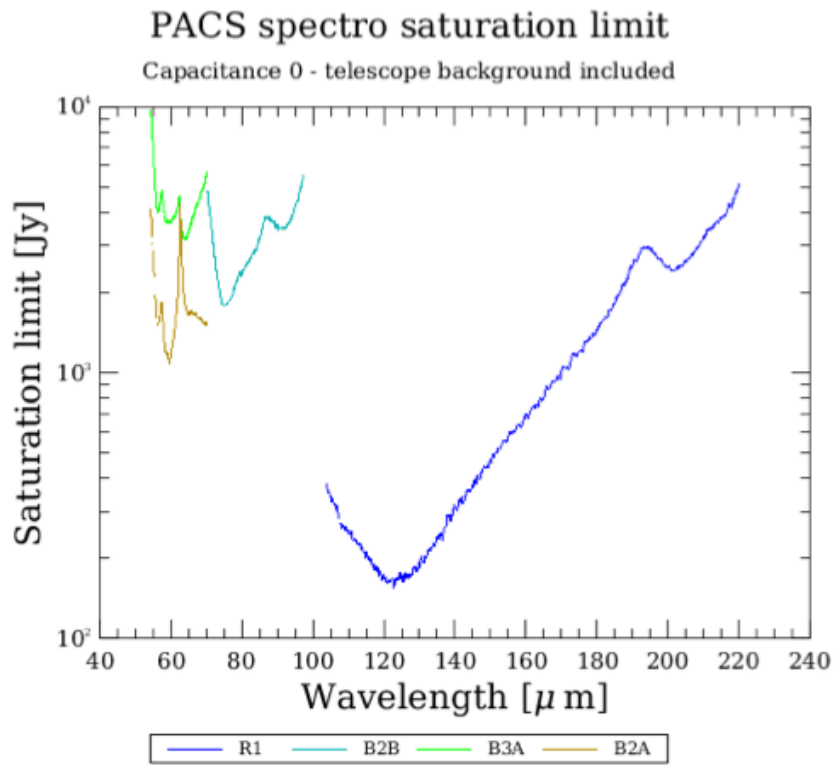


Figure 4.31. Saturation limit with the (default) smallest ( $\sim 0.14$  pF) integrating capacitance (including 80% safety margin).

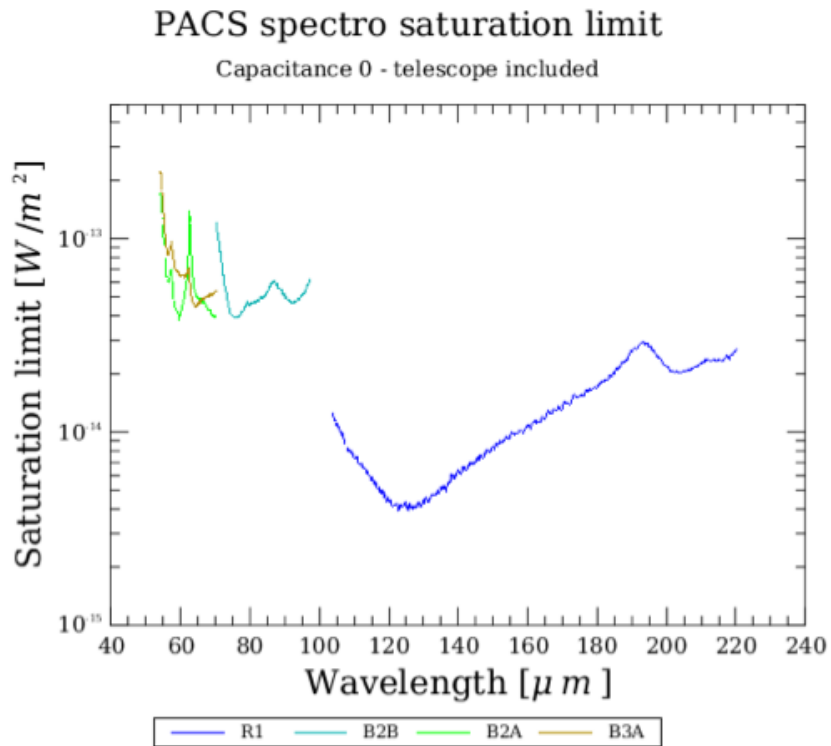


Figure 4.32. Saturation limit for unresolved lines on a zero continuum for the (default) smallest ( $\sim 0.14$  pF) integration capacitance.

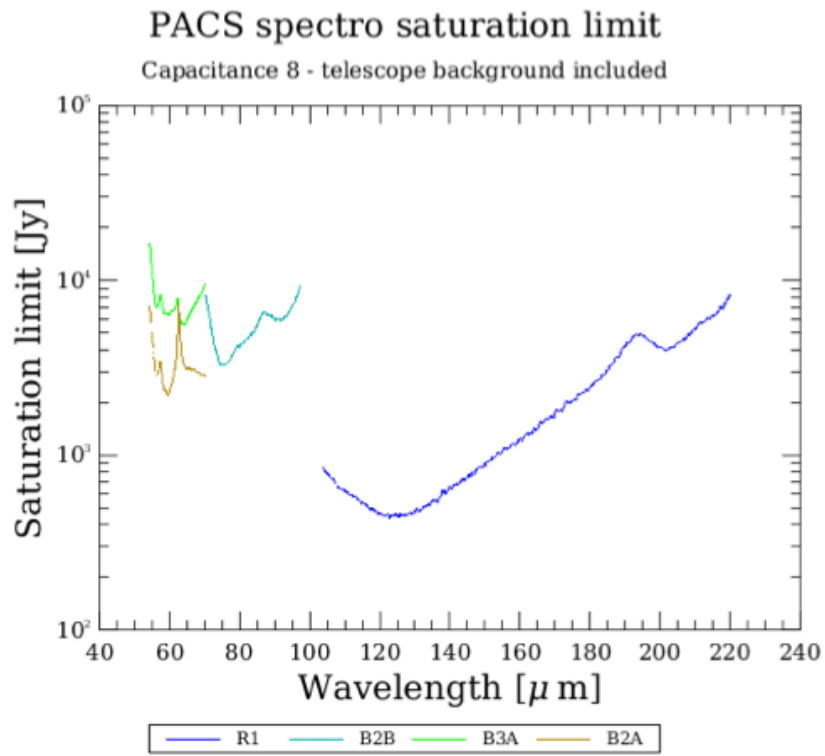


Figure 4.33. Saturation limit for the second ( $\sim 0.24$  pF) integration capacitance (including 80% safety margin)

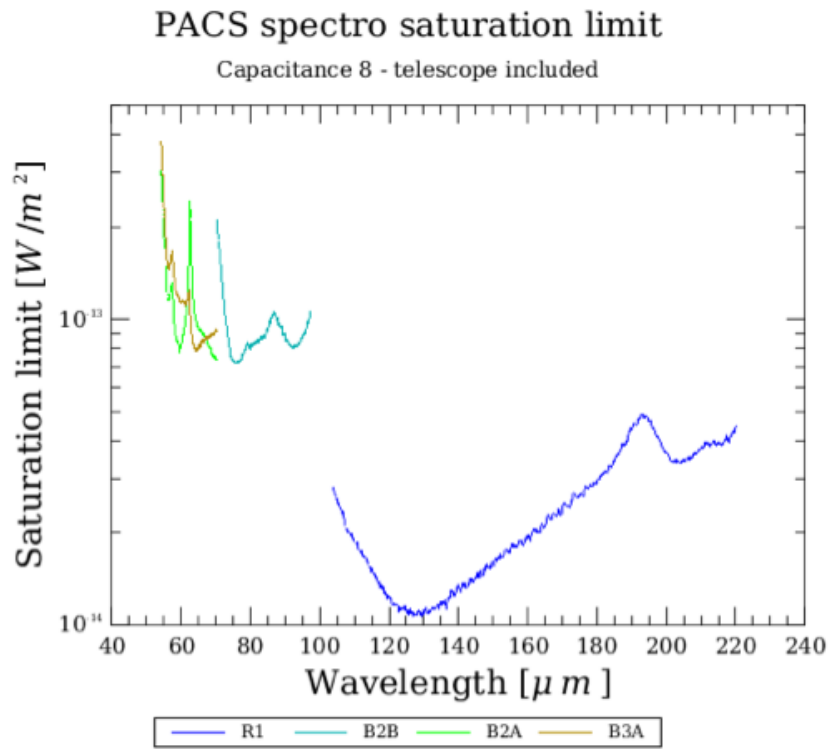


Figure 4.34. Saturation limit for unresolved lines on a zero continuum for the second ( $\sim 0.24$  pF) integrating capacitance (inc. 80% safety margin).

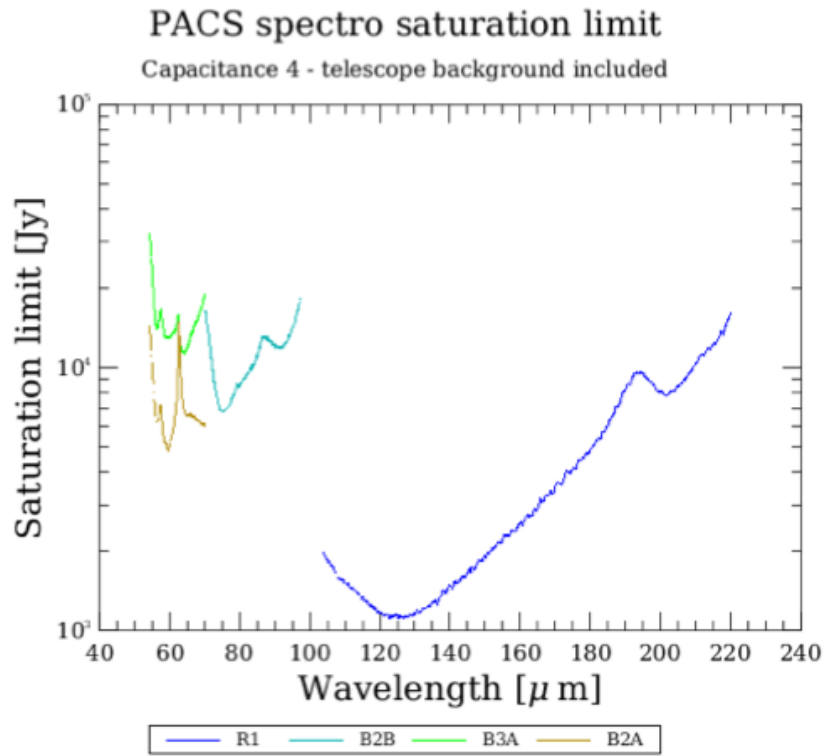


Figure 4.35. Saturation limit for the third ( $\sim 0.46$  pF) integrating capacitance (inc. 80% safety margin).

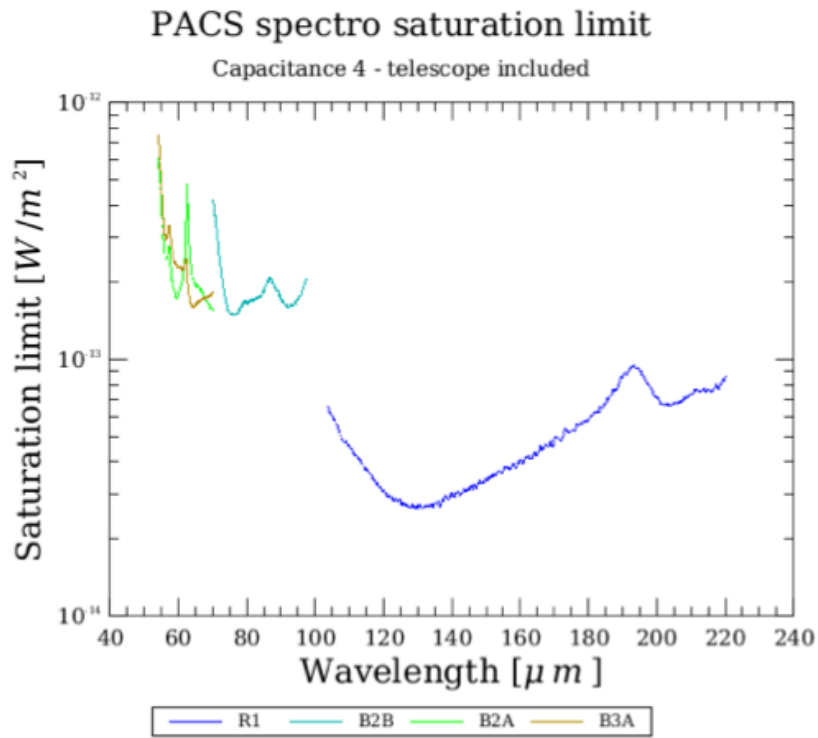


Figure 4.36. Saturation limit for unresolved lines on a zero continuum using the third ( $\sim 0.46$  pF) integration capacitance (including 80% safety margin).

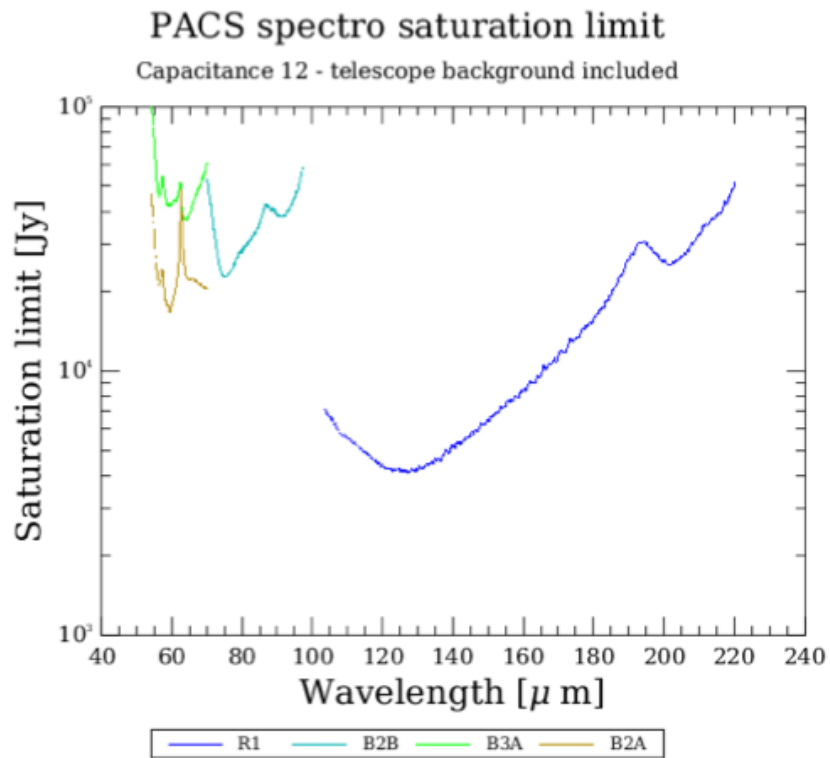


Figure 4.37. Saturation limit for the largest (~1.15 pF) integrating capacitance.

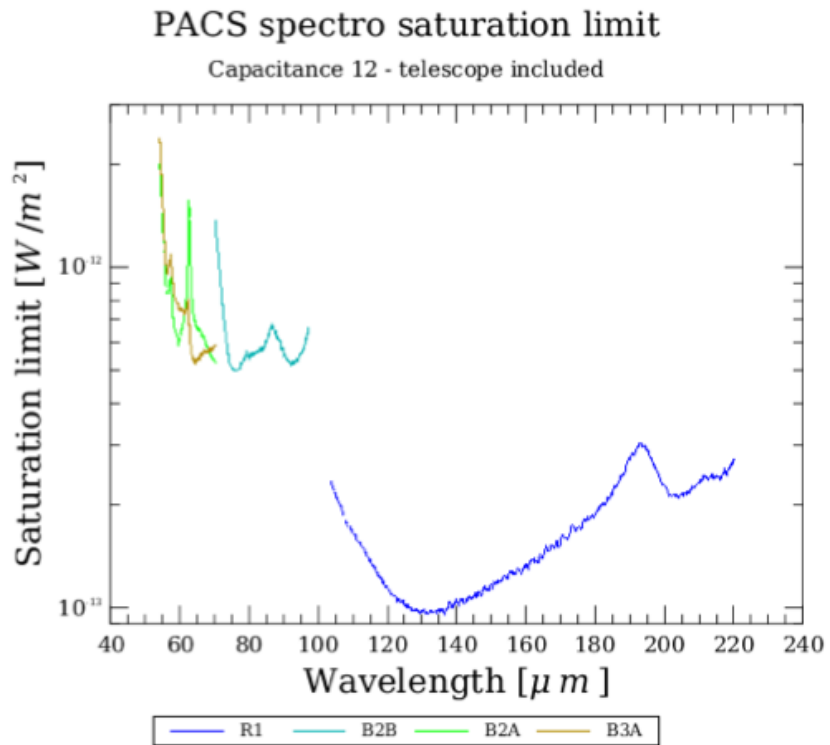


Figure 4.38. Saturation limit for unresolved lines on a zero continuum for the largest (~1.15 pF) integrating capacitance.

---

# Chapter 5. Observing with the PACS photometer

A typical PACS Observation Day (OD) contains predominantly either photometer or spectrometer observations to optimise the observing efficiency within a photometer cooler cycle. After each cooler recycling procedure (which takes about 2.5 h), there are about 2.5 ODs of PACS photometer – prime or parallel mode – observations possible. Mixed days with both sub-instruments, e.g., to observe the same target in photometry and spectroscopy close in time, are only scheduled in exceptional cases.

Three observing modes or Astronomical Observing Templates (AOT) are validated on the PACS photometer side:

- Pointsource photometry mode in chopping-nodding technique
- Scan map technique (for point-sources, small and large fields)
- Scan map technique within the PACS/SPIRE parallel mode.

The originally foreseen ”small source mode” and ”large raster mode” in chopping-nodding technique are replaced by the scanmap technique for better performance and sensitivity reasons.

We refer to the [SPIRE PACS Parallel Mode Observers' Manual](#) for more information on the use of the parallel mode and describe in this chapter the chopped-noded point-source mode and the scan mapping mode, including the mini-scan map mode, intended to replace the chopped-noded mode.

All photometer configurations perform dual-band photometry with the possibility to select either the blue (60–85 $\mu$ m) or the green (85–125 $\mu$ m) filter for the short wavelength band, the red band (125–210 $\mu$ m) is always included. The two bolometer arrays provide full spatial sampling in each band.

During an observation the bolometers are read-out with 40 Hz, but due to satellite data-rate limitations there are onboard reduction and compression steps needed before the data is down-linked. In PACS prime modes the SPU averages 4 subsequent frames; in case of chopping the averaging process is synchronised with the chopper movements to avoid averaging over chopper transitions. In PACS/SPIRE parallel mode 8 consecutive frames are averaged in the blue/green bands and 4 in the red band. In addition to the averaging process there is a supplementary compression stage ”bit rounding” for high gain observations required, where the last  $n$  bits of the signal values are rounded off. The default value for  $n$  is 2 (quantisation step of  $2 \cdot 10^{-5}$  V or 4 ADUs) for all high gain PACS/SPIRE parallel mode observations, 1 for all high gain PACS prime mode observations, and 0 for all low gain observations.

Each PACS photometer observation is preceded by a 30 seconds chopped calibration measurement executed during the target acquisition phase. The chopper moves with a frequency of 0.625 Hz between the two PACS internal calibration sources. 19 chopper cycles are executed, each chopper plateau lasts for 0.8 s (32 readouts on-board) producing 8 frames in the down-link. There are always 5 seconds idle-time between the calibration block and the on-sky part for stabilisation reasons.

## 5.1. Chop-nod point-source photometry mode

The point-source photometry observing mode makes use of a chop-nod technique and shall be used for sources that are significantly smaller than a single matrix (50 arcsec x 50 arcsec), i.e. mostly point sources .

The PACS photometer chop-nod point-source mode uses the PACS chopper to move the source along the Y spacecraft axis by about 50 arcsec, corresponding to the size of about 1 blue/green bolometer matrix or the size of about half a red matrix, with a chopper frequency of 1.25 Hz. The nodding is performed by a satellite movement of the same amplitude , but perpendicular to the chopping

direction, i.e. along the Z spacecraft axis, to compensate for the different optical paths, as illustrated in Figure 5.1.

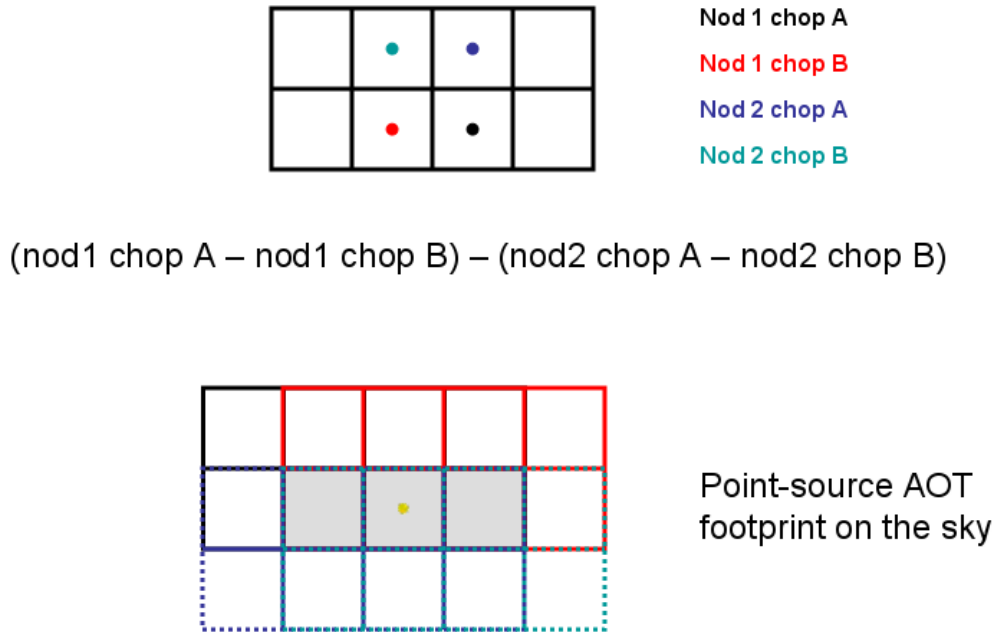


**Figure 5.1. Source positions in point-source photometry AOT. Sketch showing the source positions as a function of the nod and chopper positions. The Y-axis is to the left, the Z-axis to the top. Chop positions are defined by the internal chopper, while nod positions are defined by the satellite pointing. Dithering at each chopper position, performed with the internal chopper is not represented.**

On each nod-position the chopper executes 3x25 chopper cycles. The 3 sets of chopper patterns are either on the same array positions (no dithering) or on 3 different array positions (dither option). In the dither-option the chopper pattern is displaced along Y-direction (along the chopper direction) by about 8.5 arcsec (2.66 blue pixels or 1.33 red pixels). Each chopper plateau lasts for 0.4 second (16 readouts on-board) producing 4 frames per plateau in the down-link. The full 3x25 chopper cycles per nodposition are completed in less than 1 minute. The pattern is repeated on the second nod-position. In case of repetition factors larger than 1, the nod-cycles are repeated in the following way (example for 4 repetitions): nodA-nodB-nodB-nodA-nodA-nodB-nodB-nodA to minimise satellite slew times. The minimal duration of this observing mode with calibration and slew overheads is 5.5 min, including the fixed overhead of 3 min for the initial slew to target.

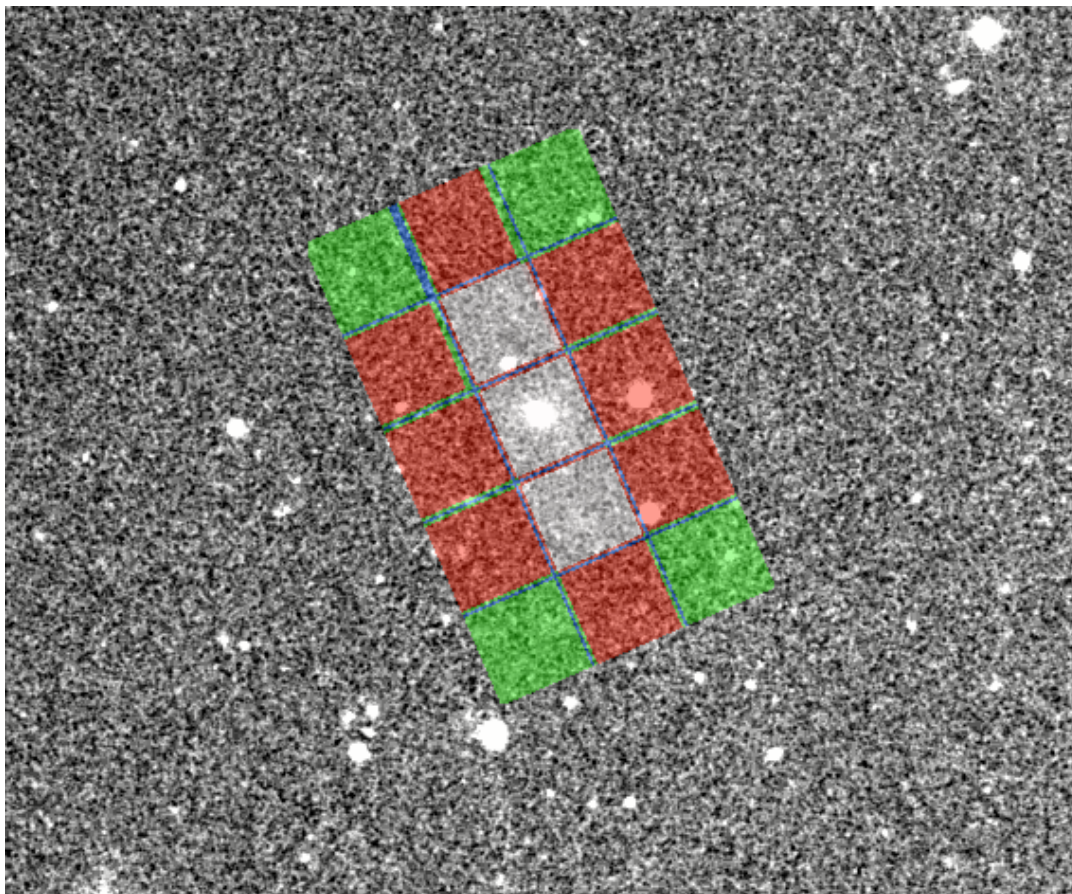


**Figure 5.2.** Exposure map of a point-source AOR in HSpot.

An example of an exposure map as generated by the HSpot exposure map tool for the blue channel is shown in Figure 5.2 .

The chop-nod point-source mode works fine for bright sources and empty fields. But the achieved sensitivities are worse by a factor 1.5-2 compared to the pre-flight prediction and the mini-scan map mode, (see Section 5.4, “Mini-scan map mode”) because the chopping frequency is not high enough to remove the  $1/f$  noise at 3 Hz.

Despite the degraded sensitivity this mode has advantages for intermediately bright sources in the range 50 mJy to about 50 Jy: a small relative pointing error (RPE) of 0.3 arcsec and high photometric reliability and reproducibility .

### 5.1.1. Chopper avoidance angle in point-source mode

In the point-source photometry mode the properly imaged field (i.e. with chopping and nodding) is rectangular : about 52 arcsec x 2.5 arcmin (see Figure 5.2). The user might therefore want to exclude some position angles of the chopping direction to avoid chopping into a bright close-by infrared source.

For this purpose an interval of chopper avoidance angles can be entered in HSpot. The chopper avoidance angle is counted positive east of north, i.e. counterclockwise in the sky, from the north to the direction of the object to avoid, i.e. the +Y spacecraft axis. As the chopper cannot rotate, this effectively defines an avoidance angle for the satellite orientation. Hence it is a scheduling constraint.

The range of position angles that will be available for a given target can be visualized with the AOR footprint overlay functionality for different observing dates in the visibility windows. The exact angle values can be determined with the 'Herschel Focal Plane' overlay functionality.



**Note**

The position angle returned by HSpot in the AOR overlays is the angle from the north to the spacecraft +Z axis counterclockwise, perpendicular to the chopping direction. Therefore the chopper avoidance angle can be derived from the position angle by adding 90 degrees (modulo 180 degrees).

**Warning**

For pointings close to the ecliptic plane, the position angle is constrained to a very narrow range of values : the inclination of the ecliptic plane, and the chopping direction is perpendicular to the ecliptic plane. For such targets, the chopping avoidance angle is at best unnecessary, and at worse renders the observation impossible. For observations at higher ecliptic latitudes, the user shall check that the range of chopping avoidance angles is compatible with the position angles in the visibility windows.

**Warning**

When a chopping avoidance angle is set, the constraint is not yet fed back in HSpot to the visibility calculation, so that the Herschel visibility windows are not affected by that constraint. The user is thus invited to assess himself the impact on the visibility of that constraint.

Table 5.1 lists the user inputs required in HSpot.

**Table 5.1. User input parameters for the point-source AOT mode**

| Parameter name          | Meaning and comments   |
|-------------------------|--|
| Filter                  | which of the two filters from the blue channel to use. In case observations in the two blue filter bands are required to be performed consecutively, two AORs shall be concatenated.   |
| Dithering               | On (dithering enabled) or Off (dithering disabled). A fixed dithering pattern is applied with an amplitude of 2.33 (blue channel) pixels with the chopper. This is intended to improve the flat-field accuracy and to produce better photometric results for faint targets.                |
| Chopper avoidance angle | Interval of position angles for the chopper avoidance zone, modulo 180 degrees. The position angle is counted positive east of north, i.e. counterclockwise in the sky, from the north to the direction of the object to avoid.  |
| Repetition factor       | Number of AB nod cycles to adjust the absolute sensitivity, maximum 120  |
| Source flux estimates   | Optional: point source flux density (in mJy) or surface brightness (in MJy/sr) for each band. It is used for signal-to-noise calculations and to change the ADC to low-gain if the flux in one of the two channel is above the ADC saturation threshold. See Section 5.3 for more details. |

## 5.2. Scan mapping mode

The scan-technique is the most frequently used Herschel observing mode. Scan maps are the default to map large areas of the sky, for galactic as well as extragalactic surveys, but meanwhile they are also recommended for small fields and even for point-sources. Scan maps are performed by slewing the spacecraft at a constant speed along parallel lines, as illustrated in Figure 5.3. The lines are actually great circles which approximates parallel lines over short distances.

The number of satellite scans, the scan leg length, the scan leg separation, and the orientation angles (in array and sky reference frames) are freely selectable by the observer. Via a repetition parameter the specified map can be repeated n times. The performance for a given map configuration and repe-

titation factor can be evaluated beforehand via sensitivity estimates and coverage maps in HSpot. The PACS/SPIRE parallel mode sky coverage maps are driven by the fixed 21 arcmin separation between the PACS and SPIRE footprints. This mode is very inefficient for small fields, the shortest possible observation requires about 45 min observing time.

Available satellite speeds are 20 or 60 arcsec/s. The highest (60"/s) speed (default value) is dedicated for large (galactic) surveys, with a degradation of the PSF in the blue channel, due to the on-board averaging of 4 frames (final 10 Hz sampling).

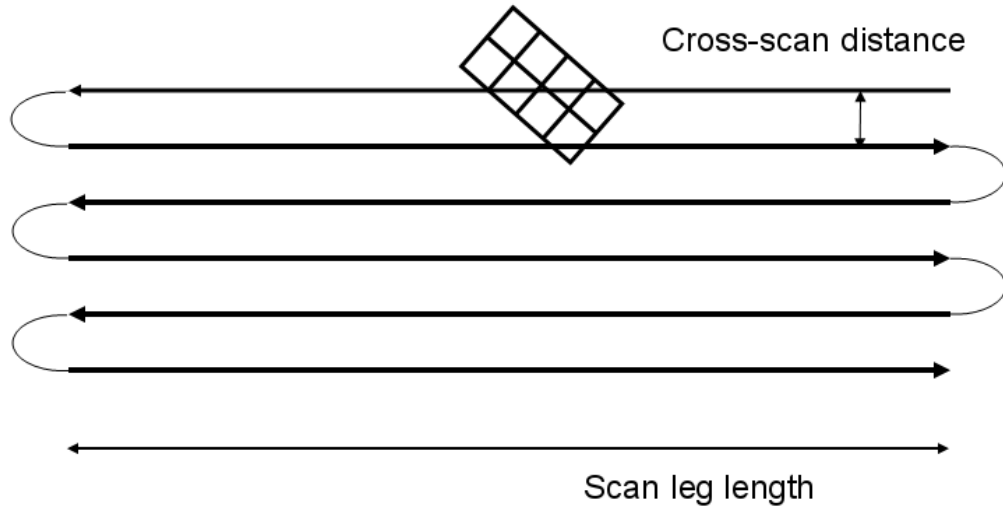


**Figure 5.3. Example of PACS photometer scan map.** Schematic of a scan map with 6 scan line legs. After the first line, the satellite turns left and continue with the next scan line in the opposite direction, just like in the raster map case. The reference scan direction is the direction of the first leg. Note that the turn around between line does take place as simplistically drawn in the figure.

During the full scan-map duration the bolometers are constantly read-out with 40 Hz, allowing for a complete time-line analysis for each pixel in the data-reduction on ground.



**Important**

A combination of two different scan directions, preferably orthogonal is recommended for a better field and PSF reconstruction. and to remove the stripping effects of the  $1/f$  noise. For this purpose two AORs can concatenated in HSpot. In the second AOR the map orientation angle is then increased by 90 degrees to get an orthogonal coverage, for instance 45 and 135 degrees orientation angle when in instrument reference frame.

Most of the PACS prime observations are performed with the 20 arcsec/s scan speed where the bolometer performance is best and the pre-flight sensitivity estimates are nearly met in the blue channel. For larger fields observed in instrument reference frame there is an option to use "homogeneous coverage" which computes the cross-scan distance in order to distribute homogeneously the time spent on each sky pixel in the map.

For short scan legs below about 10 arcmin the efficiency of this mode drops below 50% due to the relatively long time required for the satellite turn-around (deceleration, idle-time, acceleration) between individual scan legs, which takes about 20 s for small leg separations of a few arcseconds. Nevertheless, this mode has an excellent performance for very small fields and even for point-sources.

The advantages of the scan mode for small fields are the better characterisation of the source vicinity and larger scale structures in the background, the more homogeneous coverage inside the final map, the higher redundancy with respect to the impact of noisy and dead pixels and the better point-source sensitivity as compared to a chop-nod observation of similar length.

PACS scan maps can be performed either in the instrument reference frame or in sky coordinates.

### 5.2.1. Scan maps in instrument reference frame

When scan maps are performed in instrument reference frame, an 'array-to-map angle' is chosen observer, The array-to-map angle is the angle from the spacecraft +Z axis to the line scan direction in the first leg, counted positive counterclockwise in the sky. This configuration corresponds to 'reference frame' = 'array' in HSpot and is illustrated in Figure 5.4.

PACS does not have a fixed 'magic angle' like SPIRE, it is left as a free parameter to the user. It is however advised not to use 0 or 90 degrees as gaps between matrices would then stay in the final map, if a sky position is visited only by one scan line leg. An array-to-map angle of 45 degrees allows to get the same depth in two scan maps with orthogonal mapping directions.

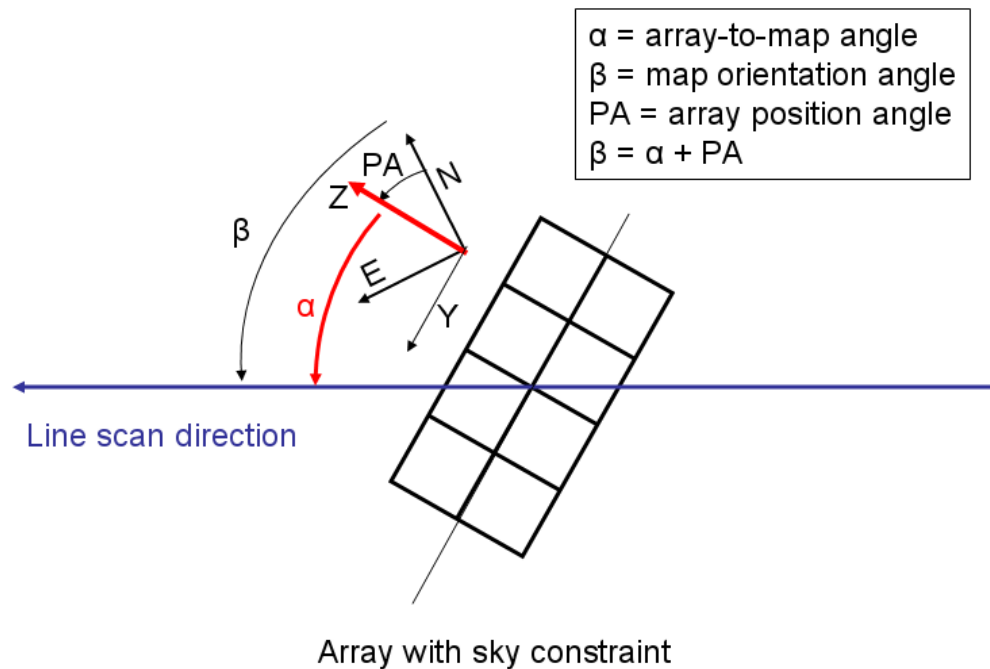


**Figure 5.4. Scan maps in instrument reference frame. The array-to-map angle ( $\alpha$ ), is defined by the user. This effectively defines the map orientation angle in the sky ( $\beta$ ), as the array position angle is not a free parameter, it is function of target coordinates and observation time. However a constraint on the map orientation angle can be put in HSpot.**

In this configuration if the 'homogeneous coverage' parameter is selected, HSpot computes the appropriate distance between scan legs ('cross-scan step') to achieve an homogeneous coverage, which is a function of the array-to-map angle selected above.



**Note**

In the case of a square scan map in instrument reference frame, the orthogonal coverage to cover the same area is achieved by simply adding 90 degrees to the array-to-map angle and recomputing the cross-scan distance. If the array-to-map angle is 45 degrees, the cross-scan distance is even the same.



**Note**

A small array-to-map angle, for instance 10 degrees (modulo 90 degrees), allows to get rid of the effect of gaps between matrices, but also to get a homogeneous exposure map toward the edges for small scan maps, hence minimizing the science time.

Scan maps defined in instrument reference frame should in principle be used to cover square areas, as the orientation of the scan map on the sky can not be known in advance, it depends on the array position angle, which itself depends on the exact observation day.

However in order to cover specific rectangular areas in the sky, a constraint on the orientation of the scan map in the sky can be introduced by selecting a range for the 'map position angle', i.e. the angle from the celestial equatorial north to the scan line direction, counted positively east of north. This corresponds to the option 'array with sky constraint' in HSpot, shown in Figure 5.4.



**Warning**

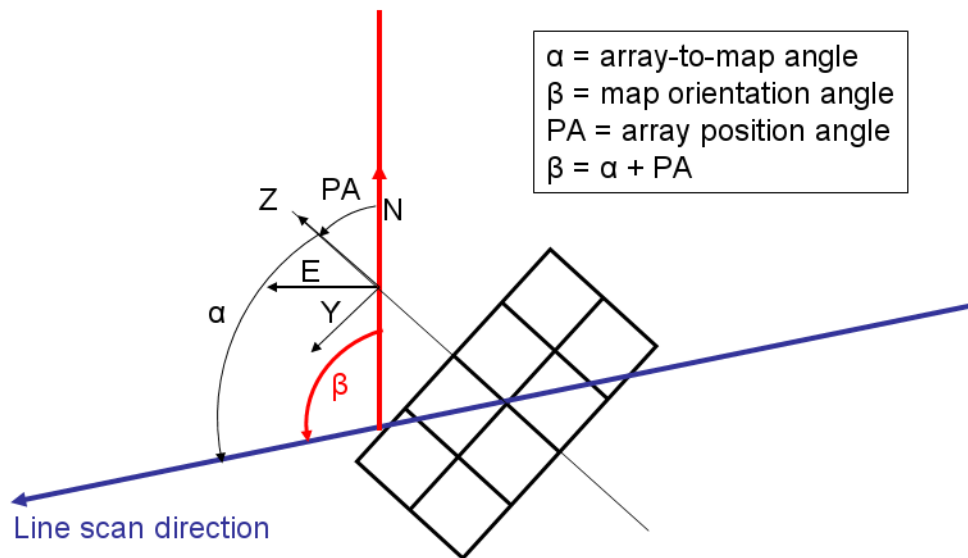
Introducing a sky constraint puts a constraint on the scheduling, and therefore shall be used only if necessary. Moreover certain combinations of array-to-map angle and ranges of map position angle might not be feasible. For instance for pointing close to the ecliptic plane, the array position angle gets constrained to a very narrow range of values (modulo 180 degrees), as the +Z axis is always pointing towards the sun (+/- 1 degree) in the ecliptic plane. Therefore the map orientation angle cannot be too different from the array-to-map angle + 90 degrees (modulo 180). This shall be checked with the overlay AOR facility in HSpot.



**Warning**

When a map orientation angle is set, the constraint is not yet fed back in HSpot to the visibility calculation, so that the Herschel visibility windows are not affected by that constraint. The user is thus invited to assess himself the impact on the visibility of the constraint.

## 5.2.2. Scan maps in sky coordinates



Sky with array constraint

**Figure 5.5.** Scan maps in sky coordinates. The map orientation angle in the sky ( $\beta$ ), is fixed by the observer, therefore there is no control on the array-to-map angle ( $\alpha$ ), which depends on the target coordinates and exact observation time. However a constraint on the array-to-map angle can be put in HSpot.

Another way to define rectangular areas in the sky with scan mapping is to select mapping in sky coordinates, with the option 'sky' in HSpot. In this configuration the map orientation angle is defined by the observer, i.e. the angle from the equatorial celestial north to the line scan direction in the first leg.

However, in this case, there is no direct control of the homogeneity of the map coverage, as the

cross-scan distance to achieve this purpose depends on the array position angle, which itself depends on the exact observation day. The user shall be very careful in selecting a cross-scan distance when in sky coordinates. Values above 105 arcsec may lead to non overlapping legs depending on the array-to-map angle. In order to allow a minimum overlap between consecutive legs, the user is advised not to select a cross-scan distance above 105 arcsec, to be immune against all possible values of the array-to-map angle.



**Note**

A cross-scan distance of 51 arcsec (i.e the size of single blue array matrix) gives relatively flat exposure maps for scan map in sky coordinates, whatever the array-to-map orientation angle.

Conversely the array-to-map angle of scan maps in sky coordinates can be constrained with the option 'sky with array constraint' in HSpot, as shown in Figure 5.5.

Again certain combinations of map orientation angle and constraints on array-to-map angle might be impossible, this shall be checked by the user with the overlay AOR functionality of HSpot.

Table 5.2 lists the user input parameters required in HSpot in scan map mode.

A decision tree to choose the most appropriate orientation reference frame a scan map is given in Figure 5.6.

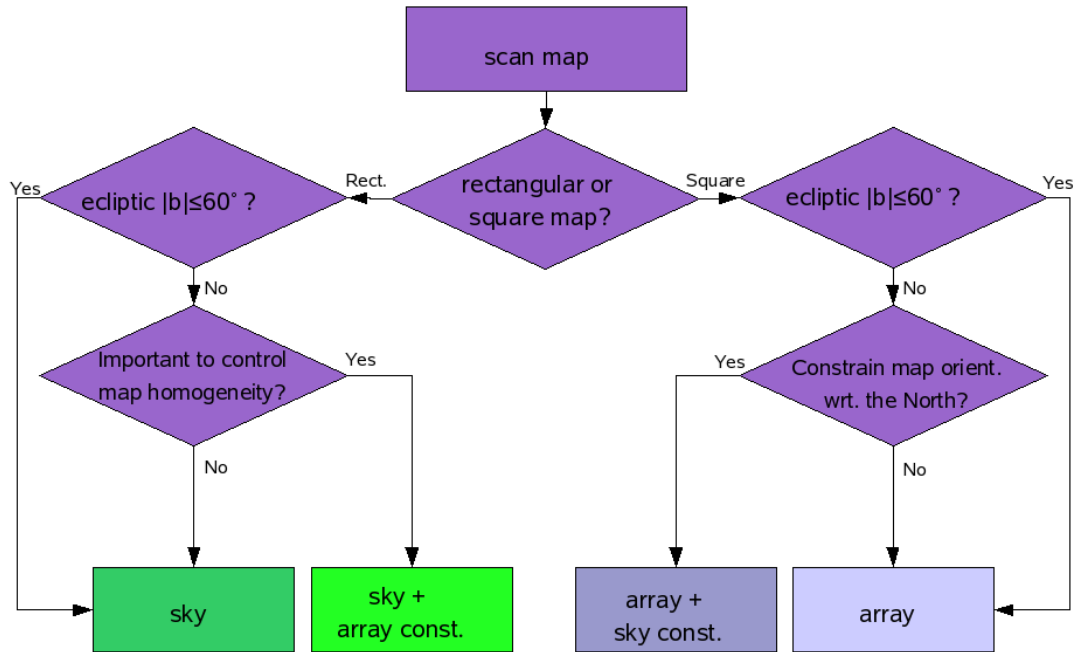


Figure 5.6. Decision tree for scan maps orientation reference frame.

Table 5.2. User input parameters for scan map mode

| Parameter name              | Signification and comments  |
|-----------------------------|---|
| Filter                      | which of the two filters from the blue channel to use. In case observations in the two blue filter bands are required to be performed consecutively, two AORs shall be concatenated.  |
| Orientation reference frame | The reference frame for the scan map orientation, "array" or "array with sky constraint" for instrument reference frame. "sky" or "sky with array constraint" for sky coordinates scans.  |
| Orientation angle           | Array-to-map angle if scan in instrument reference frame (see Figure 5.4), or map orientation angle if scan in sky coordinates (see Figure 5.5), in degrees.  |
| Orientation constraint      | Map orientation angle range if scan in instrument reference frame (see Figure 5.4), or array-to-map angle range if scan in sky coordinates (see Figure 5.5).  |
| Scan speed                  | Slew speed of the spacecraft, either high (60 arcsec/s) or standard (20 arcsec/s).  |
| Scan leg length             | Length of a line scan leg, the maximum length is 20 degrees   |
| homogeneous coverage        | If selected ('Yes'), HSpot computes the exact cross-scan distance in order to perform a homogeneous coverage, i.e. a scan map where the time spent on each sky pixel of the map is approximatively the same (discarding gaps between matrices). This choice is available only when the scan map is performed in instrument reference frame ('array'). |
| Cross-scan distance         | Distance between two scan legs, maximum = 210 arcsec, i.e. the long side of the bolometer array   |
| square map                  | If selected ('Yes'), HSpot computes the number of scan legs in order to complete a square map in the sky, which is recommended for scan maps performed in instrument reference frame, where the orientation of the map in the sky is not known in advance. However do not use in the mini-scan map case.  |
| Number of scan legs         | Number of parallel line legs in the scan map, the maximum 1500, but there is additional limit of 4 degrees for the with of the scan map, i.e. the total cross-scan distance. In case of repetition factor > 1, it is recommended to use an even number of scan legs to minimize the satellite slew overheads.   |
| Repetition factor           | number of times to repeat the scan map to adjust the absolute sensitivity, maximum 100  |
| Source flux estimates       | Optional: point source flux density (in mJy) or surface brightness (in MJy/sr) for each band. It is used for signal-to-noise calculations and to adjust the ADC to low-gain if the flux in one of the two channel is above the ADC saturation threshold. See Section 5.3 for more details.  |

### 5.2.3. Scan maps sensitivity

HSpot returns the both the averaged point-source predicted sensitivity across the map, in the column "Averaged point-source sensitivity" in the "instrument performance summary" window.

The sensitivity in the central area can be significantly better for small scan maps, where the coverage map is highly peaked towards the centre, for instance in the mini-scan map mode.



**Warning**

HSpot also returns a "central area point-source sensitivity" but this works only in the case of the mini-scan map mode

Alternatively the sensitivity can be assessed with the exposure map tool (Overlays --> Show exposure map on current image), which returns the integration on the sky in seconds from the coverage map. The point-source sensitivity can be derived by scaling the  $1\sigma$ -1 second sensitivity values given in Table 3.3 with the square root of the integration time, given by the exposure map tool, as follows:

$$\text{Sensitivity } (1\sigma) = S_0(1\sigma-1s) / \sqrt{T}$$

with  $S_0(1\sigma-1s)$  the sensitivity values given in Table 3.3 and  $T$  = on-sky integration time in seconds.

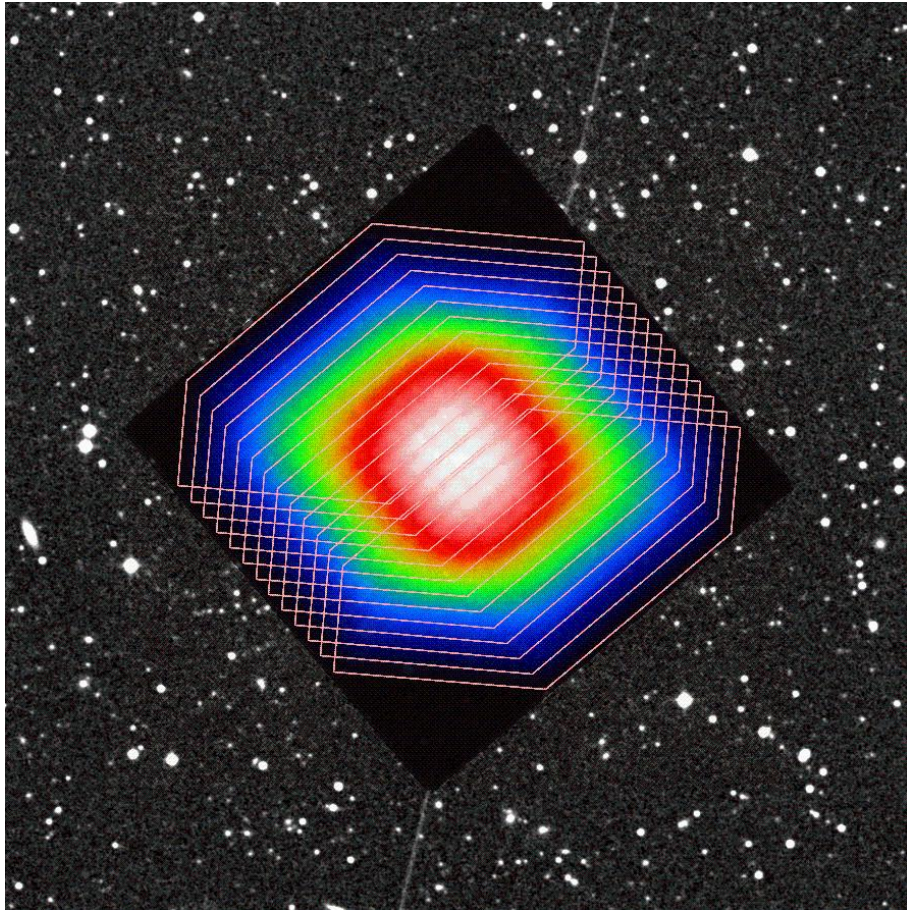


Figure 5.7. Example of a depth of coverage map for a small scan map as given by HSpot together with AOR display overlaid.

## 5.3. Gain setting for bright sources

The selection of the correct gain ("LOW" or "HIGH") is driven by source flux estimates given by the observer. The switch to low gain is required for the flux limits given in Table 5.3. Each observation – chop-nod or scan-map – can be repeated several times, driven by the observer-specified repetition factor, to increase the depth of the observation, the sensitivity scaling with the inverse of the on-target integration time (number of readouts).

**Table 5.3. PACS bolometer readout saturation levels (high-gain setting)**

| Filter | Point source [Jy] |
|--------|-------------------|
| Blue   | 220               |
| Green  | 510               |
| Red    | 1125              |

This standard ADC gain of the bolometers allows photometry on a large flux density dynamical range, from the mJy level up to about 200-1000 Jy, before the brightest pixel saturates (ADC saturation and not the detector). Hence this standard gain shall be appropriate for almost all types of scientific observations. However for very bright sources, such as planets or stars in star forming regions, a low bias gain could be needed.



**Note**

The low-gain setting increases the flux dynamic range by a factor less than 2, at the expense of losing sensitivity at low flux levels, as the noise is not properly sampled anymore with the low-gain, due to the coarser digitalization.



**Important**

The low-gain shall be used with caution and under exceptional circumstances only. If the low-gain is selected it applies to both the red and the blue channel.



## 5.4. Mini-scan map mode

We advise to use the scan mapping mode even for point-sources, in a so-called "mini-scan map" configuration, with short (3 arcmin) scan legs. The advantages for the scan map mode over the chop-nod point source mode are:

- better point-source sensitivity in all bands as a high-pass filter can be used to remove  $1/f$  noise up to higher frequencies.
- it provides a better characterisation of the close vicinity of the target and larger scale structures in the background
- also targets with positional uncertainties of 10 arcsec or more are still perfectly covered
- the final map has a much larger area of homogeneous coverage (about 50 arcsec in diameter) depending on observation configuration.
- more pixels see the target, the impact of noisy, variable and dead pixels is less problematic
- no negative beam in final map.

In case of using the scan map mode for point-sources and very small fields we propose the following configuration:

- medium scan speed (20 arcsec/s)
- scan angle in array coordinates along the array diagonal: 110 or 70 degrees
- scan length: 3.0, (the array diagonal has about 4 arcmin). The source is on-array during satellite constant-speed parts if the observer follows the mini scan-map recommendations, but during satellite turn-arounds and acceleration and deceleration phases the source is outside the array. In order to have the source always on-array during all phases one should select a scan-leg length of 2.5 arcmin. Note that scan-legs have to be multiples of 5 arcsec.
- small and even number of scans: 4, 6, 8, 10, ... for minimisation of satellite movements and a match to the array diagonal.
- small leg separation: 2...5 arcsec with the smaller separation for a larger number of scan legs and vice versa (to have the source on-array in all legs). Examples: 8 scan legs of 3 arcmin length and 4 arcsec separation. This map would then match a sky region with the width of about  $3 \times \text{FWHM}$  in the red band with very high coverage.
- repetition factor: as needed to reach the required sensitivity
- cross-scan maps: it allows to apply all kinds of map-making techniques and not just the high-pass filtering. The cross-scans are also useful to obtain higher photometric accuracy for faint sources and better spatial characterisation in the near source vicinity. It is recommended to group/concatenate the 2 cross-scan AORs to minimise slew overheads. Each AOR will have its own 30 s calibration block.

**Warning**

Do not use the homogeneous coverage in mini-scan map mode !

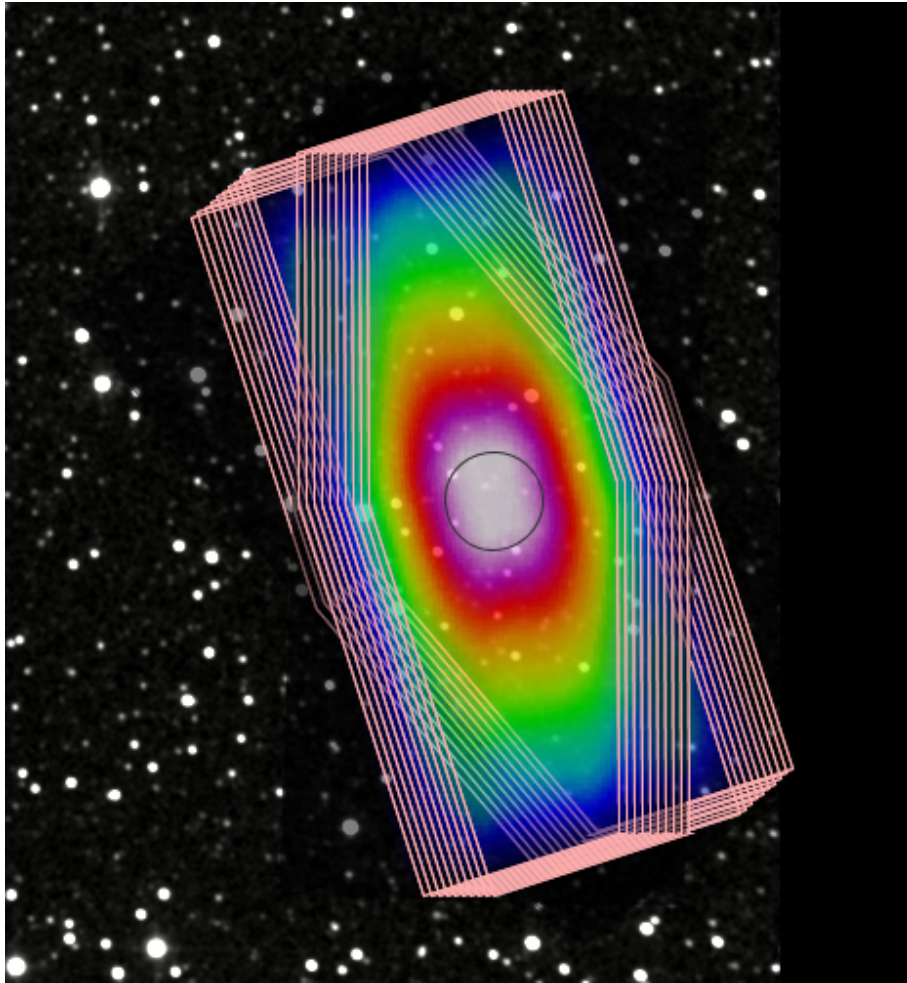


**Figure 5.8.** Coverage map for 2 mini scan-maps at array angles of 70 and 110 degrees. The homogeneous, high-coverage area (circle) is about 50 arcsec in diameter.

The 1 hour point-source sensitivities that can be achieved with this mode are reported Table 3.3



**Note**

The sensitivity in miniscan map mode is returned in the column "central area point-source sensitivity" in the "instrument performance summary" window.

Otherwise the sensitivity in the central area of the mini-scan map mode can also be directly estimated using the formula in Section 5.2.3 and computing T (on source integration time) as follows:

$$T = (\text{scan\_leg\_length}/20) * \text{number\_of\_legs} * \text{map\_repetition\_factor}$$

---

# Chapter 6. Observing with PACS spectrometer

Two observation schemes are offered for the PACS spectrometer: Line Spectroscopy and Range Spectroscopy Astronomical Observing Templates (AOTs).

- **Line Spectroscopy AOT:** A limited number of relatively narrow emission/absorption lines can be observed for either a single spectroscopic FOV (47" x 47") or for a larger raster map. The fixed angular range scanned by the grating mechanism is optimized for a given diffraction order and ensures the detection of the full profile of an unresolved line with sufficient continuum coverage symmetric to the line centre. Faint- and bright line options are available, for bright lines the redundancy in the spectral domain has been compromised in terms of the angular range scanned by the grating.
- **Range Spectroscopy AOT:** This is a more flexible and extended version of the line spectroscopy mode, where a freely defined wavelength range is scanned by stepping through the relevant angles of the grating with selectable grating sampling density (high sampling density and spectral Nyquist sampling mode). Both arrays are used at a time, spectra can be obtained from the combination of nominal- and parallel ranges. This AOT has to be used for long-range spectroscopy as well as for full coverage of broad spectral lines.

There are two PACS spectrometer observing modes used by both AOTs, background subtraction is achieved either **chopping/nodding spectroscopy** (Section 6.1.6) for single lines or larger wavelength ranges on point- or small (diameter less than 5') sources with a clean background within 6', and the **unchopped grating scan** (Section 6.1.8) for single lines or larger ranges on point- or extended sources without clean background for chopping.



#### Note

The **wavelength switching mode** (Section 6.1.9) is planned to be decommissioned, and replaced by the 2nd generation 'unchopped grating scan' mode, the optimized solution for crowded-field spectroscopy. The Herschel Science Centre will announce the release of this mode to PACS observers via Helpdesk, however, AORs can be already created in HSpot 5.0 and later versions for time estimation purposes.



#### Warning

HSpot v5.0 and later versions allow the reading of wavelength switching AORs created by older HSpot versions but time estimation has been disabled and submission to HSC is not possible. These wavelength switching observing requests can be updated to unchopped grating scan mode by switching the mode selector button in HSpot (see below for more details).

The two observing modes can be used in a single pointing, or repeated in a raster pattern on the sky. There are two sets of recommended raster patterns for mapping with full beam sampling: one for compact sources (Section 6.1.5.6), which fit within the instantaneous FOV of the spectrometer, and one for more extended sources (Section 6.1.5.5).

All spectrometer observing requests include a calibration block, a modulated measurement of the two internal calibration sources with the grating in a fixed position. The two sources are heated to different temperatures, hence provide different signal levels. The grating position is chosen to measure a reference wavelength in the bands that are measured in the sky observation. Table 6.1 lists these calibration block wavelengths. The calibration block measurement starts during the slew of the spacecraft to the target in order to optimise the use of observing time.

**Table 6.1. Key wavelengths. The wavelengths observed in the spectrometer calibration block depend on the spectral bands visited in the rest of the observation**

| bands  | wavelength range ( $\mu\text{m}$ ) | blue key wavelength | red key wavelength |
|--------|------------------------------------|---------------------|--------------------|
| B2A/R1 | 103-220                            | 60                  | 120                |
| B3A/R1 | 51-73                              | 60                  | 180                |
| B2B/R1 | 71-105                             | 75                  | 150                |

Based on the continuum and line flux estimates entered by the observer in the HSpot PACS Line/Range Editor tables, the expected maximum photoconductor signal level is estimated by the observing logic. For range spectroscopy, the expected flux at the maximum response is extrapolated via a Rayleigh-Jeans law from the reference wavelength and corresponding flux estimate. The appropriate integrating capacitance of the CRE is then chosen for the entire observation to avoid saturation. This way, observer's flux estimates can adjust the dynamic range of the observation.



**Warning**

If continuum and expected line fluxes are higher than the saturation limits for the default capacitance, it is mandatory to enter the expected continuum and line flux for every line/range in HSpot. Observations that are saturated because no HSpot flux estimates were entered by the observer will not be considered as failed for technical reasons. Saturation limits are presented in Section 4.11.

## 6.1. Line Spectroscopy AOT

This AOT is intended to observe one or several unresolved or narrow spectral line features, on fixed wavelength range of about 1 micron (but varying from 0.35 to 1.8  $\mu\text{m}$  depending on the wavelength and the grating order).

Only lines in the first (103-220  $\mu\text{m}$ ) and second order (71-105  $\mu\text{m}$ ) combination, or first and third order (51-73  $\mu\text{m}$ ) can be observed within a single AOR, to avoid filter wheels movements. If lines of second and third grating order are to be observed on the same target at the same time, two AORs shall be concatenated. Depending on the requested wavelength/grating order, only the data of one of the two detector arrays is normally of interest to the observer.

The fixed wavelength and its immediate neighborhood is observed for each chopper and grating position. For improved flat-fielding, especially for long integrations, the grating is scanned by a number of discrete steps around a specified centre position such that drifts in the detector responsivity between individual pixels are eliminated. The centre position of a grating scan is the corresponding line peak wavelength.

These grating scans provide for each line and for each of the 5 by 5 spatial pixels a short spectrum with a resolving power of  $\sim 1700$  in its highest resolution covering  $\sim 1500$  km/s but dependent on the wavelength and order.

Up to 10 lines can be studied within one observation. The relative sensitivity between the lines is controlled by using the line repetition factor, in the PACS Line Editor of the "Wavelength Settings" in HSpot, that allows to repeat a line scan several times. While the absolute sensitivity is controlled by the number of observing cycles in the "Observing Mode Settings", by dedicating a larger amount of time to this observation (integer multiples).



**Note**

A maximum of 10 repetitions in total can be specified in the table. For instance, in the case that 10 lines are selected, the "Line repetition" factor has to be 1 for each line; if 3 lines are selected then the total of the 3 repetition factors has to be less or equal to 10 (e.g. 4+5+1 or 2+3+3 ...).

Background subtraction is achieved either through standard 'chopping/nodding' (for faint/compact sources) or through 'unchopped grating scan' techniques (for line measurements especially of bright point- or extended sources) of the grating mechanism. The observer can select either chopping/nodding or unchopped grating scan in combination with one of two observing mode settings: pointed and mapping.

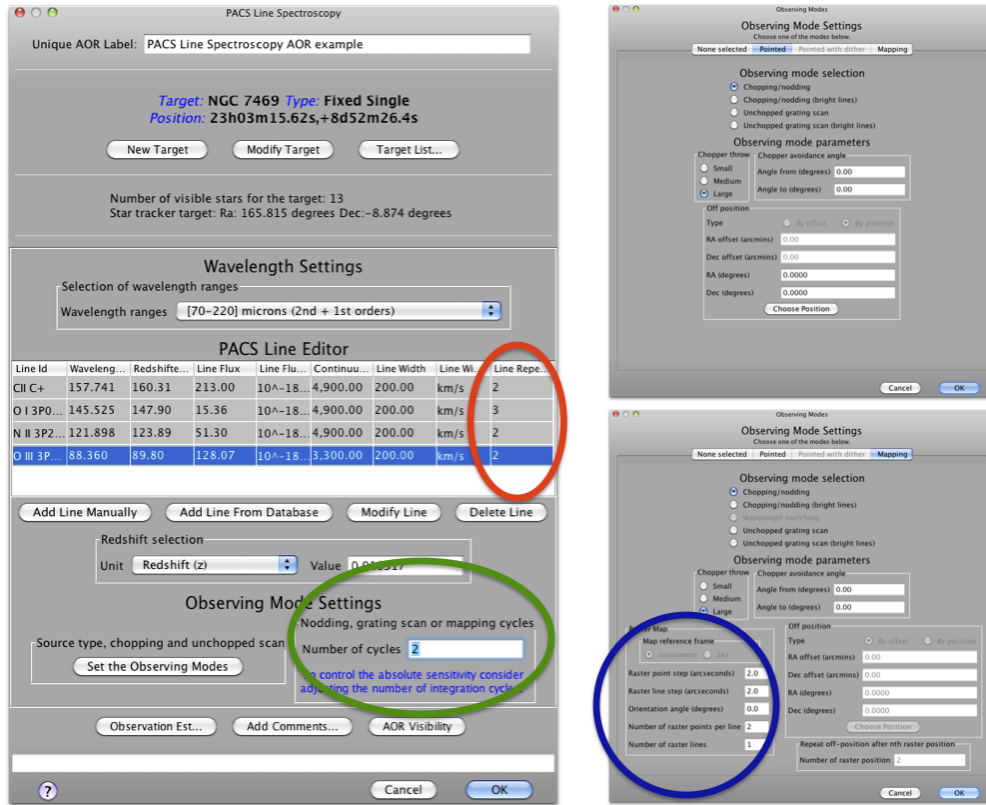


Figure 6.1. The PACS Line Spectroscopy AOT front-end is shown in HSpot v5.0 (left) and the parameter input fields for pointed mode (up right), and for mapping mode (bottom right). The coloured circles indicate ways to adjust the depth of line observations: red shows line repetitions used to adjust the relative depth of various lines in the Line Editor Table; green shows the observing cycles used to adjust the absolute sensitivity; and finally blue in the mapping mode indicates that overlapping footprints in a small raster produce deeper coverage towards the centre of the map.

### 6.1.1. Flux estimates and dynamic range

The uplink logic automatically selects the integrating capacitance based on estimated continuum and line fluxes. If an observation contains lines that fall in different flux regimes, the largest applicable capacitance will be chosen for the entire observation. If lines in the same observation fall in different flux regimes, it is recommended to split the observation into separate observations per flux regime. The HSpot Time Estimator Message (click on "Observation Estimation / PACS Time Estimator Messages") indicates if other than the default capacitance has been selected for a given combination of lines. Please note, a single bright line could trigger capacitance switching in both read and blue channels, i.e. capacitances are always kept in synch between the two channels. In case a bright red line is grouped together with faint lines in the blue channel then the observation will be sub-optimal in the blue. In such a case it is recommended to regroup lines per channel in two separate AORs.

### 6.1.2. Spectral leakage regions

Spectral regions affected by leakage are discussed in Section 4.8. The measured spectrum in these regions may contain superimposed flux originated in the parallel channel, the interpretation of spectral features (unresolved or continuum fluxes) should be avoided without consulting a PACS expert (i.e. contact Helpdesk).

### 6.1.3. Pointed mode

The default mode for point-source spectroscopy, a single pointing on the source. The integral-field

concept allows simultaneous spectral and spatial multiplexing for the most efficient detection of weak individual spectral lines with sufficient baseline coverage and high tolerance to pointing errors without compromising spatial resolution. The PACS spectrometer arrays have 5 by 5 spatial pixels covering a 47 by 47 arcseconds field-of-view respectively, both channels viewing almost identical positions on the sky. The line flux from a point source object will always be collected with the filled detector array, with most the source flux falling on the central pixel. Therefore, for the plain detection of a line source, one pointing is sufficient for a point- or compact source.

This mode allows the observer to set up a pointed observation in combination with chopping/nodding or unchopped grating scan techniques.

### 6.1.4. Pointed with dither mode



**Warning**

HSpot v5.0 and later versions allow the reading of AORs in 'Pointed with dither' mode but time estimation has been disabled and submission to HSC is not possible. This mode has been decommissioned.

It has been proven during the Performance Verification Phase that flux reconstruction from a single pointed observation is as good as in dithering mode, therefore dithering option is not recommended anymore. For sources with a well confined photocenter (point- or compact sources), the pointing mode can be changed from 'Pointed with dither' to 'Pointed'. To maintain the observation integration time, nod repetition and/or scan repetitions should be increased until the original observing time is reached. Nod or range repetition x 3 should be the appropriate change for most observations. Observations requiring spatial oversampling should use a minimum 2x2 size raster with recommended step sizes.

### 6.1.5. Mapping mode

This mode allows the observer to set up a raster map observation in combination with chopping/nodding or unchopped grating scan techniques.

In chop/nod mode, the map can only be defined in instrument coordinates, and the map size shall be restricted to 6' by 6' to obtain clean offset positions with the large chopper throw for each raster position. The user is therefore advised to build a square raster map to be position angle independent, in other words to define a map with the same number of raster points and step sizes on the X and Y axis.



**Note**

Raster lines are performed along the Z-axis (in contrast to photometer raster map where raster lines are along the Y-axis), i.e. perpendicular to the chopping axis, as can be visualized in HSpot with the AOR overlay functionality.

In unchopped grating scan mode the map can be defined in instrument- as well as sky coordinates, with a maximum size of 2 degrees, and sparsely sampled maps are possible.



**Warning**

In mapping mode, the sensitivity given by HSpot refers to each single raster point and does not take into account internal redundancy. The sensitivity shall increase roughly with the square root of the redundancy factor (number of times a sky pixel is seen by a spectrometer spatial pixel).

#### 6.1.5.1. Map orientation reference frame

The recommended raster step/line size settings (see below) have been optimised only for zero degree map orientation in instrument coordinates. In case of applying sky reference frame then optimal spatial sampling cannot be guaranteed because the PACS footprint rotation with respect to the raster line orientation depends on the position angle of the detectors footprint (determined by the day of the observation). The sky reference frame can be selected only in unchopped grating scan mode. Please note, in unchopped grating scan mode the HSpot default option is 'sky' reference, but we highly advise to switch to 'instrument' mode except for cases described in Section 6.1.5.2.

**Note**

Time constraints as well as the chopper avoidance angle may be used to put restrictions on the map orientation angle if the map is defined in 'instrument' reference frame. The time constraint can indirectly limit the array position angle in the optimal range, while the chopper avoidance can be used to avoid a certain chopping direction with respect to the target position (see details in the HSpot Users Manual). Map orientation direction restrictions are possible only for targets at high ecliptic latitude, here the spacecraft orbit may result different position angles at different observing epochs.

### 6.1.5.2. Map orientation in unchopped modes

In unchopped grating scan mode, if an AOR raster covers an elongated area (e.g. a nearby edge-on galaxy) then the observer might have no other option than using sky reference frame and turn the raster to the right direction. If the target is at higher ecliptic latitude then you may select instrument reference frame and put a time constraint on the AOR. The time window can be identified in HSpot "Overlays/AORs on images..." option by changing the tentative epoch of observation. This way the array can be rotated to the desired angle by the time dependent array position angle. Please consult the HSpot Users Manual for a detailed description how to set time constraints and what consequences apply.

If the map is defined in sky coordinates, the map "orientation angle" in the "Observing Mode Settings" HSpot panel can be used to rotate the raster map, this angle is counted from the celestial north to the raster line direction counterclockwise.

If the map is defined in sky coordinates and the observer wants to cover a contiguous area in the sky, under any position angle he shall not define a step size larger than 34 arcsec, i.e. the size of the array (47") divided by  $\sqrt{2}$ .

### 6.1.5.3. Map orientation in chopped modes

Chopped rasters cannot be rotated with a specific orientation angle, the chop direction is hard-coded in instrument reference frame with zero angle orientation (i.e. the chop direction is perpendicular to a raster line). If the target is at higher ecliptic latitude then put a time constraint on the AOR. This way the array and the whole raster can be rotated to the desired angle by a time dependent array position angle.

### 6.1.5.4. Sky mosaics

For raster maps with stepsize greater than 30" (i.e. tiling the sky rather than oversampled rasters) there are no particular recommendations for step sizes. Typical step sizes are 47" (no overlap between the different raster positions) and 38" (approximately one row or column of spatial pixels overlap between the different raster positions).

### 6.1.5.5. Nyquist sampling map of extended objects

For extended objects, mapping with oversampling, i.e. with step size smaller than one spaxel, may be very time consuming. Therefore this mapping strategy is suggested with step sizes larger than one spaxel, but such that the beam is Nyquist sampled. Taking into account that what is defined as raster point step in HSpot corresponds to the spacecraft Z axis, and the line step to the Y axis, the recommended raster step sizes (see ???) for Nyquist sampled maps of larger areas translate to the following HSpot settings:

- **Blue:** point step=16.0", line step =14.5"
- **Red:** point step=24.0", line step =22.0"

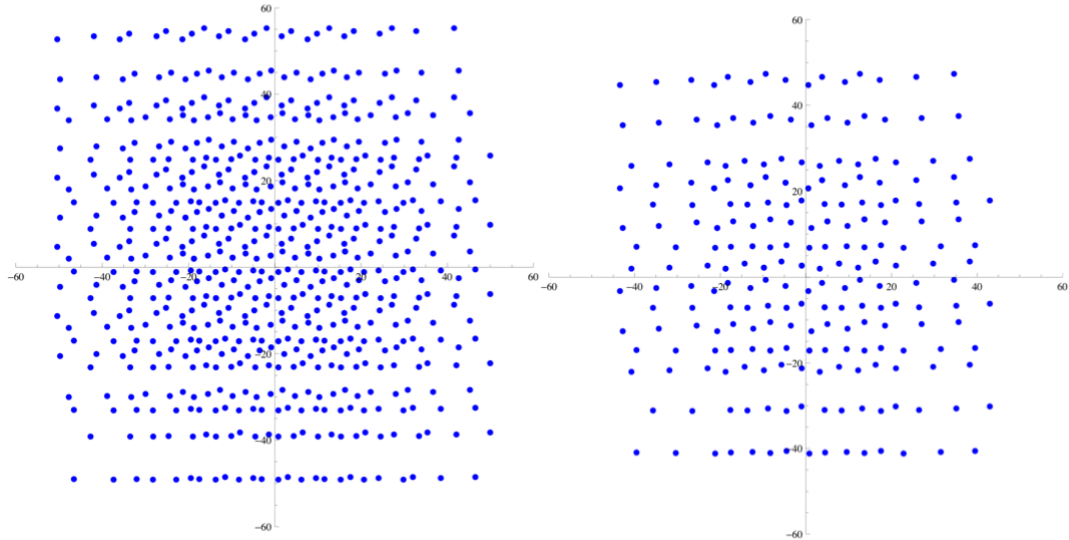


Figure 6.2. Spatial sampling by all PACS spaxels when using a 5x5 raster with step size 14.5''/16'' for the blue (left) and a 3x3 raster with step size 22''/24'' for the red (right)

### 6.1.5.6. Full PACS spatial resolution of compact objects

In order to map the sky at full PACS spatial resolution, step sizes smaller than a spaxel have to be used. Since this increases the observing time, this mode is strongly suggested to be used only for mapping point-like or almost point-like objects. In order to recover the best PACS resolution we recommend the following minimum number of raster positions and maximum step sizes:

- **Blue:** 3x3 raster with step size equal to 3.0'' in both directions
- **Red:** 2x2 raster with step size equal to 4.5'' in both directions



#### Note

For oversampled maps (Section 6.1.5.5 and Section 6.1.5.6) the optimum separation between raster points has been optimised to a reference beam size in the blue and red channels. In case an AOR contains a mix of blue and red lines/ranges then it is recommended to adopt the blue settings.

### 6.1.6. Standard chopping-nodding mode

This mode is called "Chopping/nodding" in the "observing mode settings" panel of HSpot. The chopping technique is the standard way of observing with the PACS spectrometer, this mode is recommended especially for faint lines (below 4-5 Jy peak-to-continuum) combined with faint- or bright continuum. Both line flux and continuum level can be recovered from the data. The mode could be used in a reliable way only if clean off-fields are available within a 6' radius with respect to the target coordinates.

An observing request can contain up to 10 spectral line scans across different bands with the same fixed order selection filter wheel position. For each observer defined wavelength in the PACS Line Editor, the spectrometer performs grating scans with an amplitude such that a given wavelength is seen successively by all 16 spectral pixels. The sampling density per resolution element is higher than 3 samples per FWHM of an unresolved line at all wavelengths with 43, 46 and 48 grating steps in the first, second and third order respectively (see scan parameters in Table 6.2). A single grating scan is repeated in two directions. This up/down scan can be repeated up to 10 times for a single line. Table 6.3 shows the wavelength range covered in the different bands.



**Table 6.2.** Scan parameters in line scan modes. Grating settings are shown for three bands and for the faint- and bright-line options separately; the duration of atomic observing blocks are for a single grating up- and down scan without overheads; the oversampling factor gives the number of times a given wavelength is seen by multiple pixels in the homogeneously sampled part of the observed spectrum.

| band | wavelength range ( $\mu\text{m}$ ) | grating step size | grating steps, faint lines | oversampling factor, faint lines | 1 scan duration (sec), faint lines, chop/nod | grating steps, bright lines | oversampling factor, bright lines | 1 scan duration (sec), bright lines | 1 scan duration (sec), unchopped grating scan |
|------|------------------------------------|-------------------|----------------------------|----------------------------------|--|-----------------------------|-----------------------------------|-------------------------------------|---|
| B3A  | 51-73                              | 168               | 48                         | 41.1                             | 384  | 10                          | 10.0                              | 80                                  | 384   |
| B2B  | 71-105                             | 188               | 46                         | 36.2                             | 368  | 10                          | 10.0                              | 80                                  | 368   |
| R1   | 103-220                            | 240               | 43                         | 27.9                             | 344  | 10                          | 10.0                              | 80                                  | 344   |

**Table 6.3.** Spectral coverage in line scan. The wavelength range seen in a nominal line scan varies over the spectral bands. The column 'highest sensitivity range' refers to the range that is seen by every spectral pixel.

| band | wavelength ( $\mu\text{m}$ ) | full range (km/s) | full range ( $\mu\text{m}$ ) | highest sensitivity range ( $\mu\text{m}$ ) | FWHM ( $\mu\text{m}$ ) | FWHM (km/s) |
|------|------------------------------|-------------------|------------------------------|---|------------------------|-------------|
| B3A  | 55                           | 1880              | 0.345                        | 0.095                                       | 0.021                  | 115         |
| B3A  | 72                           | 799               | 0.192                        | 0.053                                       | 0.013                  | 55          |
| B2B  | 72                           | 2658              | 0.638                        | 0.221                                       | 0.039                  | 165         |
| B2B  | 105                          | 1039              | 0.364                        | 0.126                                       | 0.028                  | 80          |
| R1   | 105                          | 5214              | 1.825                        | 0.875                                       | 0.111                  | 315         |
| R1   | 158                          | 2869              | 1.511                        | 0.724                                       | 0.126                  | 240         |
| R1   | 175                          | 2337              | 1.363                        | 0.654                                       | 0.124                  | 210         |
| R1   | 210                          | 1314              | 0.92                         | 0.441                                       | 0.098                  | 140         |

At every grating position, the detector signal is modulated between on and off source via an [on-off-off-on]-[on-off-off-on] chopping pattern. In order to take advantage of the best spectrometer sensitivity, at every chopper plateau two 1/8 second integrations of the photoconductor signals are recorded. These integration ramps of 1/8 second length are fitted on-board PACS, therefore the signal transmitted to the ground is represented by the slope of the ramp in terms of [ADU/reset interval].

The observer can choose a chopper throw of "Small", "Medium" and "Large" what referring to 6', 3' or 1.5' respectively. The apparent chopper throw is curved on the sky. This rotates the on-source spectral footprint in the two nod positions, and this rotation becomes larger with increasing chopper throw (see Section 4.5).


**Note**

It is recommended to select the "Small" (1.5') chopper throw if applicable for the target (i.e. well isolated point-sources) in order to reduce the effect of field-rotation between the two chop positions (see Figure 6.3).

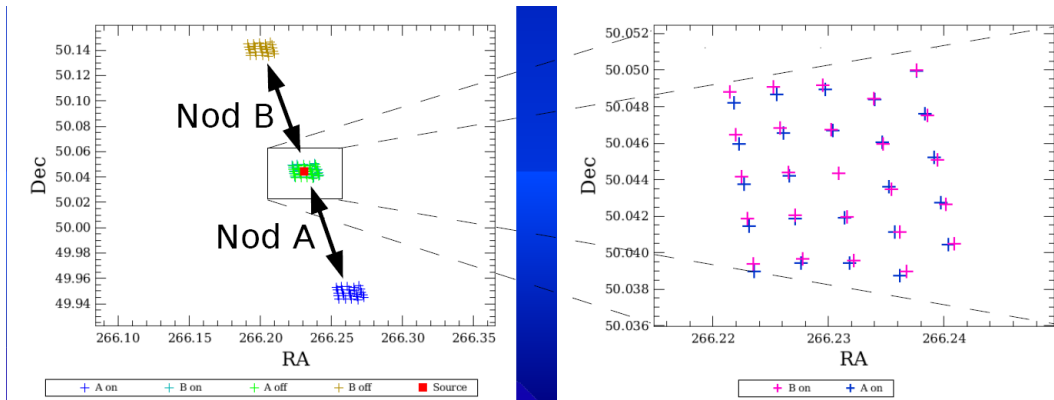


**Figure 6.3. Spatial footprint layout of the chop/nod observing mode: two chopper positions are shown for nod A and B. The zoom in the on-source position reveals the field-rotation between the two chop positions.**


**Note**

In case some disturbing sky features would fall in within the chopper throw radius around the target, the observer has to consider to setup a chopper avoidance angle constraint. The angle can be specified in equatorial coordinates counterclockwise with respect the celestial north. The avoidance angle range can be specified up to 360 degrees with a minimum range of 15 degrees, to avoid too much restrictions on scheduling. Setting up a chopper avoidance angle requires an additional constraint on mission planning, therefore this parameter should have to be used only for observations where it is absolutely necessary.

The sequence of line scans is repeated at two nod positions of the telescope. In the second nod position (nod B), the source is located in the off chopping position of the first nod (nod A). With this technique, one can eliminate the telescope background what happens to be different at the optical angle of the two chop positions:  $F(\text{observed}) = [\text{NodA}(\text{on-off})] + [\text{NodB}(\text{on-off})] / 2 = [(T2+F(\text{source})-T1) + [(T1+F(\text{source})-T2) / 2 = F(\text{source})]$ , where T1 and T2 are the telescope background fluxes at the two chopper positions. (In this term we assume the sky background is negligible compared to the telescope background.) The nod sequence can be repeated within one observation to increase the depth of the observation. Nod cycles are repeated in a way that A-B slew times are minimised, for instance, in case of two repetitions the spacecraft follows the pattern: [A-B-B-A]. In chop/nod mode in total, one half of the science time is spent on-source. The principle of line spectroscopy is illustrated in the diagram of subsequent instrument and spacecraft observing blocks in Figure 6.5.


**Note**

For low number of repetitions (up to 5-6) it is recommended to repeat line scans (increase line repetition factor), while for deeper observations line repetitions should be combined with a number of nod cycles.

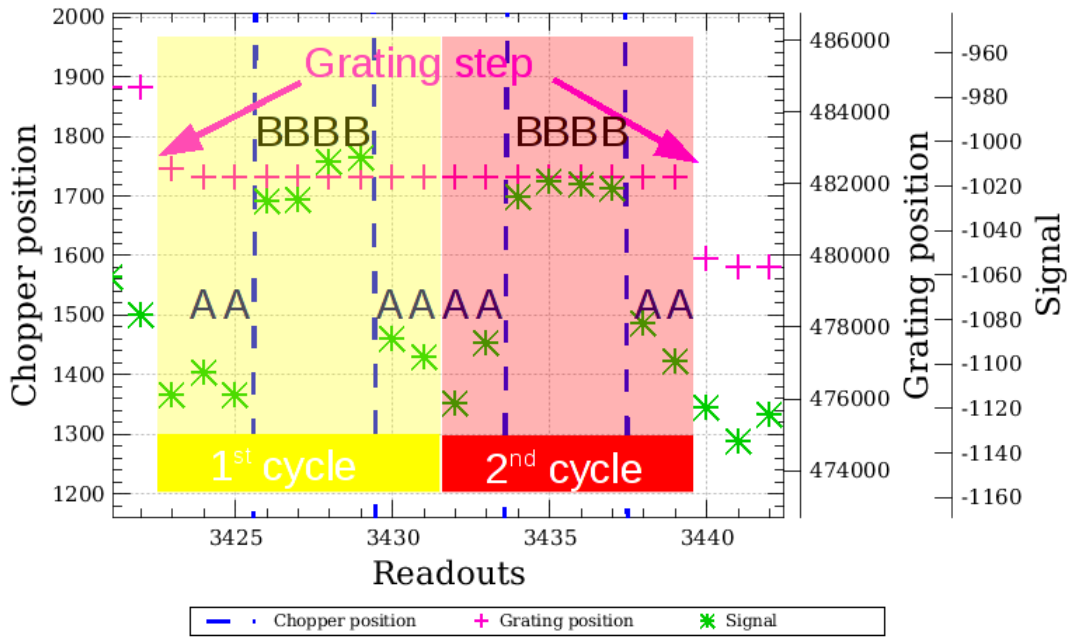


Figure 6.4. At each grating position in an up/down scan 16 ontegration ramps are taken (plus 1 for synchronisation at the beginning). The ABBA sequence represents a chopper [on-off-off-on] cycle which is repeated two times. The duration of such a grating plateau is [8 integrations] x [1/8 sec integration time] x [2 ABBA cycles] = 2 seconds.

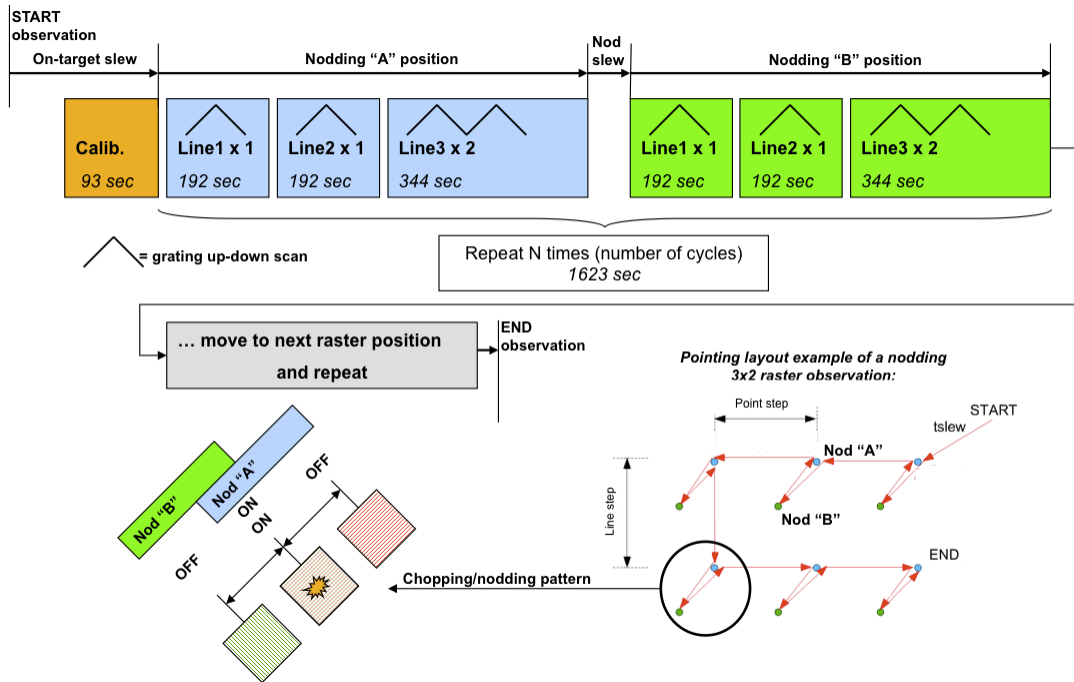


Figure 6.5. Instrument observing blocks are shown for a typical chop/nod measurement combining two lines with single repetition in B3A and a third line with two repetitions in band R1 (3rd + 1st orders setting). Line repetitions adjust the relative depth required for spectral lines, while the number of observing cycle is used to repeat the entire nodding cycle. In the bottom the spatial layout of the chop/nod scheme is sketched. Note, the raster patterns has been distorted for better visibility, in real observations, the nod slew is significantly larger than the raster step size and nodding direction is enforced along the raster columns (vertical direction).

The full wavelength range covered by the scan and the range covered to the highest sensitivity, i.e. the wavelength seen by all 16 spectral pixels are shown in Table 6.3 and compared with respective FWHM of the spectrometer at these wavelengths, for an unresolved line. The spectral coverage in line spectroscopy modes is shown in Figure 6.6. The reference for the wavelength range as specified in HSpot is spectral pixel 8, i.e. the predefined range is not covered by all spectral pixels, and the actual range in the data has S/N going up at the edges.

The spatial layout of a pointed measurement is shown on Figure 6.7 where the 25 spaxels for the four chop/nod position are projected onto the sky.

Chopping and nodding is imposed by the design of the AOT, in other words if chopping/nodding is deselected, the unchopped grating scan is selected instead, as both observing techniques are mutually exclusive.

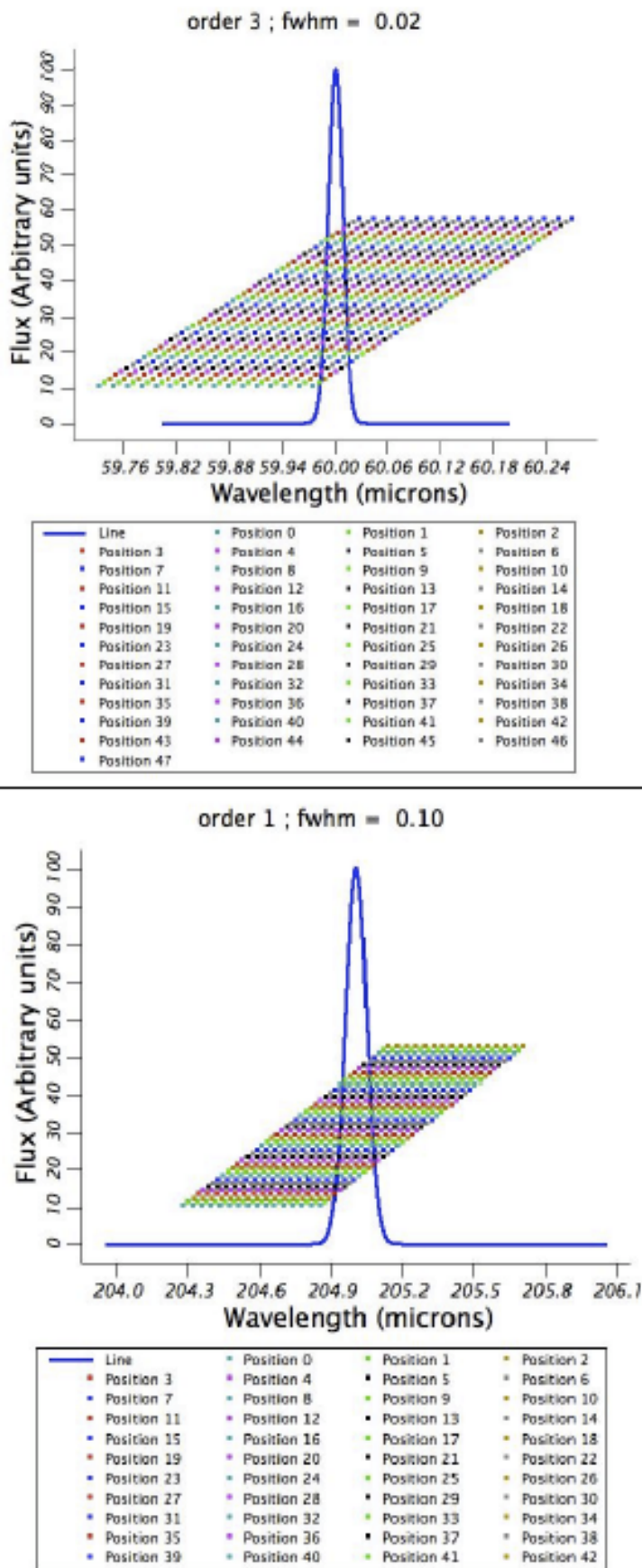


Figure 6.6. Visualization of the line scan AOT on an unresolved PACS line (here given by a Gaussian).

The grating step size and number of grating positions used is the nominal one currently coded in AOT design for standard "faint lines" summarized in Table 6.2. Top row is for a blue line at  $60\mu\text{m}$ ; bottom row is for a red line at  $205\mu\text{m}$ . In bright line mode, grating step sizes are identical but the instrument scans over only the 10 central positions. These scan patterns are identical for chopped- and unchopped modes.

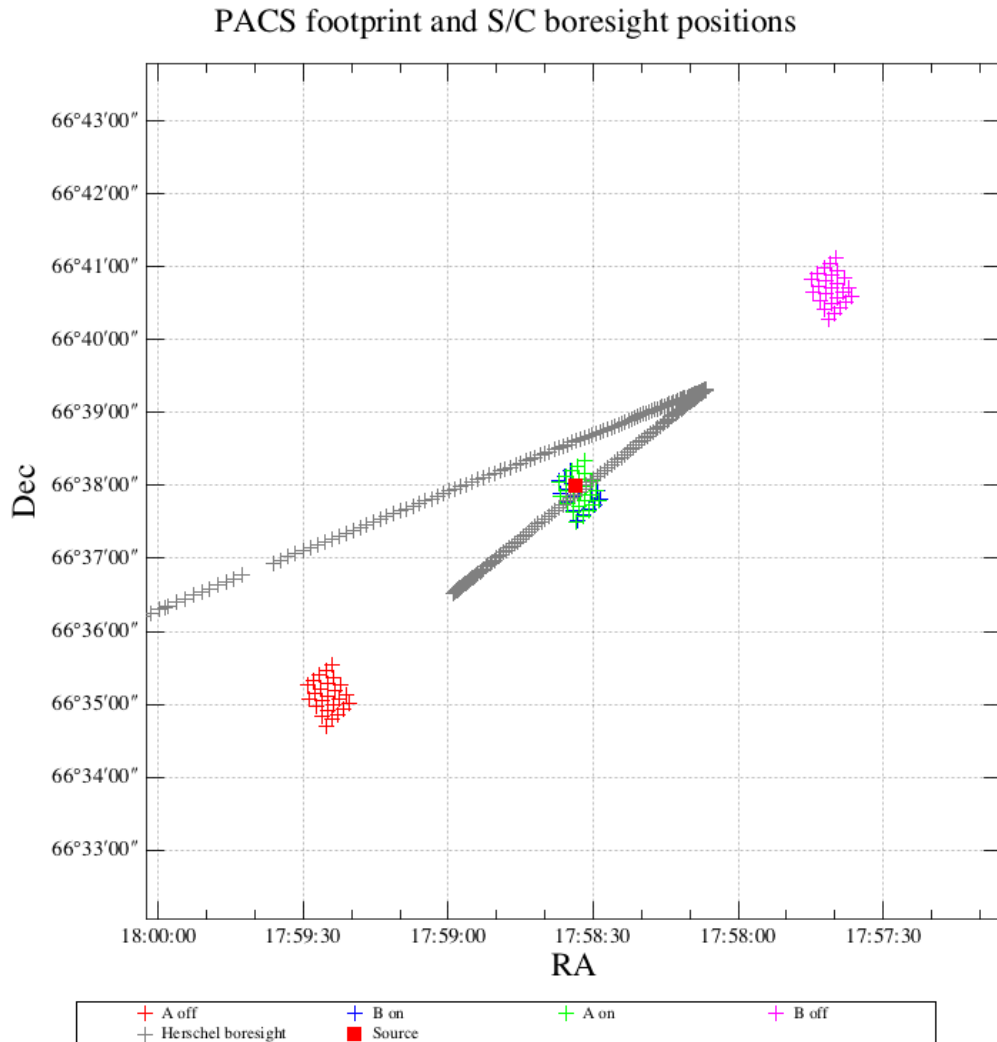


Figure 6.7. The PACS spectrometer footprint of a chop/nod pointed observation is shown for the blue band. The four fields of nod A and B positions combined with chop on- and off fields are plotted as well as the instrument boresight (grey) and target position (red). In this example observation large chopper throw ( $6'$ ) was used which is a result of a symmetrical chopping pattern around the instrument boresight.

### 6.1.7. Bright lines chopping-nodding mode

This mode is devoted to bright lines where it is not needed to spend as much time per line as in the standard chopping/nodding mode with a single repetition. Up and down grating scans are performed but only with 10 grating steps, i.e. the on-sky time about 3-4 times shorter than in the standard chopping/nodding mode depending on the band. A comparison of bright line mode scan parameters can be found in Table 6.2.

The observing efficiency of this mode is rather poor because of fixed incompressible overheads (nod slew time and instrument overheads). The minimum total observing time (one line, one cycle) is

303s versus 583s in the standard chopping/nodding, while it is about twice less sensitive: the sensitivity ratio per resolution element in the highest sensitivity part of the coverage is about 0.6. (Sensitivity ratio is driven by the respective oversampling factors,  $\sqrt{10 / 27.9}$ ) If several lines are observed the modes becomes more attractive, but line repetition factor as well as nodding cycles should be equal or less than 3.

In bright line mode, even for unresolved lines, the central 3 pixels in a 16 pixel module do not "see" the continuum, they scan over the line profile only. This could make difficult a proper response correction as no flat continuum level can be determined for all the pixels.

**Note**

Since the bright line mode scans about 1/4th of the wavelength range scanned in faint line mode for broadened lines this might limit the wavelength extent of the baseline measured.

## 6.1.8. Unchopped grating scan mode

The unchopped grating scan is an alternative to the chopping/nodding mode if by chopping to a maximum of 6' the off position field-of-view cannot be on an emission free area, for instance in crowded-fields or for spectral line mapping of extended objects with diameter larger than 5' respectively. The direct way of acquiring data raises limitations on the applicable flux regime with respect to the standard chop/nod mode. This mode is not recommended for faint lines, target lines needs to be above typically  $\sim 1$  Jy peak-to-continuum and the continuum level can be recovered in a reliable way only for bright sources, i.e. at a minimum continuum level of  $\sim 20$ -30 Jy. The continuum level can be determined by off-position subtraction which could efficiently eliminate the telescope background for bright objects.

### 6.1.8.1. Unchopped faint line mode

In this default version of the unchopped grating scan mode, the line is scanned with the same grating step as in chopped line spectroscopy, i.e., every spectral pixel samples at least every 1/3 of a resolution element. The number of grating steps is fixed to 75 irrespective the spectral band in which the line is observed. Other grating scan parameters and block duration are shown in Table 6.2.

A key element in the unchopped mode is to make this technique robust against instantaneous responsivity changes caused by cosmic ray hits in the Ge:Ga detector pixels. For this purpose, the up/down grating scan have been made much faster than in the chopped mode, and every line repetition requested by the observer is doubled internally by PACS. On every grating position, four integration ramps are taken. Each integration lasts 1/8 s, resulting in a grating scan which is four times faster than the one in chop mode.

The example of an observing block sequence of the unchopped grating scan mode is sketched in Figure 6.8. In the on-source block, the observer defined line repetitions are internally multiplied by two, i.e. a single repetition is made of two fast scans. The on-source integration time in this mode is half the time PACS spends on-source in the chopped mode (including both nod positions).

In pointed mode, following an on-source block the spacecraft slews to an off-position within two degrees radius with respect to the target coordinates. The off-position has to be carefully selected for an efficient subtraction of the telescope background. Ideally, the background sky emission towards the target and towards the off-position is at the same level respectively, and the background field is free of confusing structures (i.e. the 25 spaxels see a similar level of sky emission).

The off-position is always executed with a single repetition, irrespective what the observer has defined for line repetition factor in the PACS Line Editor. This means, the duration and signal-to-noise in the off-position blocks will be lower than the on-target block, if line repetition factor has been set larger than one.

**Note**

The repetition cycle has to be used to increase the exposure, the entire on-off block is repeated as is in the chopped mode. For instance, in two cycles the spacecraft follows an [ON-OFF-OFF-ON] pointing sequence between the two positions. For deep observations, if necessary, the off-position duration could be kept identical to the on-source duration by specifying single line repetitions and higher number of observing cycles. However, this parameterization is inefficient in terms of slew-

ing overheads.



**Note**

While the scheme in the block diagram Figure 6.8 can be executed, it may turn more advisable to rather do this line by line, particularly for rasters with not too frequent off positions.



**Note**

A shorter integration time in the OFF-position results in a RMS noise of the reference continuum higher than that of the source continuum. To avoid to increase the RMS noise when subtracting the OFF-position, the OFF-position data can be binned using larger wavelength intervals. In case of flat continuum, a single value can be computed for the reference continuum.

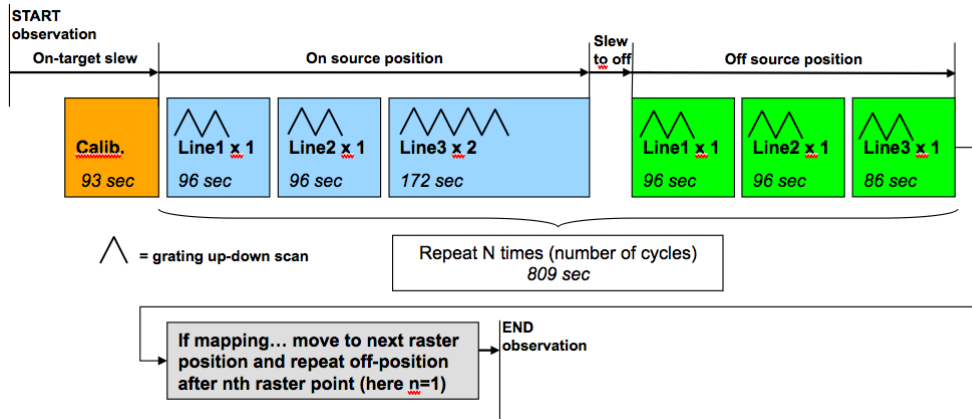


Figure 6.8. Instrument observing blocks are shown for a typical unchopped grating scan measurement combining two lines with single repetition in B3A and a third line with two repetitions in band R1 (3rd + 1st orders setting). Line repetitions adjust the relative depth required for spectral lines, while the number of observing cycles is used to repeat the entire on-off cycle. In this example, the off-position is only 6' away from the target what results only short on-off slewing overhead.

In raster mapping mode the observing block sequence is similar to the chopped mode but here the observer could define the number of raster positions to visit before moving to the off-position.



**Note**

In mapping mode, the observing cycle is repeating the entire raster. At least one OFF-position has to be specified for a single cycle, i.e. the number of raster positions to visit before moving to the OFF-position has to be equal or lower than the number of raster positions [(num. raster lines) x (num. of raster points)]

In raster mode, PACS executes an obligatory OFF-position before the first science block starts at the first raster position. For instance, in case of a 2x2 raster, with a single cycle and with an off position request after 2 raster positions, the following spatial pattern will be executed: [OFF-ON-ON-OFF-ON-ON-OFF]. The same raster with two cycles: [OFF-ON-ON-OFF-ON-ON-OFF-ON-ON-OFF-ON-ON-OFF].

### 6.1.8.2. Unchopped bright line mode

This bright-line option has been made available in HSpot version 5.3.1 and later for science cases where very high signal-to-noise ( $S/N > 100$ ) line detections are expected applying a single line repetition factor. For such bright targets, the integration time can be kept shorter than as is in the default faint-line mode, even on the expense of compromised observing performance.



**Warning**

At the time of the GT2 call, precise sensitivity numbers have not yet been characterized for the bright line mode, however, preliminary validation results indicate a loss of sensitivity not more than a factor two comparing to the default faint-line mode. For more up-to-date information please contact the Herschel Science Centre Helpdesk.



In this mode, grating scan parameters and observing logic remain unchanged, except the number of grating steps visited by a single scan. Instead of applying the default 75 steps, a bright line scan is done through 50 steps, resulting a factor 1/3 reduction in integration time. The shorter duration scan is therefore achieved via a shorter wavelength coverage, the scan speed (number of integration ramps per grating position) has not been changed. Due to instrument and spacecraft overheads the 33% gain in integration time does not apply to the total duration of a bright line AOR. Typically, a bright line AOR is shorter by 25-30% than its faint-line homologue.

**Note**

The shorter wavelength coverage on both sides of the line profile may result a higher uncertainty in the continuum level reconstruction.

## 6.1.9. Wavelength switching mode

The wavelength switching technique/mode is an alternative to the chopping/nodding mode, if by chopping to a maximum of 6 arcminutes, the OFF position field-of-view cannot be on an emission free area, for instance in crowded areas.

**Warning**

The wavelength switching mode has been deprecated in HSpot v5.0 and later versions. For crowded-field spectroscopy, and in more general, for science cases where chopping is not possible it is advised to use the unchopped range scan mode instead. Observers with AORs in wavelength switching mode could still read these observations in HSpot but time estimation is not possible any further.

In wavelength switching mode, the line is scanned with the same grating step as in chopped line spectroscopy, i.e., every spectral pixel samples at least every 1/3 of a resolution element. In wavelength switching we refer to this step as a dither step. At every dither step, the signal is modulated by moving the line over about half of the FWHM. This allows one to measure a differential line profile, canceling out the background (Figure 6.9). The modulation on every scan step follows an ABBBBAA pattern, where A is a detector integration at the initial wavelength, and B is a detector integration at the wavelength switching wavelength. This cycle is repeated 20 times in one direction, and repeated in the reverse wavelength direction. The switching amplitude is fixed for every spectral band.

In order to reconstruct the full power spectrum, a clean off- position is visited at the beginning and the end of the observation. On this position the same scan is performed. In between, the scan is performed at two or more raster positions.

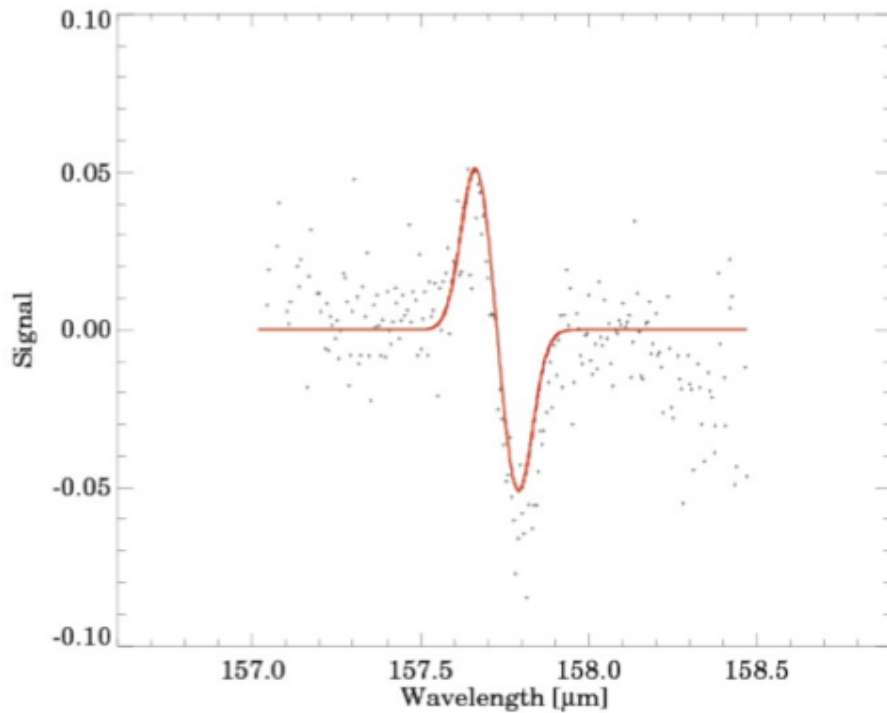


**Figure 6.9. Reconstruction of emission line flux in the differential wavelength switching mode (by fitting a differential Gaussian).**

Wavelength switching can be used for large extended sources since no clean reference is needed. But it shall be used with caution: by definition this technique eliminates the continuum information. Besides the baseline estimates, line profiles are not be reliable if:

- a noticeable gradient is present in the continuum flux over the performed wavelength throw,
- blends of line forests disturb the wavelength switch interval.

Table 6.4. User input parameters for Line Spectroscopy AOT

| Parameter name                  | Signification and comments  |
|---------------------------------|---|
| Wavelength ranges               | <p>Which of the two order combinations to use:</p> <ul style="list-style-type: none"> <li>Option 1 - "[70-220] microns (2nd + 1st orders) " - default option</li> <li>Option 2 - "[51-73] and [103-220] microns (3rd + 1st orders)"</li> </ul> <p>As a result of the selection, the (redshifted) wavelengths of line centres have to be specified in the "PACS Line Editor" table, either within the 70-220 microns band, or within the 51-73 and 103-220 microns band.</p>   |
| Wavelength (microns)            | Mandatory parameter. The rest wavelength of the line centre. If no redshift is specified, the PACS grating will perform an up- and down scan, centred around the line's central wavelength.   |
| Redshifted wavelength (microns) | Parameter calculated by , it appears only in the PACS Line Editor and indicates the redshifted wavelength of the line centre. The bottom pull-down menu allows the reference frame for the redshift to be input.  |
| Line flux unit                  | This menu gives the flexibility to switch between physical input units supported by the PACS AOT logic.   |
| Line flux                       | Optional parameter. User supplied line flux estimate in units specified by the "Line Flux Units" option. Line flux input is used for signal-to-noise estimation as well as for the optimization of the dynamic range. Leaving the parameter as the default 0.0 value means the PACS Time Estimator will not perform signal-to-noise estimation (sensitivity estimates are still provided) and default integration capacitor may be used providing the smallest dynamic range. |
| Continuum flux density (mJy)    | Optional parameter. Continuum flux density estimate at the line (redshifted) wavelength. The value of this parameter is interpreted by the PACS Time Estimator as flux density for a spectrometer resolution element. Leaving the parameter as the default 0.0 value means the PACS Time Estimator will not perform signal-to-noise estimation (sensitivity estimates are still provided) and default integration capacitor may be used providing the smallest dynamic range. |
| Line width unit                 | This menu gives the flexibility to switch between physical input units supported by the PACS AOT logic.   |
| Line width (FWHM)               | Optional parameter. The spectral line full width at half maximum value in units specified by the "Line Width Units" pull-down menu. Line width input is used only for checking purposes. It helps the observer to ensure the specified line width fits within the predefined wavelength range hard coded in the PACS Line Spectroscopy AOT logic  |
| Line repetition                 | Mandatory parameter. The relative line strength (fraction of on-source time per line) is taken into account by specifying the grating scan repetition factor for each line. A maximum of 10 repetitions in total can be specified in the table. For instance, in the case that 10 lines are selected, the "Line repetition" factor has to be 1 for each line; if 3 lines are selected then the total  |

| Parameter name                                    | Signification and comments  |
|---|---|
|   | of the 3 repetition factors has to be less or equal to 10 (e.g. 4+5+1 or 2+3+3 ...). If the sum of repetitions exceeds 10 then you must either remove spectral line(s), or reduce the scan repetition factor(s).  |
| Redshift Selection                                | The redshift selection menu allows the observer to make adjustments to the observing wavelength. The input can be specified either in known radial velocities or redshifts. Once any area in the PACS Line Editor is clicked on the "Redshifted Wavelength" field turns to show the wavelength to be observed.  |
| Nodding, unchopped grating scan or mapping cycles | The absolute sensitivity of the observation can be controlled by entering an integer number between 1 and 100. In chop mode, the on-source time is increased by repeating the nodding pattern the number of times that is entered. For each of the nod positions the sequence of line scans is repeated with the relative depth specified in the PACS Line Editor. In case of unchopped grating scan mode, this cycle is used to repeat the ON-OFF blocks the number of times that is entered.  |
| Chopper throw                                     | The chopper throw and chopper avoidance angle can be selected. The choice of "Small", "Medium" and "Large" refer to 1.5, 3.0 and 6.0 arcminutes chopper throws respectively on the sky. The chop direction is determined by the date of observation; the observer has no direct influence on this parameter. If an emission source would fall in within the chopper throw radius around the target the observer may consider setting up a chopper avoidance angle constraint. The angle is specified in Equatorial coordinates anticlockwise with respect the celestial North (East of North). The avoidance angle range can be specified up to 345 degrees.  |
| Setting the map size                              | The centre of the map is at the coordinates given by the target position. The map size along a raster line can be expressed as the number of raster points per line times the raster point step. In perpendicular direction, the map size is given by the number of raster lines times the raster line step. Mapping parameter ranges are defined as: <ul style="list-style-type: none"> <li>• Raster point step in [2, 480] arcseconds</li> <li>• Raster line step in [2, 480] arcseconds</li> <li>• Number of raster points per line in [2, 100]</li> <li>• Number of raster lines in [1, 100]</li> </ul> Please consult Section 6.1.5.4, Section 6.1.5.5 and Section 6.1.5.6 for instructions how to set up optimal step sizes.  |
| Setting the map orientation angle                 | Selecting the chop/nod mode the map (raster line) orientation is defined by the chopping direction, the observer has no direct access to the map orientation parameter (disabled field). The sky reference frame can be selected only in unchopped grating scan mode. Please note, in unchopped grating scan mode the HSpot default option is 'sky' reference, but we highly advise to switch to 'instrument' mode if suitable for the science case. In unchopped grating scan mode, if an AOR raster covers an elongated area (e.g. a nearby edge-on galaxy) then the observer might have no other option then using sky reference frame and turn the raster to the right direction. If the target is at higher ecliptic latitudes then you may select instrument reference frame and put a time constraint on the AOR. The appropriate time window can be identified in HSpot "Overlays/AORs on images..." option by changing the |

| Parameter name                      | Signification and comments  |
|-------------------------------------|---|
|                                     | tentative epoch of observation. This way the array can be rotated to the desired angle by the time dependent array position angle.  |
| Unchopped grating scan off-position | The off-position can be specified by relative offset in arcminutes with respect the target coordinate, or alternatively, you can define an absolute position within a two degrees radius. In case you prefer to use the absolute position option then it is highly recommended to specify RA/Dec via the standard HSpot target definition window. You can have access to this window by clicking on the "Choose Position" button. This panel is enabled only for the unchopped grating scan mode. |

## 6.2. Range Spectroscopy AOT

Similarly to the Line Spectroscopy AOT, PACS in this mode allows to observe one or several spectral line features or broad ranges (up to ten), but the observer can freely specify the explored wavelength range, or use the predefined full-range templates (SED mode).

Only lines in the first (102-220  $\mu\text{m}$ ) and second order (71-105  $\mu\text{m}$ ) combination, or first and third order (51-73  $\mu\text{m}$ ) can be observed within a single AOR, to avoid filter wheel movements. If lines of second and third grating order are to be observed on the same target at the same time, two AORs shall be concatenated.

This AOT is mainly intended to cover rather limited wavelength ranges up to a few microns in high sampling mode (see below) to study broad lines (larger than a few hundred km/s), which wings would not be covered sufficiently in Line Spectroscopy AOT, or a set of closed lines. But in the second case, the relative depth of the line cannot be adjusted as in the Line Spectroscopy case.



**Note**

Contrary to the Line spectroscopy AOT, there is no way to adjust the range with a redshift for a broad line. The user has to compute the redshifted range to cover in the observation.

The Range Spectroscopy AOT is also intended to cover larger wavelength ranges up to the entire bandwidth of PACS (in SED mode) in low-sampling mode this time, otherwise integration times get quickly prohibitive. But one should remember that the power of the PACS spectrometer is its high spectral resolution rather than continuum sensitivity. Unlike in Line Spectroscopy, depending on the requested wavelength range /grating order, the observer may consider the parallel channel data for an efficient coverage of the required wavelength range, this aspect becomes more important for long-range spectroscopy.



**Note**

HSpot provides information about sensitivity and wavelength coverage in the nominal- as well as in the parallel range(s). For long-range spectroscopy, it is imperative to verify the actual wavelength coverage in both channels, in order to optimize observing strategy.

Similar to Line Spectroscopy, background subtraction is achieved either through standard 'chopping/nodding' (for faint/compact sources) or through 'unchopped grating scan' techniques (bright point- or extended sources) of the grating mechanism. The observer can select either chopping/nodding or unchopped grating scan in combination with one of two observing mode settings: pointed and mapping.

As in line spectroscopy, three chopper throws are available: "Small" (1.5 arcmin), "Medium" (3 arcmin) and "Large" (6 arcmin), except in the mapping mode, where only the large chopper throw is allowed, in order to chop out of the map. In this case the map size is also limited to 4 arcminutes.

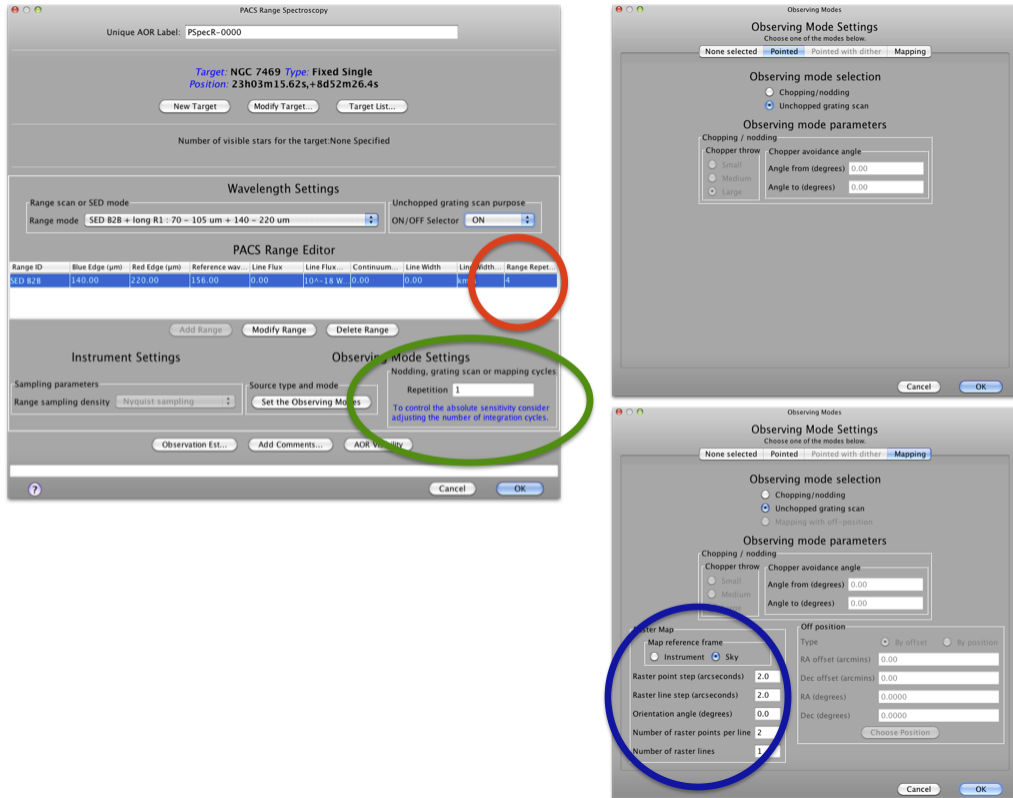


Figure 6.10. The PACS Range Spectroscopy AOT front-end is shown in HSpot v5.0 (left) and the parameter input fields for pointed mode (up right), and for mapping mode (bottom right). The coloured circles indicate ways to adjust the depth of line observations: red shows line repetitions used to adjust the relative depth of various lines in the Range Editor Table; green shows the observing cycles used to apply to adjust the absolute sensitivity; and finally blue in the mapping mode indicates that overlapping footprints in a small raster produce deeper coverage towards the centre of the map.

### 6.2.1. Flux estimates and dynamic range

For bright sources where the default integrating capacitance will result in saturation you need to enter the expected continuum flux, line flux and line width at a reference wavelength in the selected spectral channel: this can be either the nominal or parallel channel. We advise to select the reference wavelength at the highest risk of saturation (see section on saturation limits in Section 4.11). You may check parallel ranges in Figure 6.11, or alternatively, the parallel coverage can be plotted in the HSpot “Range sensitivity plot” as well as printed in the “PACS time estimator message”. The provided continuum flux estimates are used to scale a Rayleigh-Jeans law SED. Then the RJ-law SED is evaluated at the wavelength of the peak response in the red and in the blue range, and in case a non-zero line flux is provided then the peak flux falling on a single resolution element will be added to the continuum (after the RJ-law extrapolation). These flux estimates are used to select the optimal integration capacitor. If an observation contains nominal and parallel ranges that fall in different flux regimes, the largest capacitance will be chosen for the entire observation. If ranges in the same observation fall in different flux regimes, it is recommended to split the observation into separate observations per flux regime.



**Note**

Please note, the SED mode templates in the Range Editor Table do not accept line flux estimates, in these modes you could only specify a continuum flux density estimate at a given reference wavelength.

### 6.2.2. Spectral leakage regions

Spectral regions affected by leakage are discussed in Section 4.8. The measured spectrum in these regions may contain superimposed flux originated in the parallel channel, the interpretation of spectral features (unresolved or continuum fluxes) should be avoided without consulting a PACS expert (i.e. contact Helpdesk).

### 6.2.3. Pointed mode

See Section 6.1.3.

### 6.2.4. Pointed with dither mode



**Warning**

HSpot v5.0 and later versions allow the reading of AORs in Pointed with dither mode but time estimation has been disabled and submission to HSC is not possible. This mode has been decommissioned.

See Section 6.1.4.

### 6.2.5. Mapping mode

See Section 6.1.5.

### 6.2.6. Range scan modes

Range scan options can be selected in HSpot "Wavelength settings / Range scan or SED modes" pull-down menu of the Range Spectroscopy AOT. The following diffraction order combinations are available:

- Range scan in [70-105] and [102-220] microns (2nd + 1st orders)
- Range scan in [51-73] and [102-220] microns (3rd + 1st orders)
- Range scan in [51-73] and [102-146] microns (2nd + 1st orders)

Up to ten wavelength ranges (low- and high wavelength pairs) can be entered either in the 70-105 and 102-220  $\mu\text{m}$  interval (2nd and 1st orders) or in the 51-73 and 102-220  $\mu\text{m}$  interval (3rd and 1st orders). In the third option, the 51-73  $\mu\text{m}$  range is covered in the second diffraction order, the corresponding range in the red channel is 102-146  $\mu\text{m}$ . This option provides higher continuum sensitivity but lower spectral resolution in the 51-73  $\mu\text{m}$  range (see Section 4.10), therefore its use is only recommended for observing broad spectral features, very strong lines or when the primary scientific interest is the determination of the continuum level over long spectral ranges.



**Note**

Band B2A is also superior to B3A (in terms of sensitivity) in cases where the line is resolved. I.e. if the purpose is to detect a broad line (e.g. in ULIRGs or AGN) and measure a flux (rather than have a high resolution line profile) B2A is more sensitive (i.e. faster).

The mode provides two different grating sampling densities of the up/down scans:

- either the **high sampling density**, the same step sizes as in line spectroscopy (Table 6.3) but here for customized ranges, corresponding an objective of more than 3 samples per FWHM of an unresolved line in each pixel at all wavelengths,
- or the coarser **Nyquist sampling** (considering the 16 spectral pixels of the instantaneous PACS coverage), with grating step size of 6.25 spectral pixels.

The reason of applying the faster Nyquist sampling is twofold: broad ranges can be covered within a reasonable amount of time, and deeper observations can be achieved by applying a higher number of up/down scans what provides sufficient redundancy and robustness against response changes on longer time scales (typically longer than half an hour). Scan parameters of range scan mode and full-scan durations are summarized in Table 6.5.


**Note**

The reference for the wavelength range as specified in HSpot is spectral pixel 8, i.e. the specified range is not covered by all spectral pixels, and the actual range in the data set is a bit larger than specified (with S/N going up at the edges).

**Table 6.5. Scan parameters in range scan modes. Grating settings are shown for four grating orders and for high sampling density and Nyquist sampling options separately; the duration of atomic observing blocks are for a single grating up- and down scan without overheads on a full range; the oversampling factor gives the number of times a given wavelength is seen by multiple pixels in the homogeneously sampled part of the observed spectrum.**

| band | wavelength range ( $\mu\text{m}$ ) | grating step size, high density | grating step size, Nyquist/SED | over-sampling factor, high density | over-sampling factor, Nyquist/SED | 1 full scan duration (sec), high density | 1 full scan duration (sec), Nyquist | 1 full scan duration (sec), chopped/un-chopped SED |
|------|------------------------------------|---------------------------------|--------------------------------|------------------------------------|-----------------------------------|--|-------------------------------------|--|
| B3A  | 51-73                              | 168                             | 2220                           | 41.1                               | 3.1                               | 31512                                    | 2384                                | 2728/682   |
| B2A  | 51-73                              | 188                             | 2300                           | 36.7                               | 3.0                               | 28160                                    | 2304                                | 1032/258   |
| B2B  | 71-105                             | 188                             | 2400                           | 36.2                               | 2.8                               | 26728                                    | 2096                                | 2096/524   |
| R1   | 102-220                            | 240                             | 2500                           | 27.9                               | 2.7                               | 34264                                    | 3288                                | parallel range                                     |

In "high sampling density" mode integration times can be very long, for instance a full up/down scan in the first order takes more than 5.5 hours. The time scale of the detector drifts does not allow such a long scan, as the time spend on one nod position will be too long.

In order to improve data quality for deep Nyquist sampled observations, a spectral dithering scheme has been implemented: for repeated ranges the subsequent scans are performed with a small offset so that one spectral resolution element is seen by as many pixels as possible. You can take advantage of this dithering for range repetition factor equal or larger than 2.

The Nyquist sampling shall therefore be the default for large wavelength range coverages as it allows obviously faster scans than the high sampling density option but at the expense of sensitivity.



### Grating angle – wavelength relation in Littow configuration

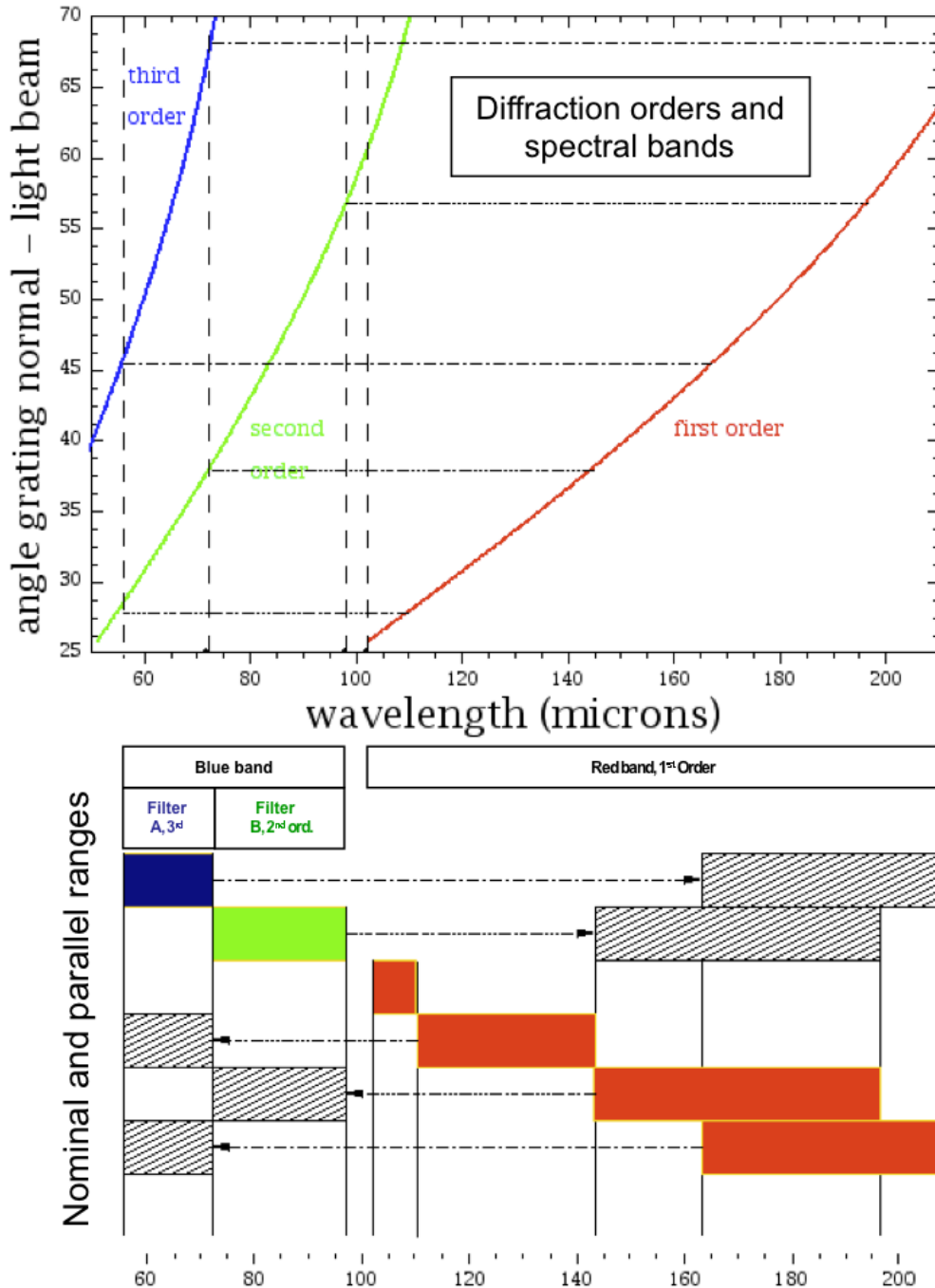


Figure 6.11. Wavelength as a function of spectrometer grating position (incident angle of light beam). Colours represent the three grating orders in use, the chart in the bottom shows nominal- and parallel ranges.

Figure 6.11 shows the parallel ranges covered for a primary defined wavelength range. Note that this information is provided directly in HSpot in the time estimation report as well as in the sensitivity plots. Sensitivity plots can be generated on-line with HSpot including for the parallel range(s) in the other spectral orders covered simultaneously and "for free". The parallel ranges can also be estimated quickly with Figure 6.11. As a general rule:

- for every scan range defined in the 2nd or 3rd order there is a parallel scan covered in the 1st or-

der,

- for a scan defined in the 1st order there might 1 or 2 parallel ranges in the 2nd and 3rd orders.



#### Warning

Grating step sizes are always determined for the primary nominal range! In practice this means, the same wavelength range could be observed with different step sizes depending in which order the range was defined (see Table 6.5). For instance, the 80-90 microns range is observed with step size 188 in the 2nd order but could be covered as well in parallel to the 160-180 microns 1st order range with 240 grating step size. The latter will result sub-optimal wavelength sampling in the 2nd order, therefore observers should always define the primary range for the wavelength of the main scientific interest.

PacsRangeSpectroscopy AOT is suitable for broad lines or for long-range coverage, and conceptually, this template is not meant for observing narrower ranges than what the default wavelength coverage of Line Spectroscopy AOT provides (designed for unresolved lines). This would mean an inadequate use of the system, however, HSpot has no hard protection to prevent observers doing this. In practice, Range Spectroscopy AORs should never be created with fewer grating steps than what Line Spectroscopy would provide at the same central wavelength in the same diffraction order. The actual coverage in grating positions can be found in the Time Estimator Message under "Info for range XX [um]". For instance, an info print line such as "Grat Order/StepSize/NbSteps 2/2400/262" (the last number is in your interest). From this line the value of "NbSteps" can be compared with the Line Spectroscopy design values provided in the 3rd column of Table 6.2. In essence, the number of grating steps in Range Spectroscopy has to be always larger than 168, 188 or 240 in high sampling density in bands B3A, B2B or R1.

In Line Spectroscopy AOT, the highest sensitivity range (uniform coverage) is at least  $\sim 4x$  larger than the FWHM of an unresolved line. In case of Range Spectroscopy AOT the calculation of sufficient margins on both sides of a broad line remains a task for the observer. In order to make sure the entire line profile is fully covered by the uniformly sampled part of the range you need to apply the PACS instantaneous coverage as a margin on both blue- and red-edge of the requested range (in case of high sampling density and especially for faint lines). The wavelength margin is provided in column "Instantaneous spectral coverage (16 pixels)" of Table 4.1.



#### Note

The calculation of highest sensitivity range and adjustment of range borders to the homogeneously sampled part might be a necessary step only for short ranges (i.e. observing broad lines) and only in case of faint detections.

### 6.2.6.1. Standard chopping/nodding mode

The principles of chopping/nodding in range spectroscopy is very similar to its implementation in line spectroscopy as described in Section 6.1.6. In range spectroscopy, chopping/nodding can be combined either with high sampling density scan or with the coarser and shallower Nyquist sampling option.

In order to increase the depth of high sampling density range scans, even for relatively short ranges, it is advised to increase more the number of nodding cycles rather than the range repetition factor, as the timescale of the drifts in detector sensitivities should be considered shorter than an hour they will be better corrected with shorter nodding cycle durations.

The sensitivities for the SED mode and high-sampling density mode mode are displayed in Section 4.10 for a single up-and-down scan and one nodding cycle.



#### Note

Sensitivity plots can be easily produced in HSpot: go to the Range Spectroscopy AOT, define a full wavelength range in Nyquist- or high sampling density and adjust the repetition factors. By clicking on 'Observation estimation' and then 'Range sensitivity plots' a pop-up window will show both line- and continuum sensitivities as a function of wavelength for the integration time defined in the AOR.

## 6.2.6.2. Unchopped grating scan mode

The principles of unchopped mode in range spectroscopy is very similar to its implementation in line spectroscopy as described in Section 6.1.8. In range spectroscopy, the unchopped grating scan mode can be combined either with high sampling density scan or with the coarser and shallower Nyquist sampling option.

We summarize important particularities in range spectroscopy unchopped mode the observer has to be aware of. This mode does not provide a built-in option to visit an OFF-position. The reason behind this feature is related to highly variable timescales: depending on the observer defined wavelength range and sampling density the duration of a single up/down scan could vary between few hundred seconds to few hours, therefore it is unrealistic to automatise the best OFF-position frequency and OFF durations based on the highly flexible range settings. Instead, we advise observers to visit an OFF-position in a separate AOR.

Total integration times over the reference field needs to be equal to the on-source integration, however, the off-integration can be split-up to various individual scans (AORs). For instance, an on-source integration with 4 scans could have two off-scans of each 2 repetitions, one before- and the other after the on-source AORs. In such a case the three AORs need to be concatenated: OFF1-ON-OFF2.

The equal off-integration is a mandatory requirement for range-scans and SED mode observations, since it has been found that the subtraction of the “off” (taken with sufficient S/N) will significantly improve the shape of the continuum, correcting for 2nd order effects in the RSRF. It would be possible to use the same “off” for more than one set of “on”s if the “on” observations were short duration range scans. An “off” observation should be taken either before or after a long range-scan observation. For shorter ranges, the user should try to obtain an “off” every 30-60 minutes.

In brief, the off-position needs to be observed for two purposes:

- 1) For bright sources ( $> 20\text{Jy}$ ) differencing the “on” and “off” can provide a source continuum comparable with chop-nod observations. However experiments have shown that for faint sources responsivity drifts on these long timescales make continuum measurements very uncertain and currently cannot be recovered reliably.
- 2) Observations taken in the “off” position can allow small uncertainties in the relative spectral response function to be corrected in the “on” observation. This is especially valuable for range-scan observations where the subtraction of the “off” can significantly improve the quality of the “on” spectrum.



### Note

In HSpot version 5.3.1 and later a new input field has been introduced "Unchopped grating scan purpose - ON/OFF Selector". You can indicate with this parameter whether the AOR is targeting on-source, or alternatively, the purpose of the observation is taking a reference off-field spectrum. This selector has no impact on commanding, neither on the way the AOR is executed. However, the data processing system will be able to recognize the corresponding OBSIDs (Observation IDs) as on- or off-scans and the pipeline can arrange automatic off-subtraction based on this information. The off-subtracted spectrum will appear as Level 2.5 product in the Science Archive for the on-source OBSID.

## 6.2.7. SED mode

This observing mode is intended to cover the full PACS wavelength range in Nyquist sampling to get the far-infrared SED (Spectral Energy Distribution) of a target. In HSpot, SED options are pre-defined templates with fixed wavelength range and with fixed Nyquist sampling density.



### Note

A full PACS SED is obtained within 1 hour in order 1 (red detector) and order 2 (blue detector) with two PACS range spectroscopy AORs of a single repetition. In these scans, both nominal- and parallel data have to be taken into account.

Three SED options are offered:

- **SED B2B + long R1: [70-105]  $\mu\text{m}$  + [140-220]  $\mu\text{m}$**  data obtained in the first and second diffraction orders, total duration is 2438 seconds.
- **SED B2A + short R1: [51-73]  $\mu\text{m}$  + [102-146]  $\mu\text{m}$** , in the range 55 and 73  $\mu\text{m}$  data obtained in the first and second diffraction orders but covering the short part, total duration is 1310 seconds. This scan offers a better continuum sensitivity in the blue range than the 'SED B3A' option, but a worse line sensitivity because of the much worse spectral resolution of the 2nd order compared to the 3rd order.
- **SED B3A + long R1: [47-73]  $\mu\text{m}$  + [140-219]  $\mu\text{m}$** , For sources where the order 3 spectral resolution is required e.g. because you look at a source with a rich line spectrum where lines can be blended, this additional AOR of 3110 seconds can be added.



**Note**

To cover the full PACS spectrometer wavelength range (51-220  $\mu\text{m}$ ), two AORs in 'SED B2B' and 'SED B2A' and/or 'SED B3A' have to be concatenated. A single AOR can have only a single SED option defined.

For deeper exposure increase the range repetition factor. A spectral dithering scheme has been implemented for SED scans similar to the Nyquist sampled range scans: the different scans will be performed with a small offset so that one spectral resolution element is seen by as many pixels as possible. In case more than two SED scans are required then it is advised to combine range repetitions with observing cycles.

Table 6.6. User input parameters for Range Spectroscopy AOT

| Parameter name     | Signification and comments  |
|--------------------|---|
| Wavelength ranges  | <p>Which of the torder combinations to use or SED templates:</p> <ul style="list-style-type: none"> <li>• Option 1 - "Range scan in [70-105] and [102-220] microns (2nd + 1st orders)" - default option</li> <li>• Option 2 - "Range scan in [51-73] and [102-220] microns (3rd + 1st orders)"</li> <li>• Option 3 - "Range scan in [51-73] and [102-146] microns (2nd + 1st orders)"</li> <li>• Option 4 - <b>This mode has been deprecated.</b> "SED Red [71-210] microns (2nd + 1st orders)"</li> <li>• Option 5 - <b>This mode has been deprecated.</b> "SED Blue [55-73] microns (3rd order)"</li> <li>• Option 6 - <b>This mode has been deprecated.</b> "SED Blue high sensitivity [60-73] microns (extended 2nd order)"</li> <li>• Option 7 - "SED B2B + long R1: [70-105] <math>\mu\text{m}</math> + [140-220] <math>\mu\text{m}</math>"</li> <li>• Option 8 - "SED B2A + short R1: [51-73] <math>\mu\text{m}</math> + [102-146] <math>\mu\text{m}</math>"</li> <li>• Option 9 - "SED B3A + long R1: [47-73] <math>\mu\text{m}</math> + [140-219] <math>\mu\text{m}</math>"</li> </ul> <p>As a result of the selection, the wavelengths ranges to be specified in the "PACS Range Editor" table have to be, either within the 70-220 microns band, or within the 51-73 and 103-220 microns band.</p> |
| ON/OFF Selector    | Optional parameter. Default value is "Undefined", if unchopped grating scan mode is enabled then either "ON" or "OFF" can be selected depending on the purpose of the observation.  |
| Blue edge(microns) | Mandatory parameter. The starting wavelength of the range to be observed. The PACS grating will perform an up and down scan starting at this wavelength. The "Blue Edge" must have a shorter wavelength than the "Red Edge", the minimum permitted separation is 1 micron. Note, sampling by the 16 pixels is not homogeneous at the border of ranges, i.e. the S/N increases at the two extremities. Observers need to broaden ranges if homogeneous S/N is an issue for the observation.  |
| Red edge(microns)  | Mandatory parameter. The longest red wavelength of the range to be observed. The PACS grating will perform an up and down scan terminating at this wavelength.  |
| Line flux unit     | This menu gives the flexibility to switch between physical input units supported by the PACS AOT logic.   |
| Line flux          | Optional parameter. User supplied line flux estimate in units specified by the "Line Flux Units" option. Line flux input is used for signal-to-noise estimation as well as for the optimization of the dynamic range. Leaving the   |

| Parameter name                                    | Signification and comments   |
|---|--|
|   | parameter as the default 0.0 value means the PACS Time Estimator will not perform signal-to-noise estimation (sensitivity estimates are still provided) and default integration capacitor may be used providing the smallest dynamic range.  |
| Continuum flux density (mJy)                      | Optional parameter. Continuum flux density estimate at the line (redshifted) wavelength. The value of this parameter is interpreted by the PACS Time Estimator as flux density for a spectrometer resolution element. Leaving the parameter as the default 0.0 value means the PACS Time Estimator will not perform signal-to-noise estimation (sensitivity estimates are still provided) and default integration capacitor may be used providing the smallest dynamic range.  |
| Line width unit                                   | This menu gives the flexibility to switch between physical input units supported by the PACS AOT logic.  |
| Line width (FWHM)                                 | Optional parameter. The spectral line full width at half maximum value in units specified by the "Line Width Units" pull-down menu. Line width input is used only for checking purposes. It helps the observer to ensure the specified line width fits within the requested wavelength range.  |
| Range repetition                                  | Mandatory parameter. The relative range strength (fraction of on-source time per line) is taken into account by specifying the grating scan repetition factor for each range. A maximum of 10 repetitions in total can be specified in the table. For instance, in the case that 10 ranges are selected, the "Range repetition" factor has to be 1 for each range; if 3 ranges are selected then the total of the 3 repetition factors has to be less or equal to 10 (e.g. 4+5+1 or 2+3+3 ...). If the sum of repetitions exceeds 10 then you must either remove spectral range(s), or reduce the scan repetition factor(s).                                 |
| Nodding, unchopped grating scan or mapping cycles | The absolute sensitivity of the observation can be controlled by entering an integer number between 1 and 100. In chop mode, the on-source time is increased by repeating the nodding pattern the number of times that is entered. For each of the nod positions the sequence of line scans is repeated with the relative depth specified in the PACS Range Editor.  |
| Chopper throw                                     | The chopper throw and chopper avoidance angle can be selected. The choice of "Small", "Medium" and "Large" refer to 1.5, 3.0 and 6.0 arcminutes chopper throws respectively on the sky. The chop direction is determined by the date of observation; the observer has no direct influence on this parameter. If an emission source would fall in within the chopper throw radius around the target the observer may consider setting up a chopper avoidance angle constraint. The angle is specified in Equatorial coordinates anticlockwise with respect the celestial North (East of North). The avoidance angle range can be specified up to 345 degrees. |
| Setting the map size                              | <p>The centre of the map is at the coordinates given by the target position. The map size along a raster line can be expressed as the number of raster points per line times the raster point step. In perpendicular direction, the map size is given by the number of raster lines times the raster line step. Mapping parameter ranges are defined as:</p> <ul style="list-style-type: none"> <li>• Raster point step in [2, 480] arcseconds</li> <li>• Raster line step in [2, 480] arcseconds</li> <li>• Number of raster points per line in [2, 100]</li> </ul>   |

| Parameter name                    | Signification and comments  |
|-----------------------------------|---|
|                                   | <ul style="list-style-type: none"> <li>• Number of raster lines in [1, 100]</li> </ul> <p>Please consult Section 6.1.5.4, Section 6.1.5.5 and Section 6.1.5.6 for instructions how to set up optimal step sizes.</p>  |
| Setting the map orientation angle | <p>Selecting the chop/nod mode the map (raster line) orientation is defined by the chopping direction, the observer has no direct access to the map orientation parameter (disabled field). The sky reference frame can be selected only in unchopped grating scan mode. Please note, in unchopped grating scan mode the HSpot default option is 'sky' reference, but we highly advise to switch to 'instrument' mode if suitable for the science case. In unchopped grating scan mode, if an AOR raster covers an elongated area (e.g. a nearby edge-on galaxy) then the observer might have no other option then using sky reference frame and turn the raster to the right direction. If the target is at higher ecliptic latitudes then you may select instrument reference frame and put a time constraint on the AOR. The appropriate time window can be identified in HSpot "Overlays/AORs on images..." option by changing the tentative epoch of observation. This way the array can be rotated to the desired angle by the time dependent array position angle.</p> |

---

# Chapter 7. Pipeline processing and data products

This chapter describes :

- the standard processing steps (pipeline) for the different photometry and spectroscopy observation modes of the PACS instrument. The pipeline steps are coded as java/jython tasks using well-defined interfaces. To be able to use the most recent calibration information version controlled calibration files (FITS format) are loaded during the pipeline processing.
- the different intermediate formats of the PACS data throughout the reduction (For a more detailed description of the pipeline, refer to the PACS Data Processing User's Manual).

## 7.1. PACS photometer standard data processing

### 7.1.1. Scan map pipeline processing issues

The current automatic pipeline processing provides reductions up to PACS photometer level 1 (detector readouts calibrated and converted to physical units) and level 2 products (fits maps). At this point in the Herschel mission, the goal of the pipeline is to deliver useable, but not necessarily optimal, products. Instead, the automatic pipelines are optimized for stability, speed and delivering browse quality data. The pipelines are expected to mature as both the instrument effects and the understanding on how to mitigate said effects evolves. The major data processing modules of the pipeline are discussed below:

- **Cosmic rays removal:** The default deglitching algorithm for PACS photometer is the multi-resolution median transform (MMT), which uses wavelet scales (Starck et al, 1998, PASP, 110, 193S) to differentiate between a cosmic ray hit and signal. The method produces reasonable results except for bright point-like sources (e.g. compact galactic nuclei, etc.) and fast (60"/sec) scan speeds. Under such conditions, MMT incorrectly masks point source cores. Users are advised to check the coverage map to look for any gaps in exposure depth at the location of point sources. The optional module, "2nd order deglitching" can be used in the interactive data processing as a replacement for MMT deglitching. "2nd order deglitching" uses spatial redundancy and sigma-clipping to reject cosmic ray hits.
- **Cross-talk correction:** The red bolometer array shows cross-talk between column 0 and 16. That is, when a source is present in column 16, its flux is also observed in column 0. Investigations on proper removal of cross-talks are underway. Users are currently advised to mask all signal in columns 0 and 16 to avoid any artifacts from cross-talk in the final maps when observing very bright (point-)sources
- **Offset drift correction:** Offset drift correction is performed by applying a simple high-pass filter on the data. This is adequate for point source fields, but not for structured fields and may result in dark halo artefacts. Increasing the filter window so that it covers a scan leg length already improves the map in the case of structured objects.
- **Map reconstruction:** Map reconstruction with photProject is a simple projection of the data cube on the map grid, considering the intersection areas of the native pixels with the map pixels. For this purpose the ra/dec coordinates of the four corners of each detector pixel in the cube are computed on the fly in photProject. An alternative, optimal map maker, MADmap (Cantalupo et al. 2009), is provided in the data processing environment. This is a java implementation of the original MADmap C code. MADmap uses optimal map-making techniques to produce the best-fit solution for the final reconstructed maps. The primary advantage of MADmap is that it does



not require the use of high-pass filter to mitigate  $1/f$  noise and thus preserves spatial structures up to the size of final maps. Currently, MADmap is only available as an interactive tool and requires pre-processing to remove correlated signal drifts prior to optimal map reconstruction. MADmap additionally requires apriori knowledge of the detector noise properties (as the inverse of the time-time noise correlation matrix). Investigations on the noise filters are underway from the in-flight data. Current version of the data processing environment relies on pre-launch estimates from ground-based tests. Users wishing to use MADmap for their data processing needs should contact the helpdesks at ESA or NHSC for further information.

## 7.1.2. Level 2 pipeline products for scan maps generated with HCSS in the HSA archive

There are 3 types of products in the level 2 produced by the pipeline for the PACS photometer in scan map mode. MADmap has been disabled from the HSC pipeline with HCSS 2.0, hence the second product (HPPMMAP) is not available in recently processed scan maps observations. These maps are produced by automatic pipeline scripts and shall only be considered as a preview, and not for science directly.

- **HPPPMAPB & HPPPMAPR** stands for "Herschel Pacs Photometer PhotProject MAP Blue/Red" This refers to maps produced by the photProject task, i.e. a simple projection of each frame (10Hz), after running a temporal high-pass filter with a width of  $n=20$  (i.e. subtracting a median with a width of  $2*n+1$  frames). This allows to filter a significant part of the  $1/f$  noise at the expense of removing completely ALL spatial scales larger than this width (i.e. typically larger than 1 arcmin), and creating negative undershooting around bright sources along the scan direction. To preserve extended emission, the pipeline script shall be re-run with higher width in the high pass filtering and masking bright source when necessary or an alternative map-making algorithm/tool. This processing is mostly targeted to detect point-sources with good sensitivity. Scan maps are in Jy/pixel.
- **HPPMMAPB & HPPMMAPR** stands for "Herschel Pacs Photometer MADMap Blue/Red" MADmap maps are currently disabled from the HSC pipeline, until scan and crossed-scan maps can be processed together.
- **HPPNMAPB & HPPNMAPR** stands for "Herschel Pacs Photometer Naive Map Blue/Red" Averaged signal map after pixel-to-pixel offset correction. This image is used by MADmap as its first value for the sky map and is subsequently improved and optimized iteratively as described above, hence the full optimized matrix inversion has not been performed on the data. Again these products are not available in recent HSC pipeline maps.

## 7.2. Spectroscopy processing levels and data products

There is a Herschel-wide convention on processing levels of the different instruments. There are different classes of products created at the Level 0, 0.5, 1 and 2 of the pipeline. A more detailed product description is given in the PACS Data Reduction Guide (PDRG) and also the Herschel Products Definitions Document (HPDD), both of which are available via the HIPE help. Here we give you a summary of these information. For all the products described here the red and blue ranges are separate products. They are identified by an R or a B at the end of the product name. The product names start with HPS, which stands for Herschel Pacs Spectroscopy.

- *Level 0 data:* Level 0 products are complete sets of data as a starting point for scientific data reduction. Level 0 products may reach a data volume of 200 MB/hour. For all standard observing modes, the scientific information is contained in the structures called HPSFITB/R (objects of the Frames class), which constitute the starting point for the pipeline. These contain all measured slopes described in section 2.4.5, i.e. the 18 x 25 x time-line slopes for one camera. Correct interpretation of the signal requires knowledge of the instrument status at every time. That can be found in sub-structures of these Frames, but level0 products also contain many useful additional information, like spacecraft pointing, time correlation, and selected spacecraft housekeeping information, raw data (i.e. un-fitted ramps) for some selected pixels, etc. Finally, level 0 contain the calibration data needed for data analysis. The fit-ramps products (HPSFITB/R) are of dimensions 18 x 25 x time-line, the averaged ramps products (HPSAVGB/R) are of dimensions 18 x 25 x time-line x 4. A fit-ramps HPSFITB/R product contains, for each pixel (18x25), one value for each ramp taken over the course of the observation; these values are the slopes that have been fit to each and every ramp. The averaged-ramps product contains, for each pixel, 4 values per ramp taken over the course of the observation; these being the set-of-4 averages taken for each ramp. The pipeline starts on the HPSFIT products.
- *Level 0.5 data :* Processing until this level is AOT independent. Additional information like processing flags and masks (saturation, damaged pixel, signals affected by chopper and grating transitions) is added, block selections generated, basic unit conversions applied (digital readouts to Volts/s) and for the spectrometer the wavelength calibration (inclusive velocity correction) is done. Also the center of field coordinates are computed for every frame and sky coordinates are assigned for every pixel. The only products here are the fit-ramps, the HPSFITB/R, of dimensions of 18 x 25 x nb of slopes.
- *Level 1 data:* The automatic data generation of level 1 products is partly AOT dependent. Detector readouts are flux calibrated and converted to physical units, in principle instrument and observatory independent. Level 1 processing includes the flux calibration and adds further status information to the product (e.g. chopper angle, masks, etc.). These are the biggest products in the processing chain and may reach 2GB/h in the case of spectroscopy. The spectroscopy Level 1 product (PacsCube - HPS3DB/R) contains fully calibrated 5 x 5 x nb of slopes cubes per pointing/spectral range.
- *Level 2 data:* Further processed level-1 data to such a level that scientific analysis can be performed. Processing to this level contains actual spectra and is highly AOT dependent. For optimal results many of the processing steps involved to generate level-2 data may require human interaction, based both on instrument understanding as well as understanding of the scientific aims of the observation. These data products are at browse quality level and should be suitable for publishing following an interactive enhancement.

The level 2 data product contains noise filtered, regularly sampled data cubes HPS3DRB/R of dimensions  $\lambda \times 5 \times 5$ ; and a combined cube projected on the WCS: HPS3DPB/R of dimensions  $\lambda \times N \times M$ , where 'N' and 'M' are the spatial dimensions of the projected map. This cube is constructed by rebinning the integral field cube (oversampled in wavelength, different projection per wavelength layer due to distortions) onto the same sky / wavelength grid of the instrumental resolution. The cube flux values are Jy/pixel, the wavelength is in microns.

In case of mapping observations (rasters), the pipeline loops over all raster positions and com-

bines the rasters into a single grid by adding up for each new spaxel the fluxes of the contributing old spaxels, multiplied by their overlap weights. The HPS3DP product is worth using even for pointed observations (i.e. no rastering) because it does not just add together, or mosaic, multiple pointings, but also sets the correct spatial grid for each wavelength of your cube: for the PACS spectrometer, each wavelength sees a slightly different spatial position, even for spectra within a single spaxel.

- *Level 3 data:* These are the publishable science products where level-2 data products are used as input. These products are not only from the specific instrument, but are usually combined with theoretical models, other observations, laboratory data, catalogues, etc. Their formats should be VO compatible and these data products should be suitable for VO access.

---

# Chapter 8. Change record

Version 2.0, 20 May 2010

- **New issue based on in-flight experience (Performance Verification phase and Science Demonstration phase): all sections re-written.**

Version 2.1, 28 May 2010

- **Various minor corrections and typo/formatting corrections.**
- **Analytic formula to compute sensitivity in mini-scan map mode given in Section 5.4**
- **Warning added in Section 5.2.3 that the column "central area point-source sensitivity" is only applicable in the mini-scan map mode.**

---

# References

[\[RD1\] Herschel Observers' Manual](#) *HERSCHEL-HSC-DOC-0876*

[RD2] *PACS Calibration Document*, PACS-MA-GS-001, January 27, 2009, issue 1.0, Ulrich Klaas et al.

*PACS responsivity from standard stars observations*, SAp-PACS-HA-0713-09, 29 October 2009, Aussel, H.

*MADmap: A Massively Parallel Maximum Likelihood Cosmic Microwave Background Map-maker*, Cantalupo, C. M.; Borrill, J. D.; Jaffe, A. H.; Kisner, T. S.; Stompor, R. 2009, ApJS, 187, 212

*Dehaes, S., Bauwens, E., Decin, L., et al. 2010, A&A (submitted)*

*Fletcher, L. N., Drossart, P., Burgdorf, M., et al. 2010, A&A, 514, A17*

*Mueller, T. G., Lagerros, J. S. V. 2002, A&A, 381, 324-339*

*The Photodetector Array Camera and Spectrometer (PACS) on the Herschel Space Observatory*, Poglitsch et al. 2010, A&A Herschel special issue

*Schulz, B., Huth, S., Laureijs, R. J., et al. 2002, A&A, 381, 1110*

*Shirahata, M., Matsuura, S., Hasegawa, S., et al. 2009, PASJ, 61, 737*